Cortical Dynamics Associated with Freezing of Gait and its Severity in Parkinson's Disease: An Integrative EEG-Based Analysis for Biomarkers and Detection

by

Fatemeh Karimi

A thesis

presented to the University of Waterloo

in fulfillment of the

thesis requirement for the degree of

Doctor of Philosophy

in

Systems Design Engineering

Waterloo, Ontario, Canada, 2024

Examining Committee Membership

The following kindly served on the Examining Committee for this thesis. The decision of the Examining Committee is by a majority vote.

External Examiner	Yiwen Wang Associate Professor Department of Electronic and Computer Engineering Department of Chemical and Biological Engineering Robotics Institute Center for Aging Science The Hong Kong University of Science and Technology
Supervisor	Ning Jiang Professor National Clinical Research Center for Geriatrics (WCH) West China Hospital, Sichuan University
Internal Member	Bryan Tripp Associate Professor Systems Design Engineering Department University of Waterloo
Internal Member	John Yeow Professor Systems Design Engineering Department University of Waterloo
Internal-external	James Tung Associate Professor Mechanical And Mechatronics Engineering University of Waterloo

Author's Declaration

This thesis consists of material all of which I authored or co-authored: see Statement of Contributions included in the thesis. This is a true copy of the thesis, including any required final revisions, as accepted by my examiners. I understand that my thesis may be made electronically available to the public.

Statement of Contributions

This thesis consists of two published papers and one journal manuscript written for publication. Dr. Ning Jiang, as Fatemeh Karimi's supervisor, assisted with project conceptualization, and creation of the data collection and analysis protocols. Dr. Jiang participated in editing manuscripts submitted and published in peer-reviewed journals that are presented in Chapters 3 to 5. The first draft was always written by Fatemeh Karimi, and she was involved in the editing process at all stages.

Dr. Quincy Almeida assisted in modifying and finalizing the data collection protocol, as well as patient assessments. He also participated in editing manuscripts submitted and published in peer-reviewed journals that are presented in Chapters 3 to 5.

Fatemeh Karimi, with the assistance from Jiansheng Niu and Kim Gouweleeuw, recruited participants and performed data collections. Jiansheng Niu assisted with EMG and EEG data preprocessing for the paper presented in Chapter 3.

Abstract

Freezing of gait (FOG) is a complex and debilitating gait disturbance in Parkinson's disease (PD) that significantly impacts mobility and quality of life in PD patients. FOG affects approximately 86.5% of individuals with advanced PD and up to 37.8% in the early stages of the disease. Unfortunately, dopaminergic medication provides limited benefits for FOG, and the lack of a clear understanding of its underlying neurophysiological mechanisms has resulted in limited efficacy of alternative treatment options based on emerging technologies such as brain-computer interface (BCI), deep brain stimulation (DBS), transcranial magnetic stimulation (TMS), and transcranial direct current stimulation (tDCS). Electroencephalogram (EEG), as a portable and noninvasive cortical recording technique, records oscillations representing the collective neural activity underlying the neural communication in the brain. EEG contains various components exhibiting a variety of possible characteristics across spatial and temporal scales. Integrative EEG analysis in PD patients with FOG holds the potential to establish new and efficient FOG rehabilitation pathways, while also introducing biomarkers for diagnosing FOG, monitoring its progression, predicting treatment response, and evaluating the effectiveness of therapeutic interventions.

In this study, we adopted a comprehensive approach. First, we analyzed power and phase-related EEG features in PD patients with different levels of FOG as well as PD patients without FOG and age-matched healthy controls (HC) during a simple lower limb task. We then

extended the findings to more realistic and complex walking tasks. For this purpose, a total of 41 individuals, including patients with freezing (N = 14, 11 males), patients without freezing (N = 14, 13 males), and HC (N = 13, 10 males), were recruited. All participants performed two sets of tasks: ankle dorsiflexion (AD) while seated and walking tasks. PD patients with FOG were further classified into mild and severe cases to investigate EEG features associated with freezing severity. Initially, we examined the morphological features of a specific EEG signature called Movement Related Cortical Potential (MRCP) during AD task. Additionally, we investigated power activities of distinct frequency bands (theta, alpha, and beta) during the same task across different participant groups and channels. In the second stage, we explored phase-related features of MRCP and other frequency bands in superficial and deeper networks by applying a spatial filter called surface Laplacian (SL). Lastly, considering the observed alterations in power and phase of different frequency bands during the simple lower limb task (AD), we investigated phase amplitude coupling (PAC) between various frequency bands during normal walking condition (NW) and FOG episodes (FE) in PD patients with FOG and compared the results with PD patients without FOG and HC during normal walking.

The initial results of this thesis, focused on the cortical dynamics during AD, revealed significant differences between patients with severe FOG and both HC and patients without FOG. Moreover, patients with mild and severe FOG exhibited distinct cortical activity patterns. In patients with FOG, the initial component of MRCP was significantly reduced compared to

HC (P = 0.002), and its magnitude was influenced by the severity of FOG. Notably, patients with FOG demonstrated a remarkable absence of desynchronization in the beta frequency band, particularly in the low-beta range over primary motor cortex (M1), prior to movement initiation, which was also correlated with the severity of FOG condition. Low-beta and high-beta activities represented unique characteristics for each group. While HC exhibited beta event-related desynchronization over M1 before movement, patients with FOG showed partial replacement of this pattern by theta band synchronization. Patients with severe FOG also showed some degree of theta band synchronization over the contralateral SMA.

Regarding the phase-related features of FOG during AD task, frontoparietal theta phase synchrony emerged as a distinctive characteristic in the superficial layers of PD patients with FOG. In deeper networks, interhemispheric frontoparietal alpha phase synchrony was significantly dominant in PD patients with FOG, in contrast to beta phase synchrony observed in PD patients without FOG. Furthermore, alpha phase synchrony was more widely distributed in PD patients with severe FOG, particularly exhibiting higher levels of frontoparietal alpha phase synchrony. In addition to FOG-related abnormalities found in the phase-locking value (PLV) analysis during AD task, PAC analysis was performed on frequency bands with PLV abnormalities during this task. PAC analysis revealed abnormal coupling between theta and low-beta frequency bands in PD patients with severe FOG at the superficial layers over frontal areas. In deeper networks, both theta and alpha frequency bands showed significant PAC over

parietal areas in PD patients with severe FOG. Alpha and low-beta bands also exhibited PAC over frontal areas in PD groups with FOG.

PAC analysis comparing normal walking (NW) to freezing episodes (FE) also identified significant differences between these conditions in PD patients both with and without FOG, as well as in HC. Our results demonstrated that PAC between theta and low-beta frequencies in PD patients with FOG during FE exhibited higher statistical significance compared to PAC in PD patients with FOG during NW, PD patients without FOG during NW, and HC during NW, specifically over the (pre-) SMA and parietal areas ($p<0.01$). Additionally, the findings showed elevated PAC between alpha and low-beta frequency bands in the parietal area during FE ($p<0.01$). There was also a higher PAC between theta and alpha frequency bands in PD patients with FOG compared to the other two groups ($p<0.01$), regardless of the experimental condition.

This thesis makes several contributions to current literature bridging both neurophysiological and engineering domains. Our findings highlight the critical role and potential of phase-related EEG signal features in postulating a unified mechanism for FOG. These results also suggest PLV and PAC during AD task as prospective EEG-based biomarkers for diagnosing and monitoring FOG. Additionally, these results provide novel perspectives for developing non-pharmacological strategies for FOG intervention and rehabilitation.

Acknowledgements

Over eight years, numerous individuals have supported my thesis journey. I'm profoundly grateful to my supervisor, Prof. Ning Jiang, for his guidance and support. Thanks to Dr. Quincy Almeida for his advice on strengthening the research plan and his assistance in the process of patient recruitment and assessment, and my thesis committee members, Dr. Brian Tripp, Dr. John Yeow, and Dr. James Tung. My gratitude extends to all participants, whose commitment fueled my passion.

I am endlessly thankful to my husband, Morteza, who has been my go-to in times of challenges. A million, billion, zillion, trillion, and maghzilion thanks go my sweet, lovely son, Nikrad, for being full of life and taking me to his beautiful, colorful world, and reminding me of the meaning of life. My parents also deserve immense appreciation for their lifelong support.

I owe much to Dr. Reza Gharib for his insight, support, and for enlightening me on the importance of history, art, science, and philosophy over the years.

I would like to thank my friends within and outside our lab: Nargess Heydari, Jiansheng Niu, Mina Sharif, and Sarah Mahrokhzad for their support in my research and personal life.

I also would like to thank UW and Canada that were kind to me and allowed me to see a new world. This research was supported in part by the Natural Sciences and Engineering Research Council of Canada (NSERC).

Dedication

I dedicate this thesis to Morteza, Nikrad, Mom, and Dad for their love and support. This accomplishment belongs to us all.

Table of Contents

List of Figures

List of Tables

List of Abbreviations

AD: Ankle Dorsiflexion
AMICA: Adaptive Mixture Independent Component Analysis
ASR: Artifact Subspace Reconstruction
BCI: Brain-Computer Interfaces
CFC: Cross-Frequency Coupling
CFS: Cross Frequency Phase Synchrony
CV: Correlation of variation
DBS: deep brain stimulation
EEG: Electroencephalography
EMG: Electromyogram
FOG: Freezing of Gait
GP: Globus Pallidus
GPe: Globus Pallidus external
GPi: internal segment of the globus pallidus
HC: Healthy Controls
ICA: Independent Component Analysis
LED: Levodopa Equivalent Dose
MLR: Mesencephalic Locomotor Region
MP: Motor Potential
MMP: movement-monitoring potential
MRCP: Movement Related Cortical Potential
NAc: Nucleus Accumbens
PAC: Phase Amplitude Coupling
PCA: Principal Component Analysis
PD: Parkinson's Disease
PLV: Phase Locking Value
PPN: Pedunculopontine Nucleus
PWO: Particle Swarm Optimization
SMA: Supplementary Motor Area
SNR: Signal-to-Noise Ratio
SNc: Substantia Nigra pars compacta
STD: Standard Deviation
STN: Subthalamic Nucleus
SL: Surface Laplacian
TA: Tibialis Anterior
TMS: Transcranial Magnetic Stimulation

tDCS: transcranial Direct Current Stimulation
VP: Ventral Pallidum
UPDRS: Unified Parkinson's Disease Rating Scale
WM: Working Memory

Chapter 1

Introduction

Freezing of Gait (FOG) is a prevalent symptom observed in the advanced stages of Parkinson's Disease (PD), which is characterized by the inability to generate effective stepping [1][2]. FOG significantly affects the quality of life of individuals with PD by causing balance impairment and increasing the risk of falls, which leads to higher morbidity and mortality rates among PD patients [3]. The occurrence of FOG is influenced by various factors and situational contexts including emotional states, cognitive factors, and environmental conditions. It often manifests during gait initiation, turning, maneuvering through narrow passages, or when approaching particular destinations such as chairs [4]. Despite extensive research on the clinical and physiological aspects of FOG, it remains one of the least understood symptoms in PD. The multisystem nature and high variability of FOG add to the difficulty in formulating a precise and universally applicable definition for this phenomenon [2]. However, in 2010, a definition gained wide acceptance: FOG is a ”*brief, episodic absence or marked reduction of forward progression of the feet despite the intension to walk*” [5][6].

The lack of comprehensive knowledge and understanding of FOG also restricts the development of effective therapeutic or interventional approaches. While certain pharmacological interventions (e.g., dopaminergic and non-dopaminergic), deep brain stimulation (DBS), and physical rehabilitation techniques have shown efficacy in alleviating

FOG symptoms in specific individuals, their effectiveness has been proven challenging and limited especially when dealing with advanced FOG cases [7]. This challenge primarily arises from the complex nature of gait, which necessitates the simultaneous coordination and integration of multiple neural structures and functions. Particularly, walking is a complex process, involving the integration of automatic movements, processing of sensory inputs, and intentional adjustments. Achieving normal gait thus requires a precise equilibrium among various neuronal systems that interact with one another [8]. Consequently, enhancing and integrating our comprehension of the underlying neural mechanisms driving FOG will be foundational for the development of more precise and efficient therapeutic and rehabilitation approaches, addressing the complex interplay of factors involved in FOG [9][10][11][12].

Brain dynamics are essential in locomotion control, orchestrating a wide array of motor, perceptual, and cognitive functions. Specifically, brain oscillations are proposed to fulfill a functional integration role, addressing the question of how functions performed by one part of the nervous system are integrated with those of another [13]. The intricate involvement of multiple neural networks and diverse brain structures in gait control indicates the importance of brain dynamics, which are generated by various cortical and subcortical structures. Consequently, investigating brain dynamics presents promising paths for gaining an integrative comprehension of the underlying mechanisms of FOG that can lead to the introduction of novel FOG biomarkers, and effective detection of this phenomenon. In addition, such investigation can provide valuable resources for the development of innovative

technology-based therapies and rehabilitation systems specifically for individuals with PD patients experiencing FOG. Recent research suggests that beyond subcortical regions, cortical involvement also significantly contributes to FOG. Key cortical regions, specifically the supplementary motor area (SMA) and the primary motor cortex (M1), are crucial in motor planning and execution. Studies investigating FOG have revealed alterations in cortical dynamics and activity patterns in these regions during FOG episodes. Understanding the cortical involvement in FOG can therefore provide valuable insights into the underlying mechanisms and guide the development of targeted interventions to alleviate this complex symptom.

Electroencephalogram (EEG) contains information of the rhythmic activities of brain electric potential fields at the cortical level. Identifying EEG signatures associated with FOG holds promise for the identification of reliable biomarkers and is one of the key steps toward developing effective therapies for FOG [14]. Considering advancements and emerging techniques based on EEG as a non-invasive and portable technology, understanding of the abnormal cerebral oscillatory activities associated with FOG not only enhances our insights into the underlying mechanisms of FOG but also paves the way for clinical use of EEG for FOG diagnosis and monitoring, and opens avenues for potential non-medication-based treatments and therapeutic interventions. Examples of these interventions include adaptive closed-loop DBS, as well as innovative treatment or rehabilitation options based on brain-

computer interfaces (BCI), transcranial magnetic stimulation (TMS), and transcranial electric current stimulation (tECS).

Neural correlates between EEG oscillations and FOG have been increasingly explored, especially over the last decade [15]-[28]. Although researchers have explored movement-related cortical potentials (MRCPs) and brain oscillations in different frequency bands, such as theta, alpha, beta, and gamma, the field of FOG research still lacks integrated EEG features to form a comprehensive picture of the changes in EEG characteristics associated with FOG. Particularly, most studies employed EEG analysis to study neural changes or to detect FOG events by focusing primarily on spectral power across different EEG frequency bands. Investigations into other EEG features and algorithms are thus required to provide the necessary clues for identifying meaningful signatures of FOG.

This research aims to explore novel EEG features associated with FOG and its severity through a hierarchical and purposeful approach. The findings of the research could potentially serve as biomarkers for diagnosis and monitoring, or as EEG modalities for the development and control of non-invasive, BCI-based assistive and rehabilitative devices or adaptive DBS. The specific objectives of this study are as follows:

1) To identify and extract novel EEG features associated with FOG and its severity in PD patients with varying levels of FOG. This will be accomplished through the study of brain oscillations in different patient populations, taking into account the functional role

of each frequency sub-band and the hierarchical relationship between lower and higher frequency bands. This step aims to introduce potential biomarkers for FOG diagnosis and monitoring using EEG features during a simple lower limb movement task. The objectives are further detailed as:

a) To determine the morphological features of MRCP as a low-frequency movement-related brain rhythm in relation to FOG and its severity.

b) To determine power-based EEG features associated with FOG and its severity in higher frequency bands, such as theta, alpha, and beta and their sub-bands.

c) To identify phase-related features, as an independent measure from power-based features, in relation to FOG in MRCP and higher frequency bands including theta, alpha, and beta and their sub-bands.

d) To investigate the abnormalities in phase-amplitude coupling (PAC) features, *i.e.* the coupling characteristics between the phase of lower frequencies and the amplitude of higher frequencies, related to FOG and its severity.

2) To analyze EEG alterations that contribute to the occurrence of FOG episodes. This objective aims to understand the distinctive patterns and changes in EEG signals during FOG episodes, in order to gain deeper insights into the underlying mechanisms of FOG. Furthermore, this objective seeks to introduce potential EEG signatures of FOG that can be utilized in FOG rehabilitation or assistive devices

based on BCIs or adaptive DBS. The investigation of these features was conducted during realistic walking tasks and based on the findings obtained from the previous objectives, thereby providing a cohesive and integrated understanding of the EEG correlates of FOG.

The rest of the thesis is structured as the following. Chapter 2, the background and literature review, provides essential background information and preliminary knowledge about the cortical and subcortical structures involved in FOG, as well as the properties of brain oscillation and locomotion control. Chapter 3 presents a comparative study aimed at identifying movement-related morphological and power-based EEG signatures associated with FOG and its severity during a simple lower limb movement task. The study examines multiple cortical regions and conducts a detailed investigation of various frequency bands and their sub-bands to reveal distinctive features of PD patients with mild and severe FOG. In Chapter 4, we investigate phase-related features for the same groups and task, targeting the same electrode locations and frequency sub-bands. This chapter highlights abnormal phase synchronizations in PD patients with different levels of FOG. Here, we analyze phase synchronization over both superficial and deeper networks, using a spatial filter to identify the most significant potential EEG-based biomarkers. Following the observations in Chapters 3 and 4, Chapter 5 investigates PAC between different frequency sub-bands in relation to FOG occurrence. PAC is studied using an efficient artifact removal EEG processing algorithm and a recently introduced PAC method during both normal walking and FOG episodes. This aims to identify EEG features

associated with FOG occurrence that can potentially be utilized in BCI-based assistive and rehabilitative systems and adaptive DBS. All chapters also aim to elucidate the underlying mechanisms of FOG, deepening our understanding of the phenomena and contributing to the development of new treatment options. Finally, Chapter 6 summarizes the findings from the previous chapters and discusses challenges and potential future work.

The publications resulted from this research includes:

1. F. Karimi, Q. Almeida, N. Jiang, “Altered EEG Phase Amplitude Coupling between Theta, Alpha, and Low Beta During Freezing of Gait in Parkinson’s Disease” (ready to submit)

2. F. Karimi, Q. Almeida, N. Jiang, “Large-scale frontoparietal theta, alpha, and beta phase synchronization: A set of EEG differential characteristics for freezing of gait in Parkinson’s disease?”, Frontiers in Aging Neuroscience, 2022.

3. F. Karimi, J. Niu, K. Gouweleeuw, Q. Almeida, N. Jiang, “Movement-related EEG signatures associated with freezing of gait in Parkinson’s disease: an integrative analysis”, Brain Communications, Volume 3, Issue 4, 2021.

4. F. Karimi, J. Kofman, N. Mrachacz-Kersting, D. Farina, and N. Jiang, “Detection of movement related cortical potentials from EEG using constrained ICA for brain-computer interface applications,” Frontiers in Neuroscience., vol. 11, p. 356, Jun. 2017.

5. F. Karimi, J. Niu, Q. Almeida and N. Jiang, "Movement Related Cortical Potentials in Parkinson’s Disease Patients with Freezing of Gait", 42nd Annual International Conference of the IEEE Engineering in Medicine & Biology Society (EMBC), 2020.

6. F. Karimi and N. Jiang, "A Reference-based Source Extraction Algorithm to Extract Movement Related Cortical Potentials for Brain-Computer Interface Applications", IEEE International Conference on Systems, Man and Cybernetics (SMC), 2019.

7. F. Karimi, J. Kofman, N. Mrachcz-Kersting, D. Farina, N. Jiang, “Comparison of EEG Spatial Filters for Movement Related Cortical Potential Detection”, The 38th Annual International Conference of the IEEE Engineering in Medicine and Biology Society (EMBC), Orlando, Florida USA, 2016.

Chapter 2

Background and literature Review

This chapter reviews current theories about FOG as well as human brain structures involved in PD and locomotion control. The chapter also provides background on brain oscillations, their functions, and mechanisms.

2.1 Parkinson's Disease

Parkinson's disease (PD) is the second most common progressive multi-system neurodegenerative disease, affecting 1% of the population above 60 years [29]. The prevalence and incidence of PD are also rapidly increasing due to the aging population structure and World Health Organization Program suggest that by 2040, PD is anticipated to become the second most common cause of death [7] [30]. During the early stages of PD, the affected areas of the brain are limited to the brain stem and olfactory system (pre-symptomatic stages 1-2). Throughout stages 3-4 of the progression, the substantia nigra and other nuclei of the midbrain and forebrain become increasingly subject to the initial minor and eventually severe pathological alterations, which results into development of motor symptoms. At the terminal stages of the disease (stage 5 and 6), the neocortex is adversely affected [31]. PD symptoms are generally categorized into motor and non-motor symptoms. Classic motor symptoms of PD include low-frequency rest tremor, slowness of initiation of voluntary movements, muscular rigidity, postural instability, alterations in gait and balance. In general, motor impairments of

PD follow the degeneration of significant number (80%) of dopaminergic neurons in substantia nigra pars compacta (SNc) and depletion of dopamine in striatum. The progression of the degeneration of dopamine neurons and the consequent depletion of the dopaminergic innervation of the striatum (beginning with the putamen and then moving medially to the caudate) is correlated with an aggravation of motor symptoms, with the exception of tremor [32]. A brief timeline of the significant developments in terms of epistemic and clinical advances in PD is outlined in Figure 2-1.

2.2 Freezing of Gait

FOG is a mysterious episodic neurological phenomenon that affects around half of the advanced stage PD population and presents substantial variability within and between individual patients [33][34][35]. FOG episodes are transient disruptions of the locomotor network in which the patient is unable to initiate gait, experiences arrests in forward

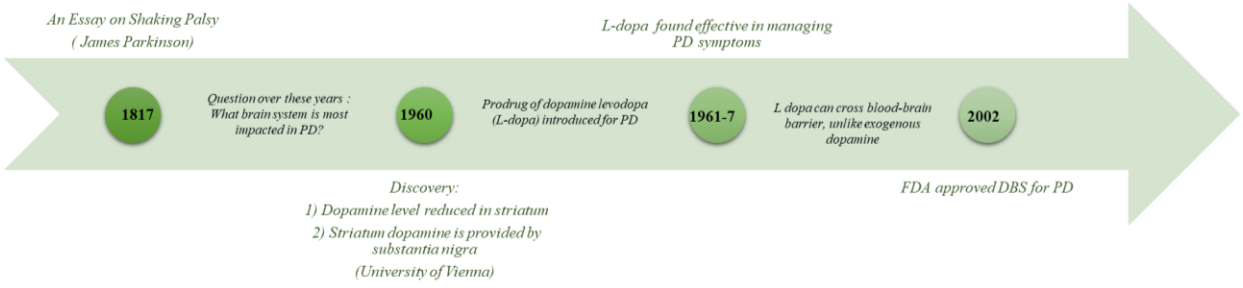

Figure 2-1. Schematic timeline of epistemic and clinical breakthroughs in PD

progression during walking, or shuffles forward with short strides ranging from millimeters to

a couple of centimeters in length [2][33]. FOG and postural instability usually coexist, and one possible characteristic of FOG is leg trembling-in-place during FOG episodes in the frequency range of 3-8 Hz. It is intriguing to note that historic PD literature rarely mentioned FOG, and its significance was fully recognized after the wide acceptance of chronic administration of levodopa. FOG is only partially responsive to dopamine replacement therapy [36][37], and pharmacologic subtypes of FOG include those that are responsive and unresponsive to levodopa [38].

Despite the growing attention toward FOG in clinical and research communities, the pathophysiology mechanism of FOG has not been yet understood due to the complexity, occasional manifestation, and multidisciplinary nature of the phenomenon [14][16][39]. Recent studies suggested the existence of subgroups among patients with FOG that can be classified by predominant freezing triggers; i.e. a motor type (freezing while turning), a cognitive type (freezing while dual-tasking), or a limbic type (freezing while anxious) [33]. Over the recent years, the FOG field has undergone a paradigm shift from being focused solely on the basal ganglia (BG) to a more holistic view that considers other brain areas. Diverse and complementary methodological domains such as neurophysiology, clinical phenomenology, neuro-modulation, neurogenetics, and multimodal neuroimaging are required to fully understand various facets of FOG. Evidence proposes a common neural pathway, encompassing the brain stem, thalamus, and BG, as a possible foundation for FOG manifestation [40]. In addition, despite all the contradictions and unknowns about the

mechanisms of FOG, the current literature suggests that FOG is a heterogeneity symptom and it is highly likely that it involves higher-level cortical modulators from both a broad host of motor perspective (e.g. prefrontal cortex (PFC), SMA, premotor cortex, and motor cortex), as well as non-motor perspective (e.g. deterioration of cortical movement planning with dual tasking, deterioration of automaticity, fear/anxiety, salience, deficits in visuomotor integration, and failure of sensory processing) [33]. Recent research suggests that FOG could be also related to dysfunctional cortical-subcortical communication [41]. Neurophysiological models that are suggested to explain the transient occurrence of FOG in four categories include [19][39]:

1) **Threshold model:** In this model, motor breakdown due to the accumulation of motor deficits over time results into a critical threshold of coordination instability during a highly coupled and bilateral task such as gait. When critical gait abnormalities such as step scaling, gait rhythmicity, and bilateral step coordination and symmetry reach a certain threshold a breakdown in locomotion results in FOG episodes [39].
2) **Interference Model**: In this model, the BG's capacity of processing motor, cognitive, and limbic inputs within a limited time window is overloaded due to insufficient dopaminergic cells [42], leading to temporary inhibition of the pedunculopontine nucleus (PPN) and, eventually, the manifestation of FOG.

3) **Cognitive Model**: This model suggests that conflict-resolution deficit, especially during time-constrained tasks which includes activation of the correct responses and suppression of the conflicting responses causes FOG [39].
4) **Decoupling Model**: This model suggests that FOG occurs when there is a disconnect between the preparatory programming and the desired motor response, leading to a halt in the automatic generation of movement. This model associated FOG with a impaired postural adjustment which is caused by an inability to couple a normal anticipatory postural adjustments (APAs) to the stepping motor pattern [43]. In a more general sense, decoupling between pre-planned motor programs and the release of an inherent movement is suggested to be linked to FOG in this model [39].
5) **Bandwidth Model:** This recent model highlights the role of cortical dysfunction, particularly in the primary motor cortex, and cognitive burden in the emergence of freezing [19]. The model comprises three key elements: the baseline occupation, which represents the level of cortical processing resources; the dynamic fluctuation, which indicates the instantaneous cognitive burden; and the bandwidth limit, which represent processing resource in human brain. When the bandwidth limit exceeds a certain threshold, information processing becomes overloaded, leading to freezing. Within this framework, PAC between beta and gamma frequency bands over primary motor cortex reflects the over-occupation of cortical processing resources, signaling the likelihood of an FOG event [19].

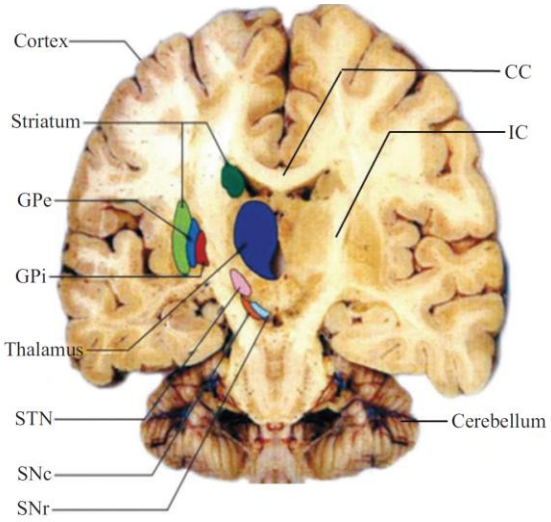

Figure 2-2. This coronal section (up-down) of the human brain shows the key components of the BG, namely the corpus callosum (CC), the external and internal segments of the globus pallidus (GPe and GPi), the internal capsule (IC), the substantia nigra compacta and reticulata (SNc and SNr), and the subthalamic nucleus (STN). Picture adopted from [277]**.**

The following section will describe the brain structures related to locomotion and FOG, as well as brain oscillations as fundamental neural mechanisms for coordinating and integrating neural activity across different brain structures and networks at cortical and subcortical levels.

2.2.1 Basal Ganglia

The basal ganglia (BG) are a group of interconnected nuclei located deep within the brain as presented in Figure 2-2. The main structures of the BG include: 1) Striatum: which is divided into caudate nucleus, putamen, and nucleus accumbens (NAc, which is not shown in the figure). 2) Globus pallidus (GP): which is divided into external segment of the globus pallidus (GPe) and internal segment of the globus pallidus (GPi), and ventral pallidum (VP, not shown

in the figure due to its anterior coronal location. 3) Subthalamic nucleus (STN). The caudate and putamen are commonly grouped together and referred to as the dorsal striatum [32].

The BG play a critical role in motor control and the modulation and execution of movement, aspects severely impacted by PD. The pathology of PD is characterized by the progressive degeneration of dopaminergic neurons in the substantia nigra. This degeneration leads to several changes within the BG circuitry, particularly disrupting the equilibrium between the direct, indirect, and hyper direct pathways—all crucial for the regulation of movement. The direct pathway facilitates movement initiation, while the indirect pathway inhibits undesired or unnecessary movements. Moreover, the hyper direct pathway, which involves a direct connection from the cortex, particularly the motor and prefrontal areas, to the STN, bypassing the striatum, is believed to be responsible for sudden changes in motor plans and conflict resolution [32].

In addition, the role of BG extends beyond mere motor control; it is also involved in cognitive and emotional processes. This becomes particularly relevant in the context of PD, as patients often experience a wide array of non-motor symptoms. These may include cognitive impairments, mood disorders, and autonomic dysfunction, reflecting the extensive connectivity and influence of the BG on various brain regions.

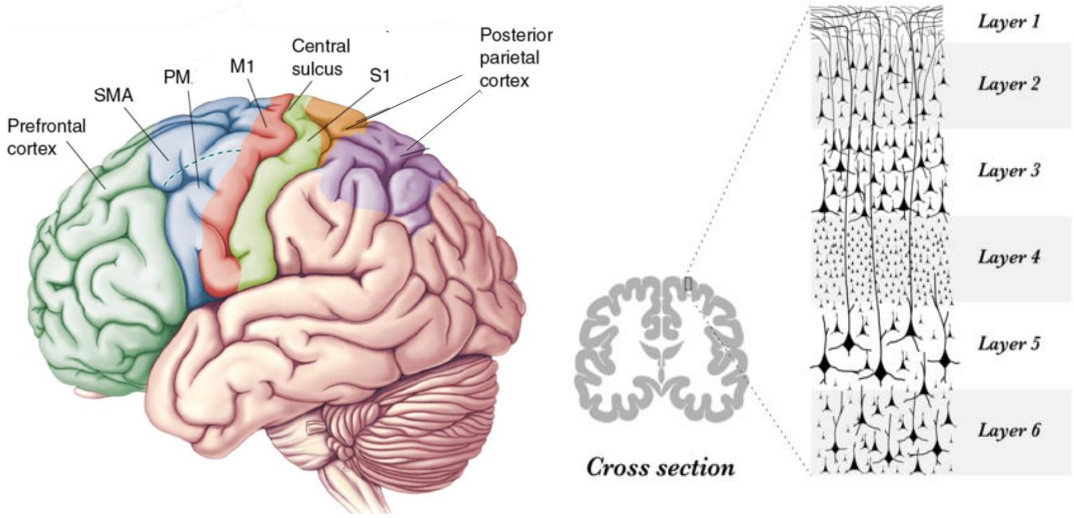

(a) (b)

Figure 2-3. a) The cerebral cortex areas involved in motor control: prefrontal cortex, SMA, pre-motor cortex (PM), primary motor cortex (M1), primary somatosensory cortex (S1), posterior parietal cortex. b) Six layers of the cortex.

The BG is situated in close proximity to the cerebral cortex and the thalamus, and these three brain structures possess a strong interconnection.

2.2.2 Cortical Motor Control

The cerebral cortex is a thin layer of neural tissue located at the top of the brain and responsible for various high-level tasks, such as processing sensory information and controlling movements. A variety of cortical areas, including the premotor cortex (PM) and the (pre-) SMA, and primary motor cortex (M1) are involved in controlling voluntary movement. The functional roles of these areas will be briefly discussed in the following

sections. The key cortical areas engaged in voluntary movements are illustrated in Figure 2-3 (a).

2.2.2.1 Cortical Layers

The neocortex is a complex structure composed of six layers of interconnected neurons. Each cortical layer plays a role in processing information, integrating sensory inputs, and controlling motor responses. This complex interplay between the layers, complemented by their connectivity with other brain structures and networks, establishes intricate communication pathways.

Layer one, being the most superficial, contains sparse cells and its specific role within the neocortex remains a subject of ongoing research [44]. The second and third layers, characterized by sparse pyramidal neurons and localized networks, are essential for various cognitive tasks, such as information processing, storage, and retrieval [45]. The fourth layer serves as the principal recipient of thalamic inputs, especially in primary sensory cortical areas, thereby playing a vital role in sensory data processing [45]. Layer five, enriched with output pyramidal neurons, sends the processed information to deeper brain structures, specifically to the striatum of the basal ganglia [45]. Particularly in regions where significant motor output is taking place, there are high numbers of large pyramidal neurons that transmit information to more profound structures and even to the spinal cord. As the deepest layer of the neocortex,

layer six plays a crucial role in regulating the flow of information between the cortex and subcortical regions. The arrangement of six cortical layers is illustrated in Figure 2-3 (b).

2.2.2.2 Supplementary Motor Area

The SMA comprises two distinct regions, namely the SMA proper and the pre-SMA, which closely interact with the BG to regulate movement [46][47]. While the precise functions of the SMA proper and pre-SMA are still being explored, these regions receive complex inputs that have undergone extensive processing by other cortical areas. The SMA proper exhibits strong connections with M1 and PM, while the pre-SMA is linked to prefrontal areas [47]. The pre-SMA receives inputs from the BG, as well as prefrontal and temporal cortical regions, and it sends a significant portion of its output to the dorsolateral prefrontal cortex and the BG [47]. Inputs to the SMA originate from the BG through the ventral anterior thalamus, as well as from the parietal and premotor cortices. The primary outputs of the SMA include connections to the PM, M1, BG, thalamic nuclei, brain stem, and spinal cord, primarily influencing other motor-related structures. Activation of the SMA prior to movement suggests its role in regulating posture preceding limb movement. Both the SMA and pre-SMA play essential roles in the learning of movement sequences and coordinating sequential movements.

2.2.2.3 Primary Motor Cortex

The primary motor cortex (M1) is directly involved in the generation of voluntary movements, primarily through its layer 5 large pyramidal cells. These cells serve as the main

outputs of the motor cortex, transmitting signals to the brainstem and the pyramidal tract. The topographical arrangements of the motor cortex suggest a role in encoding specific muscle activation for precise motor control.

2.2.2.4 Premotor Cortex

The premotor cortex (PM) plays an important role in the initiation and coordination of voluntary movements. Interacting closely with the prefrontal cortex, SMA, and posterior parietal cortex, PM receives inputs from the BG and the cerebellum via the thalamus, enabling fine-tuned motor control and the integration of sensory information with motor commands. Notably, it exhibits a strong functional relationship with the posterior parietal cortex, which provides essential spatial information for motor planning. Moreover, PM is responsible for processing sensory information, particularly visual cues, that contribute to the precise control and execution of movements.

2.2.2.5 Posterior Parietal Cortex

The posterior parietal cortex is a cortical region involved in sensory integration and spatial perception. The primary role of this area is to provide the other motor areas with information regarding the spatial relationships between objects, as well as the spatial position of the body in relation to the external environment, contributing to our ability to interact with the surrounding environment. Its intricate connections with other brain regions enable the

integration of sensory inputs and the generation of appropriate motor responses, making the posterior parietal cortex essential for sensorimotor integration and motor planning.

2.2.3 Locomotor Control

Locomotion is a rhythmic motor activity that enables humans and animals to navigate their environment. Successful locomotor control relies on the integration of postural activity and coordinated interactions among various components, including the supraspinal locomotor network and central pattern generators (CPGs), as well as various components within the nervous and musculoskeletal systems [47]. Figure 2-4 represents the framework of supraspinal control of human locomotion. While CPGs are responsible for generating rhythmic goal directed motor outputs, a hierarchy of supraspinal regions transmit signals to the CPG in the spinal cord. This interaction regulates and coordinates the rhythmic patterns of muscle activation, allowing them to adapt to changing environmental conditions. These signals serve to modify stereotypical locomotion patterns in specific situations, including gait initiation, turning, stopping, and obstacle avoidance [48]. Once an external or internal stimuli is received, cerebral cortex ,especially (pre-) SMA, sends the signal to the BG, particularly striatum, where voluntary movements are facilitated and undesired movements are inhibited [32]. When the locomotion is selected, output nuclei of BG relieve the inhibition of neurons in the mesencephalic locomotor region and pedunculopontine nucleus (MLR/PNN) which results in initiation of locomotion. BG also sends commands to Thalamus which then provides feedback

to motor cortex. In the meantime, cerebral cortex sends signals to MLR and the spinal cord through cortico-brainstem and corticospinal tracts [49].

While cerebral cortex and limbic system are responsible for volitional and emotional references, respectively, locomotion is accompanied by automatic processes, regardless of the reference, including rhythmic limb movements and the regulation of postural muscle tone that is generated by circuits in BG, the cerebellum, the brainstem, and especially the spinal cord.

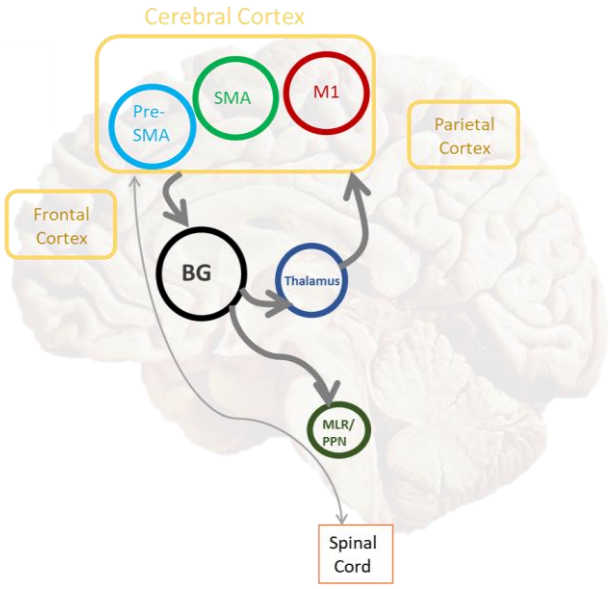

Figure 2-4. Major structures involved in in motor control hierarchy encompasses several components, including diverse cortical areas such as the frontal-parietal, supplementary motor (SMA), and motor areas, BG, thalamus, mesencephalon and pedunculopontine nucleus (MLR/PPN), and spinal central pattern generators (CPGs) in the spinal cord. Locomotor control starts in cerebral cortex with inputs from volitional or emotional references. The initiated signal then reaches the BG for refinement through BG-thalamo-cortical loop (depicted with thick gray lines). The signal flow eventually reaches brain stem and spinal cord [48].

2.2.3.1 BG-Thalamo-Cortical Loops

The BG-thalamo-cortical loops are fundamental neural circuits that play a crucial role in motor control as well as the regulation of cognitive and emotional processes. These parallel loops involve the putamen, which receives signals from the cortex. Within these circuits, the internal segment of the GPi/SNr transmits signals to the thalamus and, ultimately, back to the cortex [50]. These loops involve the interaction between BG-thalamo-cortical motor, limbic, and cognitive circuits, with different regions of the cerebral cortex contributing to movement control through these pathways. Notably, there are two distinct pathways connecting the BG and the cerebral cortex: a direct pathway that primarily facilitates cortical excitation, necessary for activating the appropriate motor program, and an indirect pathway that predominantly inhibits the cerebral cortex, crucial for suppressing competing motor programs.

2.2.3.2 Mesencephalic Locomotor Region

The mesencephalic locomotor region (MLR) is a neural region located within the midbrain including PPN. MLR plays a significant role in initiating and coordinating rhythmic movements, such as walking [47][51]. Acting as a central command center, the MLR integrates sensory information from diverse sources and generates signals that orchestrate the synchronized activation of muscles and motor patterns necessary for an efficient and stable gait.

2.3 Brain Oscillations

Brain oscillations refer to the rhythmic electrical activity of the brain, generated by neurons that communicate with each other across various brain structures. Oscillatory synchronization are pivotal for transmission of information and the establishment of interconnected neural networks [52][53]. This synchronization is known to support the capacity of the brain for efficient information processing, aligning the activities of neurons in a coordinated manner [54][55]. The significance of synchronized neural oscillations extends beyond local interactions, orchestrating the temporal coordination of activities across widespread neural circuits, from individual neurons and local assemblies to expansive networks that include deep brain nuclei and the neocortex [56]. This perspective is supported by evidence indicating the critical role of synchronized oscillations in various functions and neural processes [57][58][59]. The recording of these oscillations, primarily through techniques such as EEG, offers invaluable insights into the underlying mechanisms of brain function and dysfunction, a topic that will be elaborated in the subsequent section.

2.3.1 Electroencephalogram (EEG)

In 1875, Richard Caton made a pioneering breakthrough by utilizing a galvanometer and positioning two electrodes on an individual's scalp to record electrical time series of brain activity. This significant finding led to the combination of the terms electro-, encephalo-, and gram, giving rise to the term electroencephalogram (EEG), which specifically refers to the

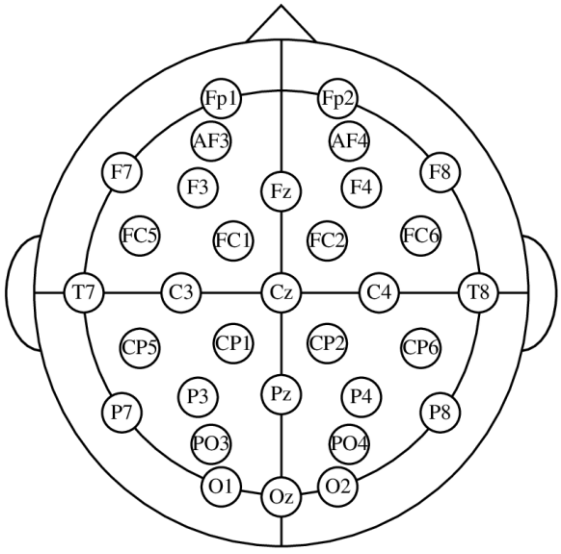

Figure 2-5: International 10-20 system with 32 channels

electrical neural activity of the brain [60]. Since the pioneering discovery of EEG and the alpha brain oscillation by Hans Berger in 1929, EEG has played a pivotal role in investigating the intricate relationship between brain oscillations and human functioning. Nowadays, EEG has evolved into a fundamental neurophysiological technique that captures the macroscopic spatio-temporal dynamics of the electric field of the brain using a set of scalp electrodes. This enables the presentation of collective neural activity from a group of neurons [61][62][63]. Figure 2-5 represents the EEG electrodes placement on the scalp using 10-20 system with 32 channels.

EEG oscillations cover a broad range of frequencies in the brain, spanning from approximately 0.02 Hz to 600 Hz. These frequencies are commonly categorized into different bands for analysis, including slow cortical potentials (SCP), delta (0.5-4 Hz), theta (4-8 Hz),

alpha (8-12 Hz), beta (12-30 Hz), and gamma (>30 Hz). Gamma oscillations, spanning the frequency range of 30 Hz to 120 Hz, have been associated with bottom-up processing in various cognitive tasks. Conversely, slower oscillations in the delta, theta, alpha, and beta frequency bands are commonly implicated in executive or top-down control functions [64]. However, it is important to note that alternative differentiations have also been proposed, indicating the complexity and multifaceted nature of these oscillatory phenomena [64]**.** Various diseases and disorders have been associated with changes in specific frequency ranges [63][65]. Still, understanding the functional role, mechanisms, and anatomical localization of these distinct frequency bands remains one of the major challenges in the field of neuroscience.

2.3.1.1 Event related synchronization/ desynchronization

Event-related synchronization (ERS) and event-related desynchronization (ERD) are EEG patterns that refer to the synchronization and desynchronization of brain activity observed during specific events. These patterns manifest as enhancements or attenuations in the amplitude of specific frequency bands and can be observed at both cortical and subcortical levels [66]. ERD typically begins around 2.0 seconds before and lasts 1.0 second after movement, occurring across various frequency bands such as 8-10 Hz, 10-12 Hz, 12-20 Hz, and 20-30 Hz [67]. In addition to these rhythmic changes, voluntary movement also leads to the occurrence of SCP shifts, which will be briefly discussed in the following section [68].

2.3.1.2 Movement Related Cortical Potentials

MRCP is an SCP characterized by a frequency band of approximately 0-5 Hz. It is identified as a low frequency negative shift in the EEG signal and is closely linked to motor planning, initiation, and execution processes. In contrast to ERD/ERS, SCPs are a distinct type of neurophysiological oscillations that specifically occur at the cortical level, typically within a frequency range of 0.5-4 Hz. The MRCP includes two pre-movement components referred to as the early Bereitschaftspotential (BP1) and late Bereitschaftspotential (BP2). BP1 emerges approximately 1.5-2 seconds prior to voluntary movement onset, while BP2 occurs around 400 milliseconds before the initiation of both real and imagined voluntary movements [24]. Notably, the MRCP reflects not only movement planning but also the monitoring of motor execution and performance. Subsequent components of the MRCP, namely the motor potential (MP) and movement-monitoring potential (MMP), are believed to represent movement execution and performance control, respectively [69][70].

Due to the role of MRCP in movement planning, researchers generally record the MRCP from EEG signals obtained from electrodes placed over the motor cortex, according to the international 10–20 System. The amplitude of MRCP is typically between 5 and 30 μV and the components of MRCP can be affected by the force and velocity of the forthcoming movement [71]. The low amplitude of MRCP compared to the normal EEG range makes it prone to be masked by brain activities with higher frequency bands [72]. Moreover, low

frequency motion artifacts and electrooculogram (EOG) locate on a similar frequency band as MRCP, but with much larger magnitudes.

2.3.1.3 Sensorimotor rhythms

The sensorimotor rhythm (SMR) is the oscillatory activity observed in electrical fields across the sensorimotor cortex. This rhythmic activity is characterized by its frequency, bandwidth, and amplitude. Within the SMR, two main components are prominent: the alpha rhythm and fluctuations in the beta range [73]. The SMR is primarily associated with the motor cortex, with contributions from somatosensory areas, where the beta and alpha components are thought to be related to motor functions and sensory processing, respectively. These dynamics can be observed in ERD during movement, movement imagery, and movement preparation, as well as in ERS following movement or during relaxation [74]. Initially, ERD is observed contralaterally to the limb involved in the movement, but as the movement progresses, bilateral ERD becomes evident [58].

The changes in alpha and beta frequencies exhibit temporal and spatial independence. The beta frequency is predominantly observed in the precentral (motor) cortex, while the alpha frequency is detected in the postcentral (somatosensory) cortex. However, the modulation of beta frequency during movement is not limited to the motor cortex alone. Connections between the motor cortex, SMA, inferior frontal gyrus, and parietal cortex also play a role in beta frequency modulation, influencing the accuracy of movement [75].

2.3.2 Brain Oscillatory Coupling

Neural assemblies operate at multiple spatial and temporal scales [76], highlighting the complexity of brain functioning. In the past, research on brain oscillations primarily focused on analyzing interactions within individual frequency bands and isolated brain regions. Considering the fact that specific neuronal structures have distinct preferred frequencies [77], and various brain regions are dominated by different frequencies [78], this approach offers insights into neural activities in particular frequency bands and brain regions, as well as certain aspects of physical and mental structures and functions. However, it presents a fragmented and incomplete picture of brain function. The primary focus of studies on the neural correlations associated with PD and FOG has also been aligned with this approach: examining individual frequency bands within isolated regions.

Research on brain oscillations has brought up a picture of coupled oscillators [78]. For the execution of complex tasks, coordinated flow of information within networks of functionally specialized brain areas is required. Neuronal oscillations are suggested to provide underlying mechanisms for this dynamic coordination in the brain [79]. Therefore, in recent years, there has been a shift in research focus towards studying brain oscillators as interconnected components within a larger system. This shift in the field has led to increased interest in functional mechanisms of neural interactions and brain oscillations to discover neural mechanisms underlying certain diseases. While the investigation of coupling principles and their functional significance remains an active area of research, two fundamental coupling

principles are believed to govern brain function: (i) amplitude modulation between any frequencies and (ii) phase coupling between frequencies [78]. Phase and power are mathematically two independent measures. In terms of brain oscillations, phase represents the timing of activity within a neural population and power reflects the number of neurons or the spatial extent of that population [52].

In the mammalian cortex, the power density of EEG or local field potential exhibits a distinctive inverse relationship with frequency (f), exemplified by a 1/f power pattern. This phenomenon signifies that the amplitude spectrum of EEG signals follows a power law that progressively decreases as the frequency increases. In fact, a wide range of physical signals,

$$S_x(f) = \frac{Constant}{|f|^{\gamma}} \qquad (2\text{-}1)$$

including EEG, originate from what is known as a 1/f process. Such signals demonstrate a power law relationship of the following form [80]:

where $S_x(f)$ is the power spectral density, f is the frequency and γ is some spectral parameter which is usually close to 1 but can lie in the range $0 < \gamma < 2$ [81]. The power-law scaling in the brain indicates a decrease in log power with frequency increase, a phenomenon consistent across all EEG signals and indicative of self-organization property of the brain. These properties of neuronal oscillators are the result of the physical architecture of neuronal networks and the limited speed of neuronal communication due to axon conduction and

synaptic delays [82] [83]. 1/f power relationship in the cortex implies that the phase of the slow frequency bands modulates the amplitude of the higher frequency bands and local events [82].

The hierarchical relationship between the phase of slower frequencies and the amplitude of higher frequencies, along with the synchronization observed across multiple brain regions, can be quantified using EEG connectivity measurements. Researchers employ various methods to study EEG connectivity, including power-based and phase-based approaches. Power-based methods examine the spectral power of EEG signals to identify brain regions that exhibit similar oscillatory patterns. On the other hand, phase-based methods focus on the phase relationships between EEG signals from different brain regions. In addition to power and phase-based measures, cross-frequency coupling (CFC) measures are used to quantify interaction between different oscillatory frequencies to provide a more comprehensive understanding of brain functions as a unified and integrated entity [55][84]. Basically, cross-frequency interactions among oscillations such as cross frequency phase synchrony (CFS) and PAC have gained attention as a plausible mechanism for the integration of information across distributed networks and the regulation of neuronal communication [64].

Phase locking value (PLV) , Phase Lag Index (PLI), Phase Slope Index (PSI), and Imaginary Coherence (ICoh) are other measures of phase connectivity [52]. PLV is a commonly used phase-based measure, which quantifies the consistency of phase differences between signals [52], identifying synchronized neural activity across brain regions.

Considering the aforementioned hierarchal relationship between the phase of the lower frequencies and the amplitude of the higher frequencies, PAC is the most common measure for quantifying CFC in physiological research [52][85][86]. PAC investigates the coupling between different frequency bands. This reflects computational and/or modulatory mechanisms that are qualitatively distinct from neural synchronizations achieved through PLV. Therefore, it provides additional insights into how different oscillatory rhythms interact and cooperate during information processing. PAC alterations have been reported in several brain disorders, including PD, which represent the importance of PAC in normal brain function and highlight its potential as a biomarker for understanding and diagnosing neurological conditions [87].

2.4 FOG Biomarkers

A biomarker is a quantifiable indicator of a biological process. The complexity of FOG, characterized by its episodic and multifactorial nature, causes significant challenges in its diagnosis, management, and treatment. Consequently, the recent shift in PD research towards introducing reliable biomarkers for FOG aims to uncover the underlying mechanisms, enhance diagnostic accuracy, and tailor individualized therapeutic strategies.

Existing biomarkers for FOG span across a wide range of methodologies, including clinical assessments, neuroimaging techniques, neurophysiological approaches, and the use of wearable sensor technologies [88][89][90][91]. Clinical scales, which mostly rely upon

subjective reports such as questionnaires, include motor and non-motor predictors like gait and balance deficits, cognitive changes, and sleep behavior disorders. While these subjective tools are beneficial, the need for objective biomarkers in clinical practice is undeniable. The objective measures not only facilitate monitoring the effects of interventions but also aid in categorizing patients, making them essential in managing FOG.

Recent advancements in objective biomarkers have been promising, particularly those derived from non-invasive techniques. Wearable sensors such as inertial measurement units (IMUs), accelerometers, gyroscopes, footswitches, and insole pressure sensors, have proven effective in providing biomarkers related to balance and gait [92][93][94][95]. This innovation represents a significant leap, offering an affordable and sensitive method for assessing FOG in clinical environments. Furthermore, neuroimaging techniques like MRI, and neurophysiological tools such as DBS and EEG, have shed light on the physiological processes and brain regions involved in FOG [96]. Structural MRI, for instance, has shown its potential in monitoring PD progression, revealing patterns of cortical thinning and occipital atrophy in patients [89]. Neural signals derived from DBS and EEG have highlighted abnormalities in brain oscillations, particularly in the beta, alpha, and theta bands, pinpointing the neural activities that coincide with FOG episodes.

While these advancements mark significant progress, the current methodologies are not without their challenges and limitations. Many of the laboratory tests, such as MRI or video-

based motion analysis systems, involve expensive and non-portable equipment, making them impractical for widespread clinical use or for multisite clinical trials. Similarly, while wearable sensors offer a significant advantage in terms of practicality and cost, they sometimes struggle to differentiate between voluntary stops and actual freezing episodes, and they often only detect FOG episodes post-occurrence [97]. On the other hand, the non-invasive nature of EEG, combined with its portability and cost-efficiency, especially when compared to MRI, position EEG as a favorable tool for both clinical and research settings. As such, integrating EEG biomarkers into the existing framework could be a transformative step in addressing the challenges posed by FOG in PD, ultimately leading to more effective therapeutic strategies.

2.5 Summary

FOG is a complex and multisystem symptom of PD that affects multiple structures of the central nervous system and particularly brain from the MLR in the brain stem to the cortical layers. Although BG is the main affected brain structure in PD, accurate and integrative interpretation of the EEG phenomena associated with FOG can reveal neural abnormalities both at the cortical and subcortical levels.

The focus of this thesis is to investigate and introduce EEG features associated with FOG in PD with a particular emphasis on novel features based on the amplitude, phase, and relationship between phase and amplitude in brain oscillations. Considering the reported abnormalities in the amplitude of different frequency bands related to PD and FOG, the study

of the phase interaction of neural oscillations, and the hierarchical relationship between the phase and amplitude of brain oscillations can provide integrated and meaningful features. These features have the potential to be used as biomarkers of FOG, control signals for BCI-based rehabilitative systems, and to optimize or augment current non-medication-based treatment options such as DBS, tECS, and TMS. Novel EEG features of FOG and FOG-related frequency modulations are investigated in MRCP frequency band as well as higher movement related frequency bands such as theta, alpha, and beta.

Chapter 3

Movement Related EEG Signatures Associated with Freezing of Gait in Parkinson's Disease: An Integrative Analysis

In this chapter, FOG-related EEG features associated with the morphology and the amplitude of MRCP, theta, alpha and beta frequency bands were investigated over (Pre-) SMA and primary motor cortex during a simple lower limb movement task in PD with FOG with different levels of severities and were compared with PD without FOG and healthy controls. The findings from this study were published in the Journal of Brain Communications under the title: "Movement-Related EEG Signatures Associated with Freezing of Gait in Parkinson's Disease: An Integrative Analysis" (Karimi F, Niu J, Gouweleeuw K, Almeida Q, Jiang N).

3.1 Introduction

Freezing of Gait (FOG) is a complex and disabling symptom in Parkinson's Disease (PD), defined as a transient and sudden episode of inability to produce effective stepping despite the intention of gait [98]. While dopaminergic treatments reduce the frequency and number of FOG episodes in most patients, the effectiveness of these treatment options is limited in PD patients with FOG, especially in severe cases, making it a challenging healthcare problem in PD [14][99][100][101][102]. Although various methodological approaches have offered some insights, the underlying mechanism of FOG is still poorly understood due to its

complexity and paroxysmal nature [33][99][103]. More recently, the focus of PD research has moved toward investigating dysfunction of all networks that involve basal ganglia (BG), including cerebellum and cortex, rather than focussing solely on the BG itself [104]. For over-learned skills such as walking, most aspects of motor function are controlled at the cortical level, and the BG's involvement is largely restricted to the regulation of movement gain [105]. At the cortical level, the pre-SMA along with SMA, and primary motor cortex (M1) are some of the main components of the locomotor network involving direct and indirect pathways between the BG and the cerebral cortex, which contribute to movement planning and execution [33]. Therefore, measuring activities of these areas prior, during, and following lower limb movements in PD patients without FOG along with PD patients with different severities of FOG, may reveal abnormalities underlying FOG.

Movement-related cortical potential (MRCP) is a type of EEG modality, which starts approximately 1.5 to 2 seconds prior to a voluntary movement onset, with the frequency band and amplitude of 0 to 5 Hz and 5 to 30 μv, respectively. Considering the prominence of BG thalamocortical projections onto (pre-)SMA, alternations in different components of MRCP might be associated with features of FOG. Time course and amplitude of MRCP sub-components including Bereitschaftspotential (BP) or contingent negative variation (CNV), in case of externally-cued movements, motor potential (MP), and movement-monitoring potential (MMP) can be influenced by psychological status and the characteristics of the

movement, such as level of movement intention, speed, precision, and movement repetition [68][71][106]. NS1 (negative slope of early BP (BP1)) and NS2 (steeper negative slope of late BP (BP2)) are two components of BP that precede the movement onset and reflect the activation of (pre-)SMA and M1, respectively [68][69][71][107][108]. Various studies have investigated MRCP in the healthy population and in PD, mostly during upper limb movements and some lower limb movements [109][110]. However, discrepancies in changes in NS1 and NS2 still exist under different interventions [107][108][111][112][113][114][115]. While increased NS1 was reported in PD patients after dopaminergic treatments; it does not influence NS2 by short-term dopaminergic treatment options [116]. On the other hand, chronic administration of L-dopa results in increased NS2 rather than NS1 [117]. NS1 was found to increase with neurofeedback treatment in both PD patients and healthy controls, while increased NS2 was achieved after pallidotomy in PD patients [118][119]. More detailed comparisons between treatment results on BP and CNV were found by using deep brain stimulation (DBS). CNV was increased during DBS; however, no difference was shown in BP [120][121]. Most studies on BP in PD involve the upper-limb movements, and, to the best knowledge of the authors, there is no research which investigates FOG with lower-limb MRCP. BP from PD patients off medication was compared with controls during gait initiation and foot movement in a sitting position [110]. Higher BP amplitude was reported when initiating a gait than moving a foot in a seated position in healthy controls, while BP amplitude in PD does not show such a difference. The same experiment was replicated by another study to explore the

relationship between BP and gait initiation failure (GIF), which is similar to the FOG symptom in PD [122]. A decreased BP amplitude was reported in GIF patients but not with PD patients, which was regarded as an important piece of evidence to the different underlying mechanisms of GIF and PD.

Event-related (de)synchronization (ERD/ERS) of different brain oscillations are other EEG features related to movement planning and execution [66]. Beta frequency band (12-35 Hz) activities have been linked to motor function at the cortical level as well as in the subthalamic nucleus (STN) and globus pallidus interna (GPi) [123]. Beta band ERD/ERS has been widely investigated in PD both at cortical and subcortical levels, and increased beta activities over the motor cortex were reported in numerous studies on PD [124][125][126][127][128]. Beta synchronizations in the STN lag beta activities in frontal and motor cortical areas with stable but different time delays in different cortical areas in PD [124]. This time delay is also different for the low and high beta frequency bands. In recent studies with PD patients with FOG and akinetic-rigid motor symptoms, abnormal dopamine resistant high beta band (21-35 Hz) activities were reported in the STN, suggesting a relationship between FOG and beta frequency sub-bands [17][124]. Maximal coherence in the high-beta activity was located in the midline cortex corresponding to the SMA, cingulate cortex, and leg area of M1. In contrast, low-beta coherence was highest in the lateral M1 region [17]. Increased beta frequency activities, especially high beta frequency range, in the STN is associated with the onset of FOG episodes [129]. In addition to abnormal beta band activities in PD, excessive

theta band (4-8 Hz) activities, which are associated with cognitive functions, were reported in central and frontal leads during FOG episodes, which, in turn, are associated with coupling between the pre-SMA and dorsal anterior cingulate [128]. Brain dynamics alternations before and during FOG episodes have been explored in a number of cortical studies that use EEG to identify neural biomarkers for detection and prediction of freezing episodes [15].

FOG as a complex multi-system lower body symptom in PD requires a deeper understanding of the underlying mechanisms of this phenomenon both at the cortical and subcortical level. New techniques and advancements in EEG, which is a non-invasive portable technology, can be used for identification of reliable biomarkers. Understanding the abnormal cerebral activities related to FOG not only provides insights into the underlying mechanism of FOG and possibly more medication-based treatments and therapeutic interventions such as adaptive closed-loop DBS but may also offer recently emerged treatment or rehabilitation options based on a brain-computer interface (BCI), transcranial magnetic stimulation (TMS), and transcranial direct current stimulation (tDCS).

In the current study, multiple EEG features of (pre-)SMA and M1 are investigated in PD with and without FOG, as well as for different severities of FOG, which are compared with healthy controls during a simple cued lower limb motor execution task.

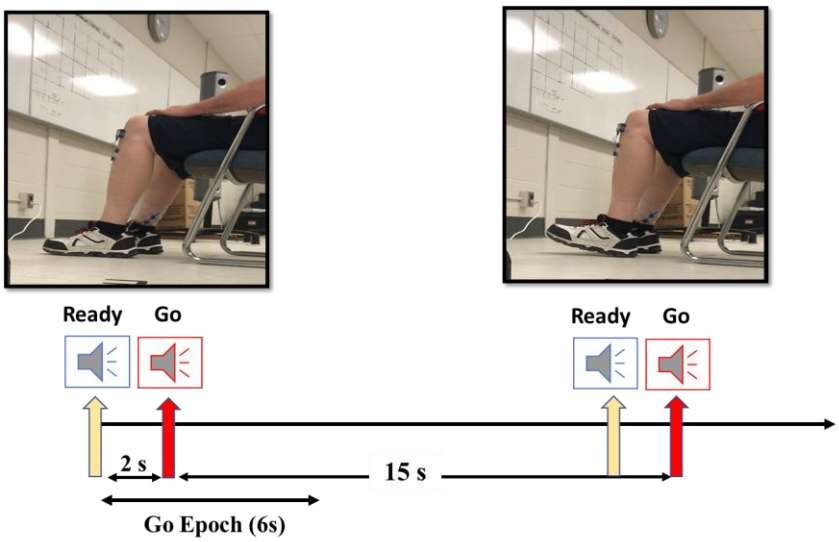

Figure 3-1. Time course of the auditory cues and 'Go' epoch for one trial of the experimental protocol.

3.2 Materials and Methods

3.2.1 Participants

This study involved 14 PD patients without FOG, 14 PD patients with FOG, and 13 age-matched healthy participants (PD without FOG: mean age = 77 years, range = 65–87 years, 3 females; PD with FOG: mean age = 74 years, range = 63–90 years, 1 female; controls: mean age = 77 years, range = 68–89 years, 3 females). The PD patients were recruited from the Movement Disorders Research and Rehabilitation Center at the Wilfrid Laurier University (MDRC; Waterloo, Ontario). Participants with any head trauma, neurological disorder, serious

vision or hearing problems, and severe movement control limitation such as dyskinesia were excluded. All patients were in their optimally medicated state to avoid the confound of exacerbated motor symptoms. Patients were assessed based on the Unified Parkinson's Disease Rating Scale (UPDRS).

PD patients with FOG were identified by the answer to question 14 in MDS-UPDRS-III (motor subsection), which confirms the presence of FOG. In addition, an experienced clinician reconfirmed the occurrence of FOG before each experiment session [130]. The procedure involved a modified Timed Up and Go (TUG) test where the participant would have started from a seated position, raised themselves out of a chair with arms across their chest, walked approximately 3 m but through a door way into an adjacent clinic room that was cluttered with other desks and chairs, then returned to in front of their chair where they completed degree turns in both the left and right directions, before sitting back down. The goal of the study was to investigate the motor cortical abnormalities associated with FOG and its severity on (pre-)SMA and M1. For this purpose, various features of MRCP and brain oscillations of PD with different degrees of FOG are compared with healthy controls as well as PD without FOG.

PD patients with FOG were divided into two subgroups of PD with mild and severe FOG. Severe freezers were defined as those who experienced observable FOG episodes whenever walking or turning that severely affect their daily activities and independence, while mild freezers were defined as those who experienced FOG occasionally when provoked only during

more complex tasks such as turning (based on patient history). In addition, the participants were instructed to perform 20 trials of videotaped walking tasks on a 10-m walkway. Participants were asked to walk after hearing an auditory "go" cue. PD with FOG who experienced FOG episodes longer than 3 seconds during turning or normal walking were considered PD with severe FOG. The videotaped walking tasks were used to determine the dominant foot for each participant.

Healthy participants were recruited from The Waterloo Research in Aging Participant (WRAP) pool at the University of Waterloo. The sample size was determined by availability of PD patients. The study was approved by the Research Ethics Board at the University of Waterloo and Wilfrid Laurier University. A written informed consent form was obtained from each participant prior to the experiment, according to the Declaration of Helsinki.

3.2.2 EEG and EMG Recordings

EEG data were recorded using a 32-channel wireless EEG system (g.Nautilus, Guger Technologies, Austria). EEG signals were sampled at a sampling rate of 250 Hz. EEG data were collected from 17 channels following 10-20 international standard positions: FP1, FP2, AF3, AF4, F3, Fz, F4, FC1, FC2, C3, Cz, C4, CP1, CP2, P3, Pz, and P4. The reference electrode was placed on the right ear lobe.

For all individuals, the EMG was acquired using an 8-channel TELEMYO 2400 system (NORAXON INC). Four wireless EMG sensors with a sampling frequency of 1000 Hz were placed on the tibialis anterior (TA) and soleus muscles (SOL) on both legs.

3.2.3 Experimental Procedures

All participants were invited to the MDRC for the experimental sessions. For PD patients, the respective clinical assessment (which included UPDRS-III to confirm motor symptom severity) was performed within two weeks of the experimental session. During the experiment, participants were instructed to perform ankle dorsiflexion (ADF) (e.g., lifting the toe) at their normal pace to the maximum possible contraction with the dominant foot while sitting in a comfortable chair with their arms rested in armrests. The participants were asked to release their toes after reaching the maximum contraction. To minimize eyes or head movements and reduce the cognitive load unrelated to the cues, they were asked to look at the center of a black '+' sign on a white background. One session with 15 trials was recorded for each participant, with an interval of 15 s between every two trials. Participants were expected to prepare for the task when they heard 'ready' and execute ADF when they heard the 'go' cue. The 'ready' and 'go' auditory cues, with a 2 s interval, were played for each trial through a speaker with a computer-generated voice. In this study, 'Go' epochs, which contain the signal from 2 s before the movement onset to 4 s after the onset, were analyzed to evaluate the cortical

Table 3-1. Mean ± standard deviations for participant demographics and clinical characteristics.

Parameters	HC	PD without FOG	PD with FOG	PD with mild FOG	PD with severe FOG
N (male/female)	13 (10/3)	14 (11/3)	14 (13/1)	7 (6/1)	5 (5/0)
Age(year)	77.61±5.65	74.5±6.67	77.64±7.41	76.7±7.5	79.6±1.14
Disease duration (year)	N/A	8.07±5.18	9.64±5.49	11±5.74	7.8±5.11
UPDRS-III	N/A	28.66±7.16	31.65±12.12	34.21±12.7	28±6.85
LED (mg/day)	N/A	449.42±358.59	639.71±419.72	585.8±265.7	969±468.03

Abbreviations: HC, Healthy Controls; UPDRS-III, Unified Parkinson's Disease Rating Scale–III; LED, Levodopa Equivalent Dose.

activities during movement preparation and execution (Figure 3-1 represents the time course of the auditory cues and extracted 'Go' epochs).

3.3 Data Processing

EEG and EMG data were analyzed offline after the experiment session using a customized Matlab function (Mathworks, USA R2020a). EMG signals recorded from the TA muscles of the dominant foot (EMG-TA) were used to identify onset timings of the ADF. EMG-TA was initially filtered using a second-order Butterworth band-pass filter with the bandwidth between 20 Hz and 120 Hz, then down-sampled to 250 Hz to maintain consistency with the EEG data. To enhance the detection accuracy of the movement onset, the Teager–Kaiser Energy Operator (TKEO) was applied to the EMG data [131]. Finally, a threshold value was manually selected for each subject to determine the movement onset. This threshold was maintained below 20 percent of the peak amplitude of the EMG-TAThe onset of the muscle activity was identified visually as the point in time where the amplitude of the EMG signal after TKEO clearly increased from baseline after the auditory "go" cue.

For EEG processing, two different pre-processing paths were performed to analyze MRCP and brain oscillations levels. To analyze the MRCP, the EEG data was initially band-pass filtered by a third-order Butterworth filter between 0.05 Hz and 5 Hz. In order to avoid phase distortions, zero-phase forward and backward filtering procedure was used. The filtered EEG data was processed by the extended infomax independent component analysis (ICA) algorithm using the *EEGLAB* function *"runica.m"* (MATLAB, CA, US). Source components containing eye blinks, severe head motion, or EMG artifacts were manually removed by visual inspections of the scalp topographies and waveforms [132]. In order to minimize bias, two independent experts identified artifactual components, and only components that were identified by both experts were removed. Lastly, trials with the peak amplitude of negativity on Cz channel outside the range of [-1.5, 2] s with respect to movement onset were removed as outliers.

For brain oscillations, similar to MRCP, EEG was first filtered by a third-order Butterworth filter between 0.05 Hz and 50 Hz, followed by ICA to remove artifactual components. For generating ERD/ERS time-frequency representation, small Laplacian filters were applied on Cz, Fc1, and Fc2 to reduce the effect of volume conduction [133]. Laplacian spatial filter was implemented by subtracting the averaged signal of the four surrounding orthogonal electrodes from the center electrode. The time-frequency representations of the power were computed using Morlet wavelets with five cycles between 1 Hz and 50 Hz, and ERD was calculated with a baseline from -4 s to -2 s [133][134]. The outliers were discarded

from further analysis based on the excessive muscle activities in both leg muscles before the auditory “go” cue, EMG activity in the opposite leg during the motor task, and head motion detected by Inertial Measurement Unit (IMU) mounted on participant’s neck. A total number of 122±2 trials in each group was used for oscillatory analysis. For participants whose left leg was dominant, the EEG channels on the left and right sides were switched during the analysis.

3.3.1 MRCP Features

Five features of MRCP over M1 (Cz channel) were studied on a single trial basis: 1) peak amplitude of negativity, 2) time course of the peak negativity, 3) NS1, 4) NS2, and 5) MRCP rebound rate [135]. EMG features include peak amplitude of the EMG-TA, the delay between peak amplitude negativity of MRCP, and peak of EMG-TA. In each trial, the peak amplitude of negativity from MRCP was defined as the lowest value between -1 s and 1.5 s with respect to the movement onset. NS1 was calculated as the difference between the amplitude of the signal 1.4 s before the peak negativity and the amplitude computed 0.4 s before peak negativity, divided by 1 s. NS2 was calculated as the difference between the amplitude of the signal 400 ms before the peak negativity and the amplitude of peak negativity, divided by 0.4 s. The rebound rate of the MRCP was calculated as the difference between the amplitude of the potential at 1.5 s after the peak negativity and the peak amplitude of negativity, divided by 1.5 s [135].

Table 3-2. Ages for all participants and UPDRS scores, duration of disease, and LED for all PD patients in each group:

Participant type	code	Gender (Male/Female)	Age	duration of disease (year)	UPDRS-III	LED
PD without FOG	1 *	M	77	6	42	100
	2	M	75	1	22	0
	3	F	87	5	37	400
	4	M	68	6	26	100
	5	F	74	7	36	100
	6	M	84	15	22	368
	7	M	65	13	18	1100
	8	F	68	4	35	700
	9	M	80	6	21	325
	10	M	75	17	35	600
	11	M	77	7	30	1000
	12	M	69	17	17	799
	13	M	66	5	29	100
	14 *	M	78	4	31	600
PD with FOG m: mild FOG s: severe FOG	1	M	89	4	49	100
	2 *	M /m	76	7	17	550
	3	M /m	80	21	38	600
	4	M / s	81	16	25	1520
	5	M /m	78	15	37	701
	6	M / s	80	8	25	1100
	7	M	63	15	13.5	900
	8	F /m	68	6	34	600
	9 *	M /s	79	3	20	1000
	10	M /s	80	4	33	1000
	11	M /m	90	7	58	100
	12	M /m	77	7	31	1000
	13	M /m	68	14	25	550
	14	M /s	78	8	37	225
Healthy Controls	1	M	83	N/A	N/A	N/A
	2 *	M	76	N/A	N/A	N/A
	3	M	77	N/A	N/A	N/A
	4	F	83	N/A	N/A	N/A
	5	M	68	N/A	N/A	N/A
	6	M	79	N/A	N/A	N/A
	7	M	68	N/A	N/A	N/A
	8	F	72	N/A	N/A	N/A
	9	M	80	N/A	N/A	N/A
	10	M	78	N/A	N/A	N/A
	11	M	89	N/A	N/A	N/A
	12	F	78	N/A	N/A	N/A
	13	M	78	N/A	N/A	N/A

*** Dominant foot of subjects with * is the left foot.**

3.3.2 Statistical Analysis

Demographic and clinical characteristics were analyzed using independent samples t-tests and one-way analysis of variance (ANOVA). To investigate the effect of FOG and its severity on features of MRCP, one-way ANOVA with a significance level of 0.05 was carried out to compare MRCP features across participant groups. To assess main effect of groups, ANOVA with three levels of group factors: Healthy, PD without FOG, and PD with FOG was

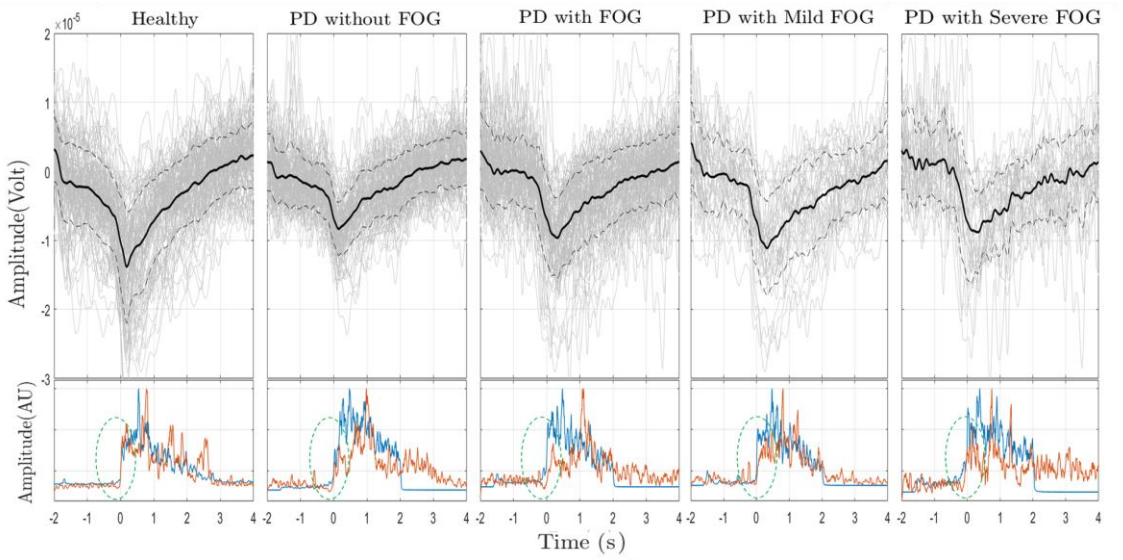

Figure 3-2. Average MRCP over 'Go' epochs from Cz channel and normalized EMG signal from TA and SOL muscles. In each group, the top plots are the epoch averages of 'Go' epochs. The thick solid line is the average over all trials, and thinner gray lines are the single trials for all subjects. The dashed lines indicate the average standard deviation in each case. In the lower row of each group, the average of the normalized EMG signal over all trials for the TA muscle (blue line) and SOL muscle (red line) are presented over the time course of the 'Go' epoch. Dashed green oval includes the time of the activity onset in TA and SOL muscles.

conducted on the data. To compare the effect of FOG severity on MRCP features, the group factor included: Healthy, PD with mild FOG, and PD with severe FOG. When a significant main effect was found, Tukey's test was used as a post-hoc test. Regarding the time-frequency representations of ERD/ERS with significant areas, significant time-frequency areas were calculated using the bootstrap re-sampling method for each group. A permutation test was applied to calculate the significant time-frequency areas when analyzing the difference between groups [136][137]. All statistical analysis was performed in Matlab 2020 a.

3.3.3 Data Availability

All derived and anonymized individual data are available at http://ieee-dataport.org/documents/fog-severity-eegemg [138].

3.4 Results

Demographic and clinical characteristics are presented in Table 3-1. Healthy controls, PD without FOG, and PD with FOG groups were matched for age (F (2,39) =1.1, P=0.3). PD without FOG and PD with FOG were also matched for UPDRS, levodopa equivalent dose (LED), and disease duration (P= 0.4, P=0.2, P=0.4, respectively). Also, PD with mild and sever FOG groups did not differ in age (P=0.4), severity of motor symptoms (UPDRS-III: P=0.4),

LED (P=0.07), disease duration (P=0.3). Individual participant details of all participants are presented in Table 3-2.

3.4.1 MRCP Features Are Associated with the Severity of FOG

The average MRCP of 'Go' epochs and standard deviation of each group for the Cz channel with background single trials within each group are presented in Figure 3-2. Normalized average EMG signals (with respect to EMG-TA) from the TA muscle (blue line) and SOL muscle (red line) over the 'Go' epoch are also shown in the lower row. Visual

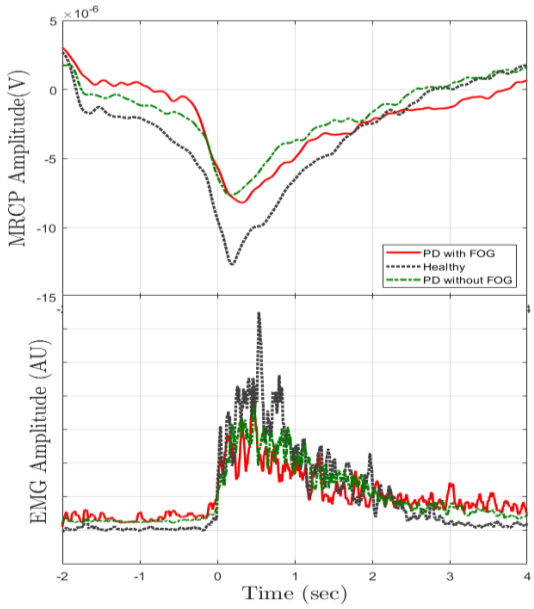

Figure 3-3. Averaged MRCP over 'Go' epochs from healthy controls and PD groups from Cz channels and the corresponding average EMG-TA. In each plot, the black dotted line, the green dashed line, the red solid line, the light blue solid line, and dark blue solid line represent the epoch average for healthy control, PD patients without FOG, and PD patients with FOG groups, respectively.

Table 3-3. Mean ± standard deviations of MRCP features over Cz, significant test statistics are marked with "*"," **", "***", "****", "*****" for different group effects.

MRCP Features	Three main groups			PD with FOG	
	HC	***PD without FOG***	***PD with FOG***	***Mild FOG***	***Severe FOG***
Peak amplitude of negativity over Cz	-16.1±7.4	-10.5±3.8*	-12.6±5.7	-13.6±6.2	-13.7±6.1
Peak amplitude of EMG-TA	946.5±274.2	737.3±319.3**	691.6±399.6***	825.5±401.7	512±221.9*****
Latency between MRCP peak and EMG-TA peak	-22.7±110.5	-67.8±121.5*	-28.4±92.3	-13.2±97.7	-35.6± 109
Time of the peak negativity over Cz	338.9±87.1	335.8±93.6	349.2±89.4	358.3±82.2	360.1±120.1
Time of the peak of EMG-TA	361.7±80.2	403.7±95.8**	377.6±71.03	371.6±57	395.8±93
NS1 of Cz	-3±5.3	-1.7±3.7	-0.8±4.7***	-1±4	-0.6±6.3****
NS2 of Cz	-12.8±11.3	-10.5±0.9	-14.4± 14.9	-13.2±12	-18.6±21.2
Rebound rate Cz	3.4±4.6	2.8±3.3	2±4.8	1.2±4.7	2.5±6.2

*** p<0.05 *PD without FOG* vs HC and *PD with FOG***
**** p<0.05 *PD without FOG* vs HC**
***** p<0.05 *PD with FOG* vs HC**
****** p<0.05 PD with severe FOG vs HC**
******* p<0.05 PD with sever FOG vs HC and PD with mild FOG**

inspections shows that the largest NS1 was observable in healthy controls and the lowest NS1 belonged to the PD with FOG and especially PD with severe FOG group. The amplitude of MRCP from PD patients, especially PD without FOG, was generally lower than healthy controls. However, it should be noted that the amplitude of the EMG signal from TA muscle seems to be consistent with MRCP amplitude (Figure 3-3 represents the relative MRCP and EMG amplitude for healthy, PD without and with FOG). A time delay between the onset of TA and SOL muscle activation was also observable in the PD with FOG group, which is visualized by the dashed green oval in Figure 3-2. MRCP features for all groups are reported in Table 3-3. Comparison between healthy, PD with and without FOG, results from the one-way ANOVA showed that the amplitude of peak negativity at Cz, the NS1, the amplitude of EMG-TA, the time of EMG-TA peak, and latency between MRCP peak and EMG peak were

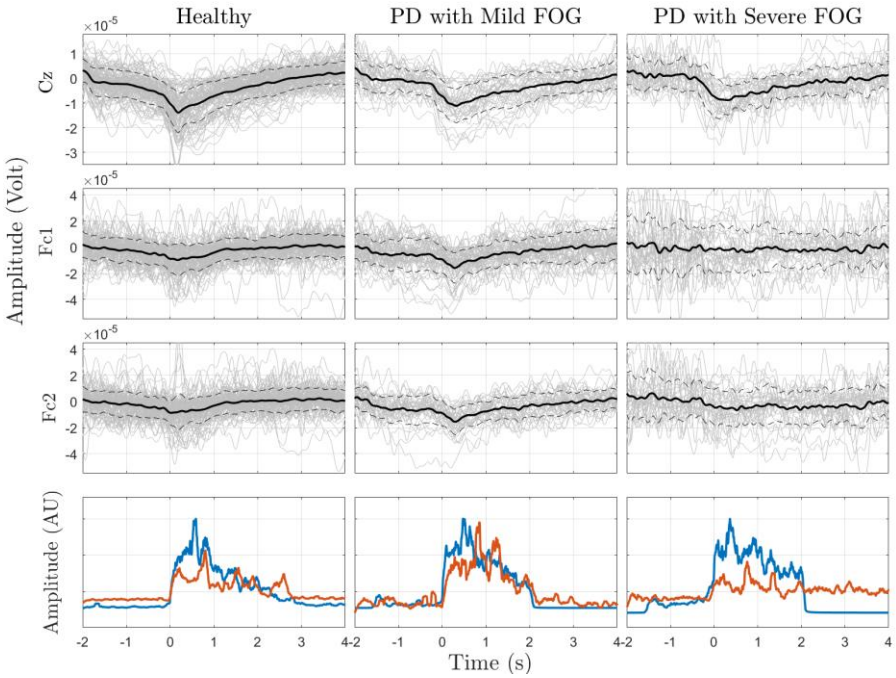

Figure 3-4. Average MRCP over 'Go' epochs from Cz, Fc1, and Fc2 channels and normalized EMG from TA and SOL muscles for healthy controls, and PD with mild and severe FOG. In each group, the top plots are the MRCP averages of 'Go' epochs. The thick solid line is the average over all trials, and the other thinner gray lines are the single trials for all subjects. In the lower row of each group, the average of EMG signal over all trials for TA muscle (blue line) and SOL muscle (red line), respectively. The dashed lines indicate the average standard deviation in each case.

significantly different among groups (peak negativity at Cz: $F(2,284) = 22.2$, $P < 0.001$, NS1: $F(2,284) = 5.8$, $P = 0.003$, amplitude of EMG-TA : $F(2,284) = 16.2$, $P < 0.001$, time of the peak of EMG-TA: $F(2,284) = 6.3$, $P = 0.002$, latency between MRCP peak, and EMG peak: $F(2,284) = 4.8$, $P = 0.008$). The multiple comparison tests indicated that the peak negativity over Cz in PD without FOG is significantly lower than healthy controls and PD with FOG ($P=0.01$, $P=0.03$, respectively). The comparison tests also showed that the NS1 from PD with

FOG was significantly lower than the NS1 from the healthy controls (P=0.002). Amplitude of EMG-TA from healthy participants were significantly higher than the PD with and without FOG (P < 00.1). The time of the EMG peak from healthy and PD without FOG was also significantly different (P = 0.001). Latency between MRCP peak and EMG peak of PD without FOG was significantly higher than healthy controls and PD with FOG (P =0.01, P=0.03, respectively). In contrast, NS2, rebound rate and the time of the peak negativity over Cz were not significantly different across the three groups: healthy, PD with FOG, and PD without FOG.

One-way ANOVA for features of MRCP over Cz for healthy participants, PD with mild, and severe FOG found significant differences for NS1 and amplitude of EMG-TA (F (2,166) =3.65 , P= 0.02) ; (F(2 , 166)= 25.1, P < 0.001), respectively. The multiple comparisons showed that NS1 from the PD with severe FOG group was significantly lower than the healthy group (P=0.02). Peak amplitude of EMG-TA from PD with severe FOG was significantly lower than both healthy and PD with mild FOG (P < 0.001). In contrast, NS2 and rebound rate were not significantly different across healthy, mild FOG, and severe FOG. Although the time

Table 3-4. Coefficient of Variation for three channels over M1 and (pre-)SMA

Coefficient of Variation of different channels	**Three main groups**			**PD with FOG**	
Name of the channel	***HC***	***PD without FOG***	**PD with FOG**	***Mild FOG***	***Severe FOG***
FC1	3.9	5.3	4.8	2.5	12.6
FC2	5.3	5.3	3.9	2.1	7.1
Cz	1.9	2.5	2.6	2.0	3.2

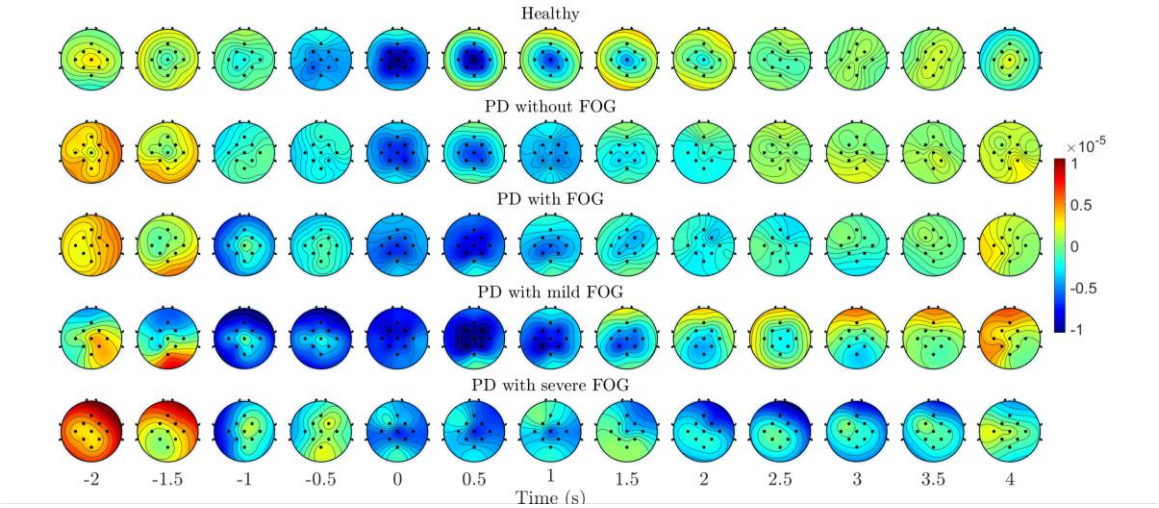

Figure 3-5. Topographic maps of five groups. Topographical plots of Healthy controls, PD patients with FOG, PD patients without FOG, PD patients with mild FOG, PD patients with severe FOG over MRCP frequency range. The voltages (Unit: Volt) of 9 electrodes are represented as different colors in topographical maps. Different topographical maps along 13 time points between -2 s and 4 s with an interval of 0.5 s.

course of peak negativity was not significantly different among groups, direct observations show that the standard deviation (SD) of PD patients with severe FOG was higher among the three groups resulting in a flatter peak negativity for this group. Direct observations also show that inconsistency between the onset of EMG activities from the TA and SOL muscles were present in PD patients with severe FOG, while absent in the other groups (the onset of EMG activities is marked with green dashed ovals). In Figure 3-4 the average MRCPs are presented for healthy, PD with mild, and severe FOG for three channels: Cz, FC1, and FC2. The most prominent difference between PD with severe FOG and healthy as well as PD with mild FOG

in MRCP frequency range, was that the averaged amplitude of the signal over (pre-)SMA (Fc1 and Fc2) were lower in the PD with severe FOG group compared to the two other groups. This difference could be a result of lower temporal consistency across trials in PD with sever FOG in (pre-)SMA. PD with severe FOG group showed less temporal consistency across trials especially over the contralateral channel (Fc1). To quantify the temporal variations of the signals over (pre-)SMA and M1, the coefficient of variation of the instantaneous potential, the standard deviation divided by mean value, was calculated and presented in Table 3-4 for all groups. The results confirm the higher temporal variation of the signals in PD with severe FOG, particularly over (pre-)SMA compared to other groups.

Figure 3-5 represents the spatiotemporal grand average of MRCP amplitude representation for all groups over 'Go' epochs from Cz. Despite healthy controls and PD without FOG, PD with different levels of FOG did not show activities over Cz at the time of the 'ready' cue (t = -2 s). Additionally, PD with sever FOG did not represent any localized activity over Cz before movement onset (t=0 s), while PD with mild represent localized activities over Cz during preparation period. PD with sever FOG also represented overactive frontal and parietal cortices during movement.

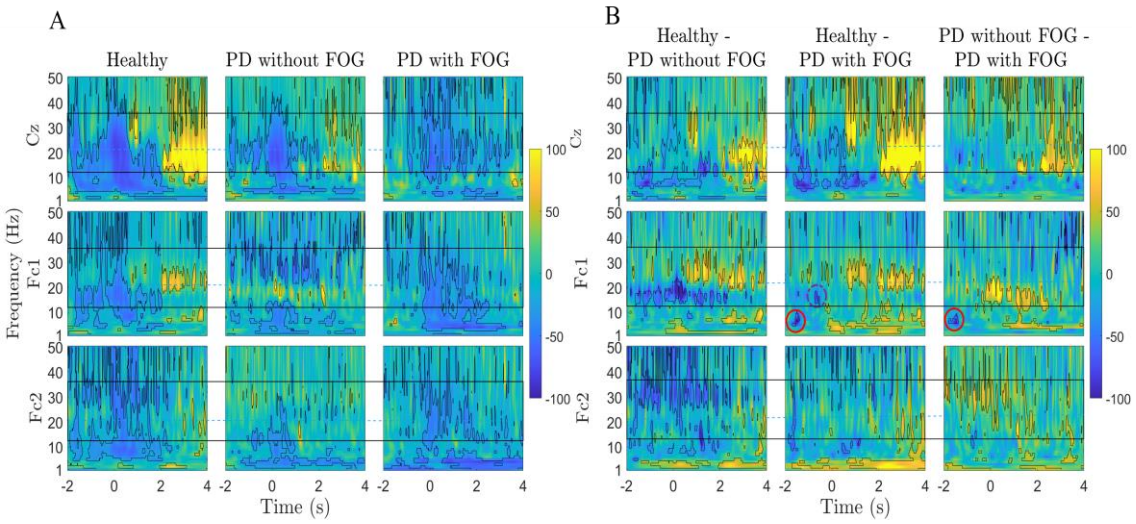

Figure 3-6. Group differences in movement related spectral power changes of healthy controls, and PD without and with FOG. Time-frequency representations of ERD/ERS and ERD/ERS differences in three channels (Cz, Fc1, Fc2) of three groups: Healthy controls, PD patients without FOG, and PD patients with FOG. In plot A, ERD/ERS indicating percentage change relative to baseline of -4 s to -2 s are represented as blue/yellow colors, respectively between 1 Hz and 50 Hz from -2 s to 4 s. significant areas are calculated with bootstrap re-sampling methods ($p < 0.05$) and outlined by black contours. In plot B, time-frequency representations of ERD/ERS differences in three channels (Cz, Fc1, Fc2) among three groups, indicated as 'Healthy - PD without FOG', 'Healthy - PD with FOG', 'PD without FOG - PD with FOG'. The solid black rectangle indicates the beta band frequency range, and the blue horizontal line separates low and high beta band frequency range, (12-21 Hz) and (21-35 Hz) respectively. Red and purple dashed circles indicate theta and low beta activity differences between PD with FOG and other groups, respectively.

3.4.2 Theta, Low Beta, and High Beta Frequency Bands Are Associated With FOG

In Figure 3-6, the time-frequency representations of the EEG signal between 1 Hz and 50 Hz of small Laplacian filtered Cz, Fc1, and Fc2 channels are presented for healthy controls, PD with FOG, and PD without FOG (figures without permutation-corrected statistical significance are presented in Figure 3-7). Over Cz, healthy participants show continued low beta band ERD before the onset of the movement as well as high beta ERD at the time of the

'ready' cue and during movement execution. PD patients without FOG presented a similar but lower low beta and high beta frequency band ERD pattern. In the PD with FOG group, the low beta ERD was highly suppressed and partially replaced by beta ERS during movement preparation and beta band ERD was interrupted during motor execution. In PD patients with FOG, some levels of theta ERS were also present prior to the movement onset over both Cz and Fc1. In addition to pre-movement differences over Cz, beta ERS was present 2 s to 4 s after movement in healthy participants, while PD patients did not show such ERS over the same time course, especially PD with FOG.

In Fc1, which was basically the contralateral channel, the distinct and contrasting high beta and low beta band activities were observable across groups. Low beta ERD during movement preparation were completely missing in PD with FOG. On the other hand, in PD without FOG, continuous low beta ERS was spanned over the whole time course of the epoch and unlike other groups, no low beta ERD was present over this channel, during movement execution. In both PD groups, high beta band ERD was observed during movement preparation and execution. This similarity might suggest a compensatory mechanism in PD.

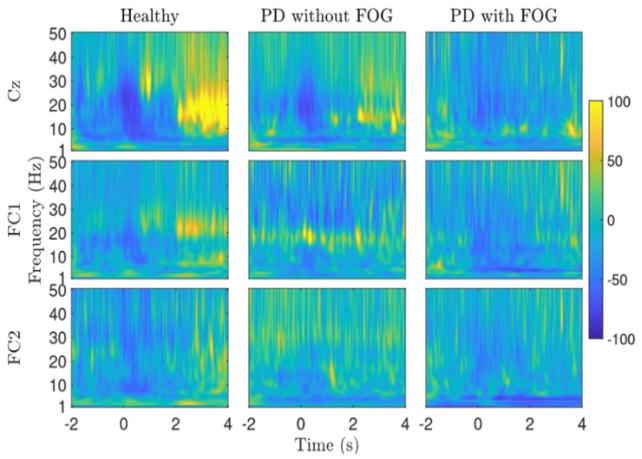

(a) Time frequency representation of ERD/ERS

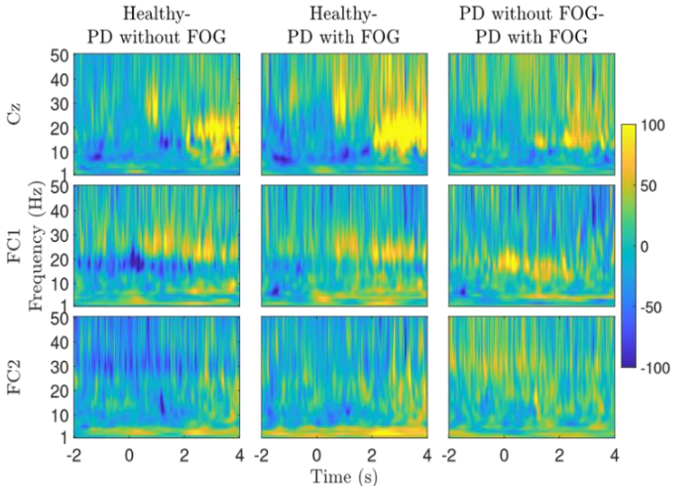

(b) Time frequency representation of ERD/ERS difference

Figure 3-7: Time-frequency representations of ERD/ERS and ERD/ERS differences in three channels (Cz, FC1, FC2) of three groups: Healthy controls, PD patients without FOG, and PD patients with FOG. In plot (a), ERD/ERS indicating percentage change relative to baseline of -4 s to -2 s are represented as blue/yellow colors, respectively between 1 Hz and 50 Hz from -2 s to 4 s. In plot (b), time-frequency representations of ERD/ERS differences in three channels (Cz, FC1, FC2) among three groups, indicated as 'Healthy - PD without FOG', 'Healthy - PD with FOG', 'PD without FOG - PD with FOG'.

In Fc2, the ipsilateral channel, the low beta ERD before the movement was more interrupted compared to Cz and Fc1 in healthy participants. In the healthy group, repetitive high beta ERD before movement was missing in PD groups. Figure 3-6 (B) represents differences between every two groups. Healthy controls and PD without FOG group did not show significant differences in beta frequency band before movement over Cz. However, PD without FOG represented delayed high beta ERD over Cz at movement onset. The healthy group and PD with FOG show significant differences in low beta activities, especially before movement. Healthy and both PD groups shared similar differences in the theta frequency band. Significant differences over Fc1, confirmed strikingly distinct high beta and low beta band activities when comparing groups.

Low beta frequency band represented main differences between PD without FOG and other group. Theta ERS before movement onset in PD with FOG represents significant difference between PD with FOG with other groups (marked with a red solid circle). Additionally, a brief significantly different low beta ERS is also observable before movement initiation in PD with FOG compared to healthy controls (marked with a purple dashed circle).

In Fc2, healthy and PD with FOG share similarities, while high beta activities represent the main difference between PD without FOG with the other two groups. In Figure 3-8, the time-frequency representations of the EEG signal between 1 Hz and 50 Hz on Cz, Fc1, and

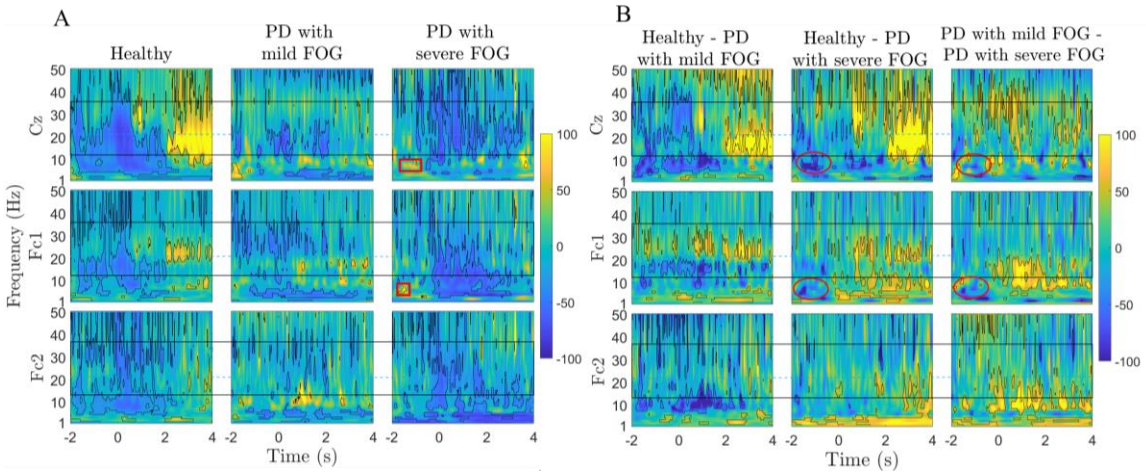

Figure 3-8: Group differences in movement related spectral power changes of healthy controls and PD with different FOG severities. Time-frequency representations of ERD/ERS in three channels (Cz, Fc1, Fc2) of three groups: Healthy controls, PD patients with mild FOG, and PD patients with severe FOG. In plot A, ERD/ ERS indicating significant areas relative to a baseline of -4 s to -2 s are represented as blue/yellow colors, respectively between 1 and 50 Hz from -2 s to 4 s. significant areas are calculated with bootstrap re-sampling methods ($p < 0.05$) and outlined by black contours. In plot B, time-frequency representations of ERD/ERS differences in three channels (Cz, Fc1, Fc2) among three groups, indicated as 'Healthy - PD with mild FOG', 'Healthy - PD with severe FOG', 'PD with mild FOG - PD with severe FOG'. significant areas are calculated with a permutation test (p-value = 0.05) and outlined by black contours. The solid black rectangle indicates the beta band frequency range, and the blue horizontal line separates low and high beta band frequency range. Red ovals show theta band activities.

Fc2 are presented for healthy controls and FOG with different severities (figure without permutation-corrected statistical significance are presented in Figure 3-9).

Theta and low beta ERS before movement represent common frequency activity patterns for both FOG severities compared to healthy controls. Theta ERS represented a longer time course during movement preparation in PD with severe FOG compared to PD with mild FOG (theta ERS is marked with red rectangles). The high beta frequent synchrony in mild FOG over

Cz represents a unique feature of this group over Cz. In Fc1, similar to PD without FOG, PD with mild FOG showed excessive high beta ERD before movement, continuous low beta synchrony over the whole epoch, which might be related to tremor in PD with mild FOG. Theta ERS over Fc1 during movement execution was a shared feature between PD with mild and severe FOG groups.

Figure 3-8 (B) represents the time-frequency differences across the healthy controls and two FOG subgroups over Cz, Fc1, and Fc2 (figure without permutation-corrected statistical significance are presented in Figure 3-9). A distinct high beta and low beta band were obvious when comparing the healthy group and PD with mild FOG, especially over Fc1, which was similar to PD without FOG. Lack of high beta band ERD during movement was the other significant EEG feature for PD with mild FOG over Cz.

For PD with severe FOG, theta band activities over Cz and Fc1 prior to the movement onset (marked with a red oval) along with excessive high beta ERD over M1 represented the two main features of this group. Fc2, the ipsilateral channel, was the only channel that did not show any level of theta ERS in PD with severe FOG. PD with mild FOG also represented the unique feature of absent low beta ERD during movement compared to healthy controls and PD with severe FOG over Fc2.

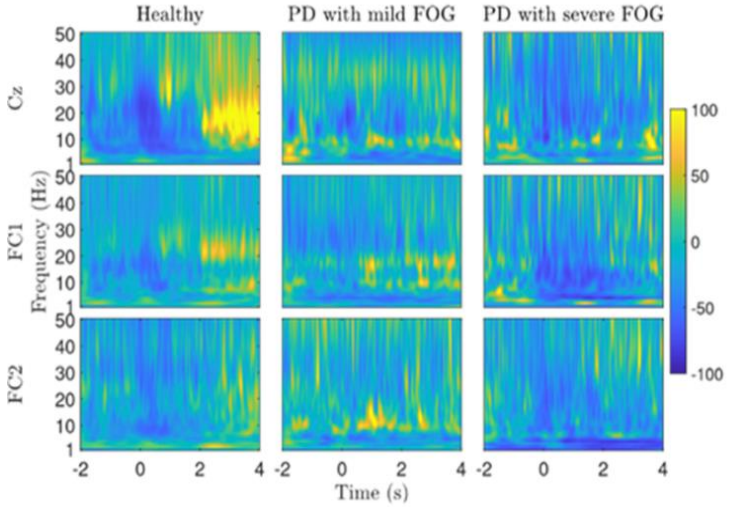

(a) Time frequency representation of ERD/ERS

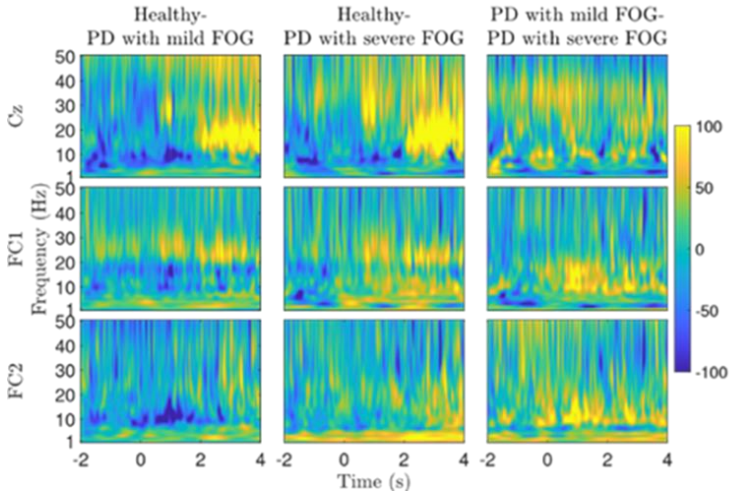

(b) Time frequency representation of ERD/ERS difference

Figure 3-9: Time-frequency representations of ERD/ERS in three channels (Cz, FC1, FC2) of three groups: Healthy controls, PD patients with mild FOG, and PD patients with severe FOG. In plot (a), ERD/ ERS indicating percentage change relative to a baseline of -4 s to -2 s are represented as blue/yellow colors, respectively between 1 and 50 Hz from -2 s to 4 s. In plot (c), time-frequency representations of ERD/ERS differences in three channels (Cz, FC1, FC2) among three groups, indicated as 'Healthy - PD with mild FOG', 'Healthy - PD with severe FOG', 'PD with mild FOG - PD with severe FOG'.

3.5 Discussion

The motor cortex is a pivotal brain structure involved in movement planning and execution through communication with the BG, cerebellum, and spinal cord. Decreased dopamine level in PD highly affects motor cortex functionality and circuitry, emphasizing the key role of cortical regions in the motor symptoms of the disease [139]. In the current study, a cue-based lower limb movement was used to investigate the motor cortical abnormalities associated with FOG and its severity during a simple lower limb motor execution task rather than FOG episodes. The results from this study showed that the motor cortical activities of PD patients with FOG are not only different from healthy controls and PD patients who do not experience FOG, but also PD with mild and severe FOG show significant differences. This might suggest the intrinsic differences between FOG subtypes and severities. One of the most significant FOG associated EEG abnormalities was the early component of MRCP. PD with severe FOG had a significantly lower NS1 compared to healthy controls, and the slope of the NS1 decreased as the severity of FOG increased. NS1 originates from the pyramidal neurons activities in pre-SMA and cingulate motor area (CMA) [68][140][141]. (Pre-)SMA, at different layers, is engaged in motor learning, integrating, and processing sequential elements, as well as planning and performing well-learned movements [71][142][143][144][145]. To perform a movement, (pre-)SMA sends BP to the BG, and for each sequence of well-learned movements, a signal from BG is sent to SMA showing the termination of the sequence [146]. Gait, as a well-learned movement sequence, critically depends on the functionality of (pre-)SMA. Impaired pre-SMA

and loss of intra-cortically projecting pyramidal cells in this cortical region was reported in PD [147][148][149][150]. In most studies, investigation of BP and SMA is limited to PD patients regardless of the type or severity of motor symptoms. The results from the NS1 differences in mild and severe freezers show the importance of further research on (pre-)SMA in patients with different FOG severities and subtypes. Additionally, building upon the existing body of MRCP research in PD, which predominantly focuses on upper limb movements, our observation of reduced BP during lower limb movements in PD patients, both with and without FOG, may indicate a generalized impairment in voluntary motor preparation across different movement types and PD subgroups. This finding is consistent with prior research, which reported decreased BP or lateralized readiness potential (LRP) during upper limb movements in PD patients [109][16][151][152]. Also, consisting with prior findings, the unaffected NS2 in patients in this study who were under chronic L-dopa treatment, may suggest specific responses of BP1 and BP2 to the long-term administration of dopaminergic medication.

Along with BP, the amplitude of MRCP was the other investigated EEG feature. The amplitude of the MRCP was lower for PD without FOG group compared to controls but independent from FOG. It should be noted that the amplitude of the MRCP has been shown to be correlated with the amplitude of EMG [153]. This suggests that the peak negativity of MRCP could be related to lower EMG amplitude, and not necessarily to FOG. Although the MRCP amplitude from PD with FOG is slightly higher than PD without FOG, they represent a lower peak of EMG signal among all groups (Table 3-3), which might be a result of time

inconsistency of muscle activities in PD patients with FOG. Analysis of the onset of EMG activities in both the TA and SOL muscle is beyond the scope of this paper; however direct observations indicate that there is an inconsistency between the onset of EMG activities from the two muscles in PD with FOG compared to other groups (green oval in Figure 3-2). Flatter peak of averaged MRCP in severe FOG and inconsistent single-trial MRCPs over (pre-)SMA and EMG onsets in both foot muscles compared to mild FOG also show that FOG might be a result of a timing issue in the muscles.

Findings of the current study also suggest distinct low and high beta band cortical abnormalities among PD patients without FOG as well as for different levels of FOG severity during movement preparation and execution (Figure 3-6 and Figure 3-8), which was consistent with the previous studies [17]. Distinct low and high beta frequency bands shared remarkable similarities and differences across groups. Lack of low beta ERD and partial ERS over Cz was a FOG associated EEG signature common between both mild and severe FOG. While PD with mild FOG represented low beta ERD over Cz at the time of the “ready” cue, PD with severe FOG group did not represent any low beta ERS before movement onset. PD with mild FOG shares some similar high and low beta activities with PD without FOG, especially over FC1. However, lack of low beta ERD during movement execution over FC2 and frequent high beta synchrony over Cz are two exclusive features of PD with mild FOG. Considering the fact that PD without FOG and PD with mild FOG show similar patterns over certain cortical regions and frequency bands, it can be suggested that mild FOG and severe FOG could be affected by

different underlying FOG mechanisms. For instance, the high beta ERD before movement over the contralateral SMA could be a compensatory mechanism stronger in PD without FOG and PD with mild FOG. On the other hand, early high beta and interrupted low beta ERD along with excessive theta ERS over Cz and Fc1 are exclusive EEG features of PD with severe FOG. This again suggests a different underlying mechanism for mild and severe FOG and possibly different FOG subtypes (e.g., motor, cognitive, limbic).

Low and high beta activities are involved in motor control at both cortical and subcortical regions. Modulation of beta activities, in general, has been introduced to play a role in internal timing, especially putaminal beta [154][155]. Distinct projections from (pre-)SMA to different parts of putamen suggest that the striatum tracks regulate movement via modulation of beta activity [156]. The power of the beta-band reflects the level of motor preparation, and beta ERS has been shown to contribute to movement inhibition [157][158]. Plus, different beta frequency bands seem to have different distributions and functionalities in different brain structures. Cortical low beta activities are related to the speed of the movement [159], and the maximum low-beta coherence was highest in the lateral M1 region [17], which corresponds to the hand areas of the motor cortex and is responsive to dopaminergic treatments [160]. By contrast, cortical and STN high beta frequency band activities have been reported to be related to self-paced movement and are less affected by dopamine [160][161]. The maximal coherence in the high-beta activity was reported in the midline cortex corresponding to the SMA, cingulate cortex, and leg area of M1 [17]. The frequency modulation patterns of the low-beta

band have been shown to be more sensitive to dopaminergic treatments compared to high-beta [162], which suggests the role of high-beta band frequency modulation in FOG, and the importance of frequency modulation of brain oscillations as a communication tool in the brain along with power modulation. It has recently been introduced that failure of cortical-subthalamic frequency modulation information processing and communication in PD can result in FOG [163]. In addition, the association of NS1 and low beta ERD over Cz with FOG severity during movement preparation suggests a possible relationship between these two EEG features.

The presence of excessive theta ERS between two auditory cues (especially over M1) changes relative to the severity of FOG with the highest and longest synchrony in PD with severe FOG over M1 followed by both high beta and low beta ERD. The presence of excessive theta ERS, associated with FOG, is consistent with the previous study [127]. This might suggest a different mechanism that controls voluntary movements in PD with FOG, particularly in severe cases. Theta activities are related to the cognitive function of the brain, motor sequence learning, and stabilization [164]. Excessive theta ERS indicates impairment of motor circuitry related to already learned movements and a relationship between the cognitive and attention impairment as well as FOG severity. Higher cognitive load of gait compared to sitting and standing could be one of the factors that contribute to FOG occurrence.

The relationship between MRCP, brain oscillations, and EMG activities is not yet completely known; however, different parts of the unified concept of motor training [165], integrated investigations of the cortical signals in different FOG subtypes and severities can shed light on underlying mechanisms of FOG and motor control in the human brain. The relationship between MRCP and FOG severities has never been investigated before. The results from this study emphasize the crucial involvement of the motor cortex in the complex pathophysiology of FOG. Further research including experiments with self-initiated, right and left, upper and lower limb movements, and motor imagery tasks in different FOG subtypes and severities can help clarify the role of the changes in MRCP characteristics as well as brain oscillations in FOG, and in human brain in general. Based on the results from this study, the abnormalities in different motor cortical areas might be used as FOG detection, and biomarkers of severe cases as particular subtypes of FOG might be more prone to severe FOG. Furthermore, impairment of motor cortical areas can offer alternative treatment options for FOG based on TMS and tDCS on motor cortical regions, which has been shown to be effective [166]. BCI-based rehabilitation systems are also emerging and promising technologies that use cortical information to rehabilitate FOG by assistive devices. Motor cortical activities are essential missing parts of the FOG dilemma, and investigation of FOG-associated malfunctions of these parts can help uncover the underlying mechanism of FOG as well as providing new treatment options.

Chapter 4

Large-Scale Frontoparietal Theta, Alpha, and Beta Phase Synchronization: A Set of EEG Differential Characteristics for Freezing of Gait in Parkinson's Disease?

This chapter is published in the Journal of Frontiers in Aging Neuroscience as:

Karimi F., Almeida Q., Jiang N., "Large-scale frontoparietal theta, alpha, and beta phase synchronization: A set of EEG differential characteristics for freezing of gait in Parkinson's disease?"

4.1 Introduction

Freezing of gait (FOG), the sudden episodic inability to move the foot forward despite the intention to walk, is a debilitating symptom of Parkinson's Disease (PD) [34][35]. The pathophysiological mechanism of the FOG phenomenon has not been understood due to its complexity and episodic nature [16][39][167]. While dopaminergic disorders of the basal ganglia (BG) are the core of PD, numerous studies have illuminated the multiplicity of brain structures and patterns of cortical activities affected by PD and FOG as well as its severity [16][168][169][33]. The majority of the current hypotheses in the literature on the underlying mechanisms of FOG suggest some level of dysfunction in the cortical structures such as supplementary motor area (SMA) and motor cortex, as well as the communication between

these regions and BG [16][170][171]. Cortical activity plays a crucial role in stabilized gait control, especially during challenging tasks such as obstacle crossing, changes in speed, and dual tasks, which are all FOG-provoking situations emphasizing on the significance of cortical networks involvement in FOG [172]. It is therefore highly likely that the mechanism of FOG involves higher-level cortical modulators from non-motor perspective (e.g. cognitive and attention-related networks) rather than only the motor perspective (e.g. prefrontal cortex (PFC), SMA, premotor cortex, and motor cortex) [33][169]. On the other hand, regarding the role of midbrain dopamine, dopaminergic system dynamics have been suggested to be the main contributors to whole-brain coordination through synchronicity and time perception [173][174][175]. Finding the links across cortical oscillations that interact with subcortical regions and might be affected by dopamine loss in PD, are thus essential in addressing current issues in deep understanding of the FOG phenomenon. The existing body of research reports abnormalities in the power spectrum and amplitude of various cortical oscillations, including movement-related cortical potentials (MRCP), theta (4-8 Hz), alpha (8- 12 Hz), low beta (12-21 Hz), and high beta (21-35 Hz) bands associated with FOG. Although there is a growing body of literature that recognizes the relationship between brain oscillations, gait and FOG [176], the field is still far from providing a systematic understanding of how brain oscillation dynamics contribute to pathological gait such as FOG.

BG plays a central role in timing and sequencing through distributed, parallel neuronal networks to connect and integrate functions [42][173][174][175][177]. The footprint of timing

dysfunction is traceable in several theories about FOG, such as motor breakdown as a result of motor deficits accumulation over time, conflict-resolution deficit, especially during time-constraint tasks, and overload of information processing capacity in motor, sensory, cognitive, and limbic inputs to BG due to insufficient dopaminergic cells in a limited time window. Considering the importance of time in underlying neurocomputational mechanisms [178]; and the independency of phase and power as dimensions of information, in this study, we take one step beyond to investigate what modulates the amplitude and power of the cortical oscillation: phase. The amplitude of higher frequency bands is controlled by the phase of the lower frequency bands [55]. Therefore, the investigation of the phase of the lower frequency bands, especially at a large scale, is crucial in the exploration of the underlying mechanisms of FOG. Although the number of studies on the phase features related to gait and FOG is limited [179], in a recent study, high beta-gamma phase-amplitude coupling (PAC) in the primary motor cortex was reported as a FOG-associated feature [19].

In the current study, we investigated the phase-locking value (PLV) of distributed cortical areas of the locomotor network (e.g., frontoparietal, SMA, and primary motor area) as well as higher-level cortical modulators (e.g., PFC) to explore neural networks associated with FOG. The PLV was explored in slow cortical potentials and low frequencies such as theta and alpha, as well as movement-related beta oscillation during a simple lower-limb movement task. Furthermore, although phase synchrony is considered to be the mechanism for neural group communication across both close and distant brain areas, PAC is mainly considered as the

mechanism to control long-distance communication based on the fact that slow oscillations can propagate at larger scales compared to fast oscillations [180]. As a result, in this study, PAC of the frequency bands was explored to investigate the possible relevance of the excessive beta power and the phase of lower frequencies in PD patients with FOG. In addition, considering the involvement of the multilayer neocortex and subcortical regions of the brain in FOG, phase features have been investigated with and without a spatial filter, Surface Laplacian (SL), that improves the spatial resolution of EEG signals and provides complementary information [181]. Prior studies about the origin of freezing in PD have been suggested to involve spatiotemporal disorder as a core motor problem which underlies freezing [182]. In a broader context, there is likely a universal mechanism and upstream cause underlying the phenomenon [183]. So, investigating phase features of brain oscillations correlated with FOG might help converge recent findings in a meaningful way to help identify unified mechanisms in FOG. This study offers a better understanding of possible underlying mechanisms for FOG, as well as biomarkers to distinguish PD patients with and without FOG based on EEG phase features. The results from this study can also help provide insight into new treatment paths to rehabilitate FOG.

4.2 Materials and Methods

4.2.1 Participants

Forty-one participants including 14 PD patients without FOG, 14 PD patients with FOG and 13 age-matched healthy control participants (PD without FOG: mean age = 77 years, range = 65–87 years, three females; PD with FOG: mean age = 74 years, range = 63–90 years, one female; healthy controls (HC): mean age = 77 years, range = 68–89 years, three females) took part in the experiment. The PD patients were recruited from the Movement Disorders Research and Rehabilitation Center (MDRC) at the Wilfrid Laurier University (Waterloo, Ontario). Participants with any head trauma, neurological disorder, severe vision or hearing problems and severe movement control limitations such as dyskinesia were excluded. All patients were in their optimally medicated state to avoid the confound of exacerbated motor symptoms. The severity of patients' motor symptoms was assessed based on the Unified Parkinson's Disease Rating Scale (UPDRS). PD patients with FOG were identified by the answer to question 14 in MDS-UPDRS-III (motor subsection), which confirms the presence of FOG. In addition, an experienced clinician reconfirmed the occurrence of FOG before each experiment session, according to the standardized protocol [130]. The procedure involved a modified Timed Up and Go test where the participant would have started from a seated position, raised themselves out of a chair with arms across their chest, walked ~3 m but through a doorway into an adjacent clinic room that was cluttered with other desks and chairs, then returned to in front of their

chair where they completed degree turns in both the left and right directions, before sitting back down. PD patients with FOG were divided into two subgroups of PD with mild and severe FOG. PD+sFOG were defined as those who experienced observable FOG episodes whenever walking or turning that severely affect their daily activities and independence, while PD+mFOG were defined as those who experienced FOG occasionally when provoked only during more complex tasks such as turning (based on patient history). In addition, the participants were instructed to perform 20 trials of videotaped walking tasks on a 10-m walkway. Participants were asked to walk after hearing an auditory 'go' cue. PD+FOG who experienced FOG episodes longer than 3 s during turning or normal walking were considered PD+sFOG. The videotaped walking tasks were used to determine the dominant foot for each participant.

HC were recruited from The Waterloo Research in Aging Participant pool at the University of Waterloo. The sample size was determined by availability of PD patients. The study was approved by the Research Ethics Board at the University of Waterloo and Wilfrid Laurier University. A written informed consent form was obtained from each participant prior to the experiment, according to the Declaration of Helsinki.

In the current study, patients were confirmed to have idiopathic Parkinson's. To maximize the number of participants experiencing FOG, any participants that met all the inclusion criteria for the study and were confirmed to experience FOG were recruited first.

Subsequently, healthy controls and PD without FOG were recruited to match for age [F (2,39) = 1.1, P = 0.3], severity using the UPDRS, levodopa equivalent dose (LED), and disease duration (P = 0.4, P =0.2 and P =0.4, respectively). PD with mild and severe FOG groups did not differ in age (P =0.4), severity of motor symptoms (UPDRS-III: P =0.4), LED (P =0.07), disease duration (P = 0.3). Individual participant details of all groups can be found in our previous paper [184]. Table 3-1 represents the participant demographics and clinical characteristics. Further details of our experimental setup can be found in our previous paper [184].

4.2.2 EEG and EMG Recordings

EEG data were recorded using a 32-channel wireless EEG system (g.Nautilus, Guger Technologies, Austria). EEG signals were sampled at a sampling rate of 250 Hz. EEG data were collected from 17 channels following 10-20 international standard positions: FP1, FP2, AF3, AF4, F3, Fz, F4, FC1, FC2, C3, Cz, C4, CP1, CP2, P3, Pz, and P4. The reference electrode was placed on the right ear lobe.

For all individuals, the EMG was acquired using an 8-channel TELEMYO 2400 system (NORAXON INC). Four wireless EMG sensors with a sampling frequency of 1000 Hz were placed on the tibialis anterior (TA) and soleus muscles (SOL) on both legs.

4.2.3 Experimental Procedures

All participants were invited to the MDRC for the experimental sessions. For PD patients, the respective clinical assessment was performed within two weeks of the experimental session. During the experiment, participants were instructed to perform ankle dorsiflexion (ADF) (e.g., lifting the toe) to the maximum possible contraction with the dominant foot, while sitting in a comfortable chair with their arms rested on armrests. To minimize eyes or head movements and reduce the cognitive load unrelated to the cues, they were asked to look at the center of a black '+' sign on a white background. One session with 15 trials was recorded for each participant, with an interval of 15 s between every two trials. Participants were expected to prepare for the task when they heard 'ready' and execute ADF when they heard the 'go' cue. The 'ready' and 'go' auditory cues, with a 2 s interval, were played for each trial through a speaker with a computer-generated voice.

4.2.4 Data Processing

EEG and EMG data were analyzed offline after the experiment session using a customized Matlab function (Mathworks, USA R2020a). EMG signals recorded from the TA muscles of the dominant foot (EMG-TA) were used to identify onset timings of the ADF. EMG was initially filtered using a second-order Butterworth band-pass filter with the bandwidth between 20 Hz and 120 Hz, and then down-sampled to 250 Hz to maintain consistency with

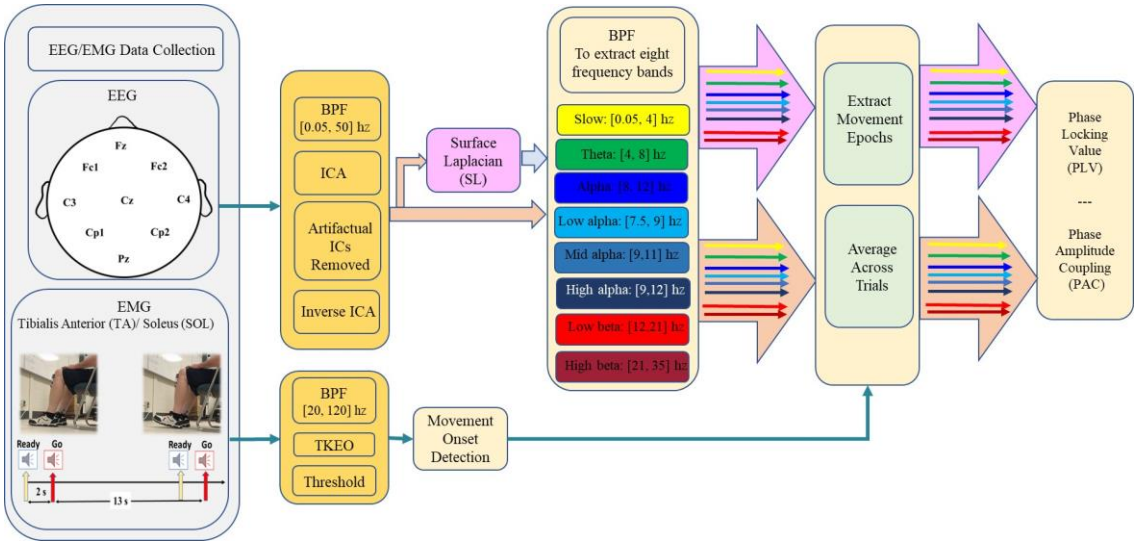

Figure 4-1. Schematic representation of experimental setup and data processing.

that of the EEG data. To enhance the detection accuracy of the movement onset, the Teager–Kaiser Energy Operator (TKEO) was applied to the EMG data [131]. By being independent of the initial phases, TKEO algorithm instantly responses to the abrupt temporal changes in the EMG signal while improving the SNR and minimizing erroneous EMG burst detection [131]. Finally, a threshold value was manually selected for each subject to determine the movement onset. The EEG data was initially band-pass filtered by a third-order Butterworth filter between 0.05 Hz and 50 Hz. The filtered EEG data were processed by independent component analysis (ICA) using the EEGLAB toolbox. Source components containing eye blinks, severe head motion or EMG artifacts were removed [132]. The phase and amplitude features are

investigated both with and without SL [133][185]. More details about the implementation of SL are provided in the next section.

The outliers were discarded from further analysis based on the excessive muscle activities in leg muscles prior to the "Go" auditory cue, motion, or other types of artifacts. Excessive muscle activities were identified when EMG amplitude was above the movement onset detection threshold in the non-dominant foot over the time interval [-3,5] s with respect to the auditory" Go" cue and/or in case EMG amplitudes from the dominant foot was above the movement onset detection threshold over the same time interval except for the time course of ADF execution ([0,5] s with respect to the auditory" Go" cue). In general, the 5 to 15 most consistent trials from each participant were manually selected, with a total number of 122±2 trials in each group. For those participants for whom their left leg was dominant, the EEG channels on the left and right sides were switched during the analysis. Figure 4-1 represents schematic for experimental setup and data processing in this study.

4.2.5 EEG Data Processing

4.2.5.1 Surface Laplacian (SL)

SL represents the second spatial derivative of the instantaneous spatial voltage distribution, which suppresses the signals with low spatial frequency (i.e., signals originating from distributed and/or deep generator sources) [181]. As a result, applying SL emphasizes on superficial, radial sources cortical generators and attenuate deeper sources, vertical

connections, and broadly distributed generators [52][186]. Forward simulations using a four-shell head model have indicated that while the maximum scalp potential is linked with broad dipole layers extending approximately 7–10 cm, the surface Laplacian maximum primarily corresponds with smaller dipole layers of about 2.5 cm, pointing towards its efficiency in targeting and delineating superficial neural activities over deeper network activities [181].While SL reduces the effect of volume conduction, the effect of this spatial filter on phase-sensitive measures such as PLV is still controversial [187][188][189]. Therefore, in this study, data has been investigated both with and without applying SL to the EEG data. In order to implement SL, the estimate of the second derivative of the scalp voltage based on a finite-difference method was used [190]. SL was applied on Fz, Cz, Fc1, Fc2, Cp1, and Cp2 by subtracting the averaged signal of the four surrounding orthogonal electrodes from the center electrode.

4.2.5.2 Phase Locking Value (PLV)

The communication between pre and post-synaptic neurons takes place via phase synchronization, both for short distances within a brain region up to long ranges between distant brain areas. PLV is a measure that represents the level of neural phase synchrony and EEG connectivity at a specific frequency range between two neural groups [188]. In other words, neural groups that oscillate at the same frequency are phase-locked to each other [191]. In this paper, PLV is calculated according to [192] :

$$PLV(n) = \frac{1}{N}\left|\sum_{k=1}^{N} e^{i(\emptyset_{(n,k)} - \varphi_{(n,k)})}\right| \quad (4\text{-}1)$$

where N is the number of trials, $\emptyset_{(n,k)}$ and $\varphi_{(n,k)}$ are instantaneous phase of two different electrodes computed by Hilbert Transformation. The magnitude of the PLV, i.e., how much two oscillations are phase-locked to each other, thus quantifies effective interactions between neural groups. PLVs were calculated for the time interval [-5,5] s, with respect to movement onset, thus including movement preparation, initialization and execution as well as time samples at rest. As the focus of this research is to investigate phase synchronization related to movement preparation that results in successful movement execution, two steps were taken: Firstly, PLV traces that represent significant PLVs outside [-3, 2] s were not reported as they were not task-relevant. Secondly, considering that the "ready" auditory cue occurred at time -2 s, the transient significant PLVs between [-3, -1] s, were not reported as significant PLVs related to movement preparation. This step was taken to limit the effect of the phase synchronizations related to "ready" auditory cue and focus on the phase synchronizations that lead to movement execution. Lastly, as time zero represents movement onset, the PLV traces that represent significance only after 1 s were not reported as significant PLVs related to movement preparation and initiation. PLVs were also baseline-corrected to the mean of the pre-stimulus period, [-10, -3] s with respect to the movement onset.

4.2.6 Time-Frequency Phase-Amplitude Coupling (PAC)

The coupling between the phase of slow oscillations and the amplitude of fast oscillations, referred to as phase-amplitude coupling (PAC), is one of the mechanisms underlying neural binding. To assess PAC between frequency bands with abnormal activities among different groups, a novel robust time-frequency-based PAC measure was implemented [180]. The method is based on a complex time-frequency distribution, named Reduced Interference Distribution (RID)-Rihaczek distribution and mean vector length (MVL). In this paper, we specifically investigated coupling between phase of slower cortical potentials ([0.5, 7.5] Hz) with the amplitude of alpha and beta frequency bands. PAC features were calculated for the two time intervals [-3, 1] s and [-3, 2] s, with respect to movement onset, thus including movement preparation, initialization and execution. Only PAC plots that represented highly distributed differences across groups over investigated frequencies were reported in comodulogram to show the coupling between high and low frequency.

4.2.7 Statistical Analysis

To determine statistical significance of PLV at different time points, Raleigh's Z score for non-uniformity of circular data was used as following [193][194]:

$$Z = N(PLV)^2 \tag{4-2}$$

The p-value of Rayleigh's test (function *circ_rtes* in Matlab) was calculated for each time point in the interval using CircStats toolbox [195]. In the test, the null hypothesis is that the

population is uniformly distributed around the circle with the alternative hypothesis that the population is not uniformly distributed, but rather has a specified mean angle. Unless specified otherwise, a significance level of 0.05 was used throughout the analysis. Correction for the false discovery rate (FDR) was also conducted using Benjamini & Hochberg test. All statistical analysis was performed in Matlab 2021 a.

4.3 Results

In Figure 4-2 and Figure 4-3, the phase-locked channels with two levels of significant PLVs are presented (top two rows) with and without SL for all groups: Healthy Control participants (HC), PD without FOG (PD-FOG), PD with mild FOG (PD+mFOG), and PD with severe FOG (PD+sFOG). Top row represent a significance level of 0.01, and lower row represent PLVs with significance level of 0.05. Different colors represent significant PLV in different frequency bands, including yellow: slow cortical potentials; green: theta; navy blue: alpha; light blue: low alpha; blue: middle alpha; dark blue: high alpha; light red: low beta; dark red: high beta. Significant PLVs (over [-1, 1] s with respect to the movement onset) are presented to determine phase-locked channels during movement preparation and execution before and after the auditory “go” cue. In the following, differences between groups are discussed in detail at two different spatial resolutions.

4.3.1 Radial Superficial Connections (With SL)

The analyses of PLV and PAC at radial and superficial networks (with SL) for different frequency bands are shown in Figure 4-2. The results revealed distinctions between PD without and with FOG groups as well as PD+mFOG and PD+sFOG, especially over theta frequency band.

4.3.1.1 Primary motor area (Cz) centrally phased locked to frontal and parietal areas in HC and PD-FOG

As seen in the top rows of Figure 4-2, a common observable feature between HC and PD-FOG is that Cz is phase-locked to Fz, over theta. Plus, Cz is phased locked to Cp1, and Cp2 over low alpha frequency band. This pattern is missing in PD+FOG groups. In addition, HC represents a strong phase synchronization ($p<0.01$) between the prefrontal area (Fz) and primary motor cortex (Cz) in theta and beta frequency bands, but no such synchronization can be seen in PD-FOG.

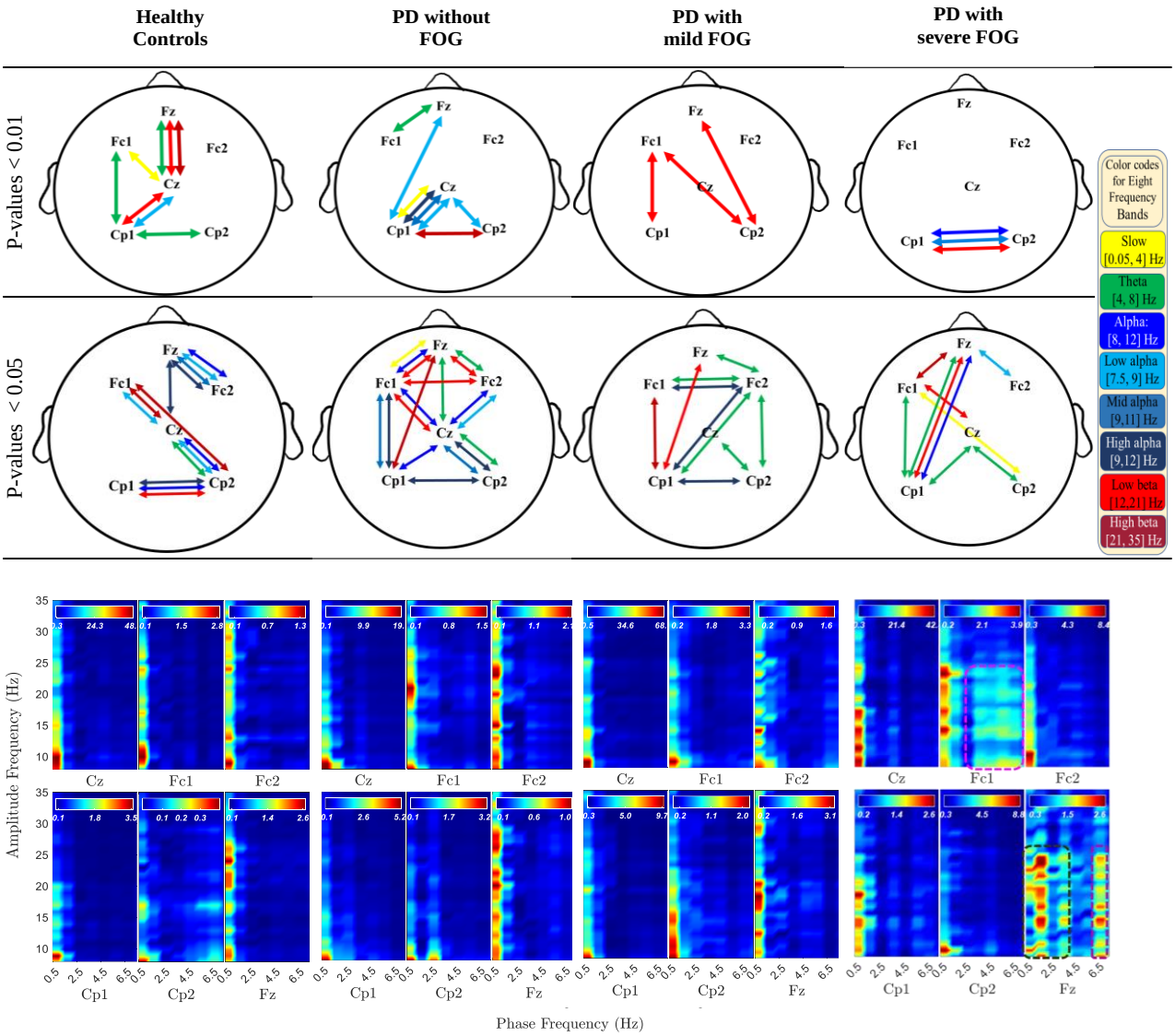

Figure 4-2. Significant PLV between different channels over different frequency bands (top two rows) and PAC between lower frequency bands (slow cortical potentials and theta) and higher frequency bands (alpha and beta frequency bands) (bottom row) with SL in all groups. In the top rows, different colors represent different frequency bands: Yellow: slow cortical potentials; green: theta; navy blue: alpha; light blue: low alpha; blue: middle alpha; dark blue: high alpha, light red: low beta; dark red: high beta. First and second row represent significant PLVs for $p < 0.01$ and $p<0.05$, FDR-corrected, respectively. In the lower row, PAC between lower frequency bands (slow cortical potentials and theta) and higher frequency bands (alpha and beta frequency bands) with SL are presented over [-3,1] s for all groups. Dashed pink lines represent the coupling of the phase of theta with alpha and low beta frequency bands. Dark green dashed lines represent the PAC between higher slow cortical potentials and alpha and beta in Fz.

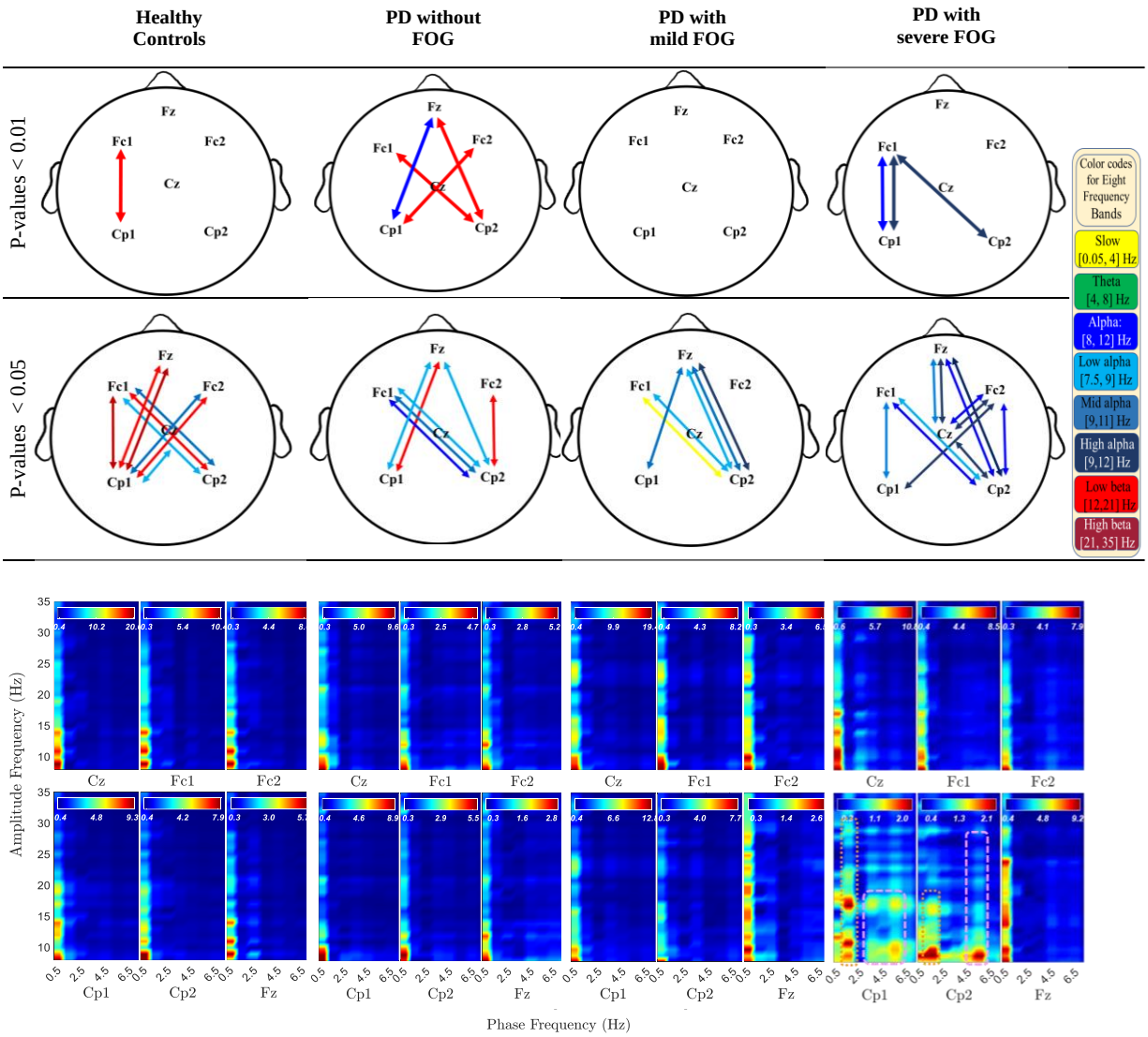

Figure 4-3. Significant PLV between different channels over different frequency bands (top two rows) and PAC between lower frequency bands (slow cortical potentials and theta) and higher frequency bands (alpha and beta frequency bands) (bottom row) without SL in all groups. In the top row, different colors represent different frequency bands: Yellow: slow cortical potentials; green: theta; navy blue: alpha; light blue: low alpha; blue: middle alpha; dark blue: high alpha, light red: low beta; dark red: high beta. First and second row represent significant PLVs for $p < 0.01$ and $p<0.05$, FDR-corrected, respectively. In the lower row, PAC between lower frequency bands (slow cortical potentials and theta) and higher frequency bands (alpha and beta frequency bands) without SL over [-3,1] s is presented for all groups. Dashed pink lines represent the coupling of the phase of theta with alpha and beta frequency bands. Pink dotted lines represent the PAC between higher slow cortical potentials and alpha and beta.

4.3.1.2 Theta between frontal areas and Cz is missing in PD+FOG

At the superficial networks, the most distributed phase synchronization is observable in the theta frequency band in all groups. HC and PD-FOG show phase synchronization between Fz and Cz. By contrast, this feature is missing in both PD groups with mild and severe FOG. In the two PD+FOG groups, unlike HC and PD-FOG, the theta phase synchrony is higher in parietal areas rather than (pre-)frontal areas and presents frontoparietal phase synchronization. More importantly, this shift in theta phase synchrony increases with the severity of FOG. While in PD+mFOG theta synchrony is observable in the (pre-) frontal areas along with large-scale phase synchrony between Cp1 and Fc2, in PD+sFOG there is no theta phase synchrony in the frontal areas. In PD+sFOG, theta phase synchrony is more pronounced in the parietal areas with dominance on the left hemisphere. While in PD+mFOG, there is interhemispheric frontoparietal theta phase synchrony between Cp1 and Fc2, PD+sFOG represents one large-scale theta phase synchrony between Cp1 and Fz. These results suggest that there is a direct relationship between large-scale interhemispheric frontoparietal theta phase synchrony at the superficial networks and FOG. The shift of this large-scale theta phase synchrony from the phase-locking between left parietal areas (Cp1) and right supplementary motor area (Fc2) in PD+mFOG to phase-locking between left parietal areas (Cp1) and prefrontal areas (Fz) in PD+sFOG, might represent the relationship between this feature and the severity of FOG.

4.3.1.3 Lack of low-alpha phase synchrony between Cp1 and Cz in PD+FOG

In Figure 4-2, significantly high low-beta phase synchrony ($p<0.01$) is observable between Cp1 and Cz in HC and PD-FOG. In these groups, the same pattern is observable between Cp2 and Cz, with lower significance in HC. In contrast, the low alpha phase synchrony between parietal areas (CP1 and Cp2) and Cz are missing in the two PD+FOG groups. PD+sFOG represents only low-alpha phase synchrony in the frontal areas between Fz and Fc2, and PD+mFOG does not represent any low alpha phase synchrony at superficial layers. However, the groups represent large-scale frontoparietal low alpha phase synchrony at deeper networks.

4.3.1.4 Lack of high-alpha phase synchronization between bilateral parietal areas in PD+sFOG

Bilateral parietal high-alpha phase synchrony between Cp1 and Cp2 is present in all groups except PD+sFOG, where a highly significant ($p<0.01$) phase synchrony is seen between Cp1 and Cp2 in low-alpha, alpha, and low-beta, as observable in the top row in Figure 4-2. On the other hand, PD+mFOG represents high alpha phase synchrony at the same significance level ($p<0.05$) as HC and PD-FOG. Interestingly, phase synchrony in mid-alpha is an exclusive phase synchrony feature of PD+sFOG between CP1 and Cp2, which is absent in all other groups.

4.3.1.5 Phase of frontal delta and theta is coupled with the amplitude of low-beta in PD+sFOG

Figure 4-2 (lower row) presents the comodulogram for PAC values between lower frequency bands ([0.5, 7.5] Hz) and higher investigated frequency bands (alpha and beta) for all channels and all groups over the movement preparation and execution [-3, 1] s with respect to the movement onset. The most striking feature is the abnormal PAC of lower frequencies and theta with the amplitude of alpha and beta frequency bands in PD+sFOG group (dashed dark green and pink lines) in Fz and Fc1. The result suggests that, unlike all other groups, in PD+sFOG, the phase of theta frequency band is coupled with the amplitude of alpha and low beta in Fc1 and Fz. In all other groups, the amplitude of alpha and beta is coupled with the phase of slow cortical potentials (less than 1.5 Hz). More importantly, in PD+sFOG, the phase of the lowest frequencies is not coupled with the amplitude of alpha and beta. Table 4-1 represents p-values for electrode pairs with significant phase synchrony when SL is utilized.

4.3.2 Deeper Neural Networks (Without SL)

PLVs without SL for different frequency bands are presented in Figure 4-3 (top two rows) with multicolor lines. These activities mainly represent large-scale crosstalk between the two hemispheres as well as frontoparietal phase synchrony in deeper networks. In addition, the phase synchrony is restricted to alpha and beta, and in one case, slow potentials.

Table 4-1. Pairs of electrodes with significant PLVs over different frequency bands with SL for all groups ($p<0.05$)

Group	SCP	Theta	Alpha	Low alpha	Mid alpha	High alpha	Low beta	High beta
HC	**Fc1-Cz (0.003)***	Cz-Cp2 (0.044) **Cz-Fz (0.0073)*** **Cp1-Cp2 (0.0007)*** **Fc1-Cp1 (0.002)***	Fz-Fc2 (0.027) Cz-Cp2 (0.044) Cp1-Cp2 (0.019)	Fc1-Cz (0.01) **Cz-Cp1 (0.00011)*** Fz-Fc2 (0.022) Cz-Cp2 (0.017)	Fz-Fc2 (0.047)	Fz-Cz (0.01) Fz-Fc2 (0.032) Cp1-Cp2 (0.022)	**Cz-Fz (0.007)*** **Cz-Cp1 (0.0013)*** Fc1-Cp1 (0.015) Cp1-Cp2 (0.032)	**Cz-Fz (0.00008)*** Cz-Fc1 (0.01) Fc1-Cp2 (0.03)
PD-FOG	**Cz-Cp1 (0.0012)***	**Fz-Fc1 (0.0023)*** Fz-Fc2 (0.041) Fz-Cz (0.013) Cz-Cp2 (0.036)	Fz-Fc1 (0.022) Cz-Fc1 (0.028) Cz-Fc2 (0.026) Cz-Cp1 (0.025)	Cz-Fc1 (0.03) **Fz-Cp1 (0.0047)*** **Cz-Cp1 (0.0037)*** **Cz-Cp2 (0.0062)***	**Cz-Cp1 (0.0037)*** Cz-Cp2 (0.041) Fc1-Cp1 (0.029)	**Cz-Cp1 (0.0016)*** Cz-Cp2 (0.038) Fc1-Cp1 (0.034) Cp1-Cp1 (0.027)	Fz-Fc1 (0.015) Fz-Fc2 (0.034) Cz-Fc1 (0.034) Fc1-Fc2 (0.018)	Fz-Cp1 (0.041) **Cp1-Cp2 (0.0038)***
PD+mFOG	-	Fz-Fc2 (0.04) Fc1-Fc2 (0.036) Fc2-Cp1 (0.045) Fc2-Cp2 (0.023) Cz- Cp2 (0.044)	-	-	-	Fc1-Fc2 (0.017) Fc2-Cp1 (0.016) Cp1-Cp2 (0.028)	**Fc1-Cp1 (0.0012)*** **Fc1-CP2 (0.005)*** **Cp2-Fz (0.0032)*** Fz-Cp1 (0.037)	Fc1-Cp1 (0.026)
PD+sFOG	Fc1-Cp2 (0.037)	Fc1-Cp1 (0.025) Cz-Cp1 (0.04) Cz-Cp2 (0.04)	**Cp1-Cp2 (0.008)***	Fz-Fc2 (0.049)	**Cp1-Cp2 (0.007)***	-	Fc1-Cz (0.013) Fz-Cp1 (0.015) **Cp1-Cp2 (0.006)***	Fz-Fc1 (0.027)

*** represents $p<0.01$**

4.3.2.1 Lack of low-beta phase synchrony in PD with FOG

From the results represented in Figure 4-3 (top rows), it is observable that while HC and PD-FOG groups have significant frontoparietal inter-hemispheric phase synchrony in low beta frequency band, PD groups with FOG surprisingly do not show any level of phase synchrony in this frequency range.

4.3.2.2 Frontoparietal Alpha band phase synchrony in PD+FOG represents right-hemisphere dominance

In Figure 4-3 (top rows), both PD+FOG groups represent high levels of alpha phase synchronization at deeper networks, especially in PD+sFOG. Interestingly, in PD+sFOG, alpha is the only frequency band that shows phase synchrony, with the greatest number of connections in the right parietal area. Highest levels of phase synchrony ($p<0.01$) are observable between Fc1-Cp1 and Fc1-Cp2. Moreover, alpha frequency band represents high levels of phase synchrony in Fc1-Cp1. Besides the connection between parietal channels and Fc1, significant PLVs are also observable between Fz-Cz over mid alpha and high alpha. Importantly, PD+mFOG shares PLV similarity with PD+sFOG between Cp2-Fz over high alpha and Cp2-Fc1 over low alpha. However, PD+mFOG shows lower levels of phase synchrony compared to PD+sFOG. Similar to PD+FOG, in PD-FOG, phase synchrony between parietal areas and Fz over alpha sub-bands is observable, which is missing in HC.

4.3.2.3 Fz and Cz are phased locked through two alpha frequency sub-bands, in PD+sFOG

The only connection between Fz and Cz, at both superficial and deeper networks, in PD+sFOG is observable in mid alpha and high alpha when no SL is applied. This feature is exclusive to PD+sFOG, meaning that PD+mFOG does not show any significant level of phase synchrony between Fz and Cz, both with and without applying SL. On the other hand, the phase synchrony between Fz and Cz in HC and PD-FOG is observable in more superficial layers with theta phase synchrony as the common feature between both groups without FOG.

4.3.2.4 Frontoparietal low-beta band phase synchrony in PD-FOG, represents right-hemisphere dominance

In PD-FOG, frontoparietal interhemispheric low beta phase synchrony was highly significant ($p<0.01$), which is an exclusive feature of this group. The phase synchrony in low beta frequency bands connects Cp1 to Fc2, and more interestingly, Cp2 to Fz and Fc1 in PD-FOG. As shown in Figure 4-3, the phase synchrony between Cp2 and Fz is only observable in PD patients, with a difference in frequency bands. PD-FOG represents large-scale frontoparietal phase synchrony in low beta, while PD+FOG represents phase synchrony mainly in the alpha frequency sub-bands between Cp2 and Fz. It should be noted that, like PD-FOG, frontoparietal interhemispheric low beta phase synchrony (Fc1-Cp2 and Fc2-Cp1) was also observable in HC but with lower significance ($p<0.05$). Table 4-2 represents all p-values for electrode pairs with significant phase synchrony.

4.3.2.5 Phase of high alpha is coupled with the amplitude of low beta in PD with FOG

Figure 4-4 represents PAC between alpha and beta frequency bands in six channels without SL and over [-3, 2] s for all groups, which covers movement preparation and execution. The most notable differences are observable in PD+sFOG, which represents PAC between all alpha frequency sub-bands, including high alpha and low beta in Fz and Fc1. Similar PAC is observable in PD+mFOG in Fc1. In Figure 4-4, red dotted squares represent abnormal PAC between alpha and beta in PD with FOG groups. It should be noted that PAC between alpha and beta frequency bands was investigated over two different time intervals: [-3, 1] s and [-3, 2] s. High PAC between high alpha and beta was more pronounced over the latter time interval. Also, same time interval, [-3, 2] s, was investigated when SL is applied, and the results show the abnormal PAC between the alpha and beta frequency bands in PD+sFOG is no longer consistently high at the superficial layers.

4.4 Discussion

Current knowledge of brain oscillation dynamics associated with FOG is very limited and does not reflect an integrative view towards this phenomenon [147]. Excessive theta and beta power has been repeatedly reported as FOG-related cortical abnormalities. In this study, we explored PLVs of eight frequency bands between 0.05 Hz to 35 Hz in HC and PD without and with different FOG severities. Two different spatial resolutions were investigated by utilizing a spatial filter, SL, to determine the abnormal phase synchronizations associated with

Table 4-2. Pairs of electrodes with significant PLVs over different frequency bands without SL for all groups (p<0.01)

Group	SCP	Theta	Alpha	Low alpha	Mid alpha	High alpha	Low beta	High beta
HC	-	-	-	Cz-Cp1 (0.047) Fc1-Cp2 (0.04)	Fc1-Cp2 (0.031) Fc2-Cp1 (0.031)	-	Fz-Cp1 (0.046) **Fc1-Cp1 (0.0074)*** Fc1-Cp2 (0.016) Fc1-Cp1 (0.027)	Fc1-Cp1 (0.024) Fz-Cp1 (0.013)
PD-FOG	Fz-Fc1 (0.042)	-	**Fz-Cp1 (0.0008)*** Fc1-Cp2 (0.021)	Fz-Cp1 (0.033) Fc1-Cp2 (0.031) Fz-Cp2 (0.026)	Fc1-Cp2 (0.025)	-	**Fz-Cp2 (0.0032)*** Fz-Cp1 (0.011) **Fc1-Cp2 (0.0051)*** **Fc2-Cp1 (0.0098)*** Fc2-Cp2 (0.01) Cz-Fc1 (0.018)	-
PD+mFOG	Fc1-Cp2 (0.05)	-	Fz-Cp2 (0.036)	Fc1-Cp2 (0.031)	Fz-Cp1 (0.028) Fz-Cp2 (0.03)	Fz-Cp2 (0.035)	-	-
PD+sFOG	-	-	**Fc1-Cp1 (0.0093)*** Cz-Fc2 (0.018) Fc2-Cp2 (0.036) Fc1-Cp2 (0.021) Fz-Cp2 (0.035)	Fc1-Cp2 (0.049)	Fz-Cz (0.032) Fc1-Cp1 (0.04)	Fz-Cz (0.03) Cz-Fc2 (0.02) Fz-Cp2 (0.027) Cz-Cp2 (0.046) **Fc1-Cp2 (0.0094)*** Fc2-Cp1 (0.02) **Fc1-Cp1 (0.0046)***	-	-

*** represents p<0.01**

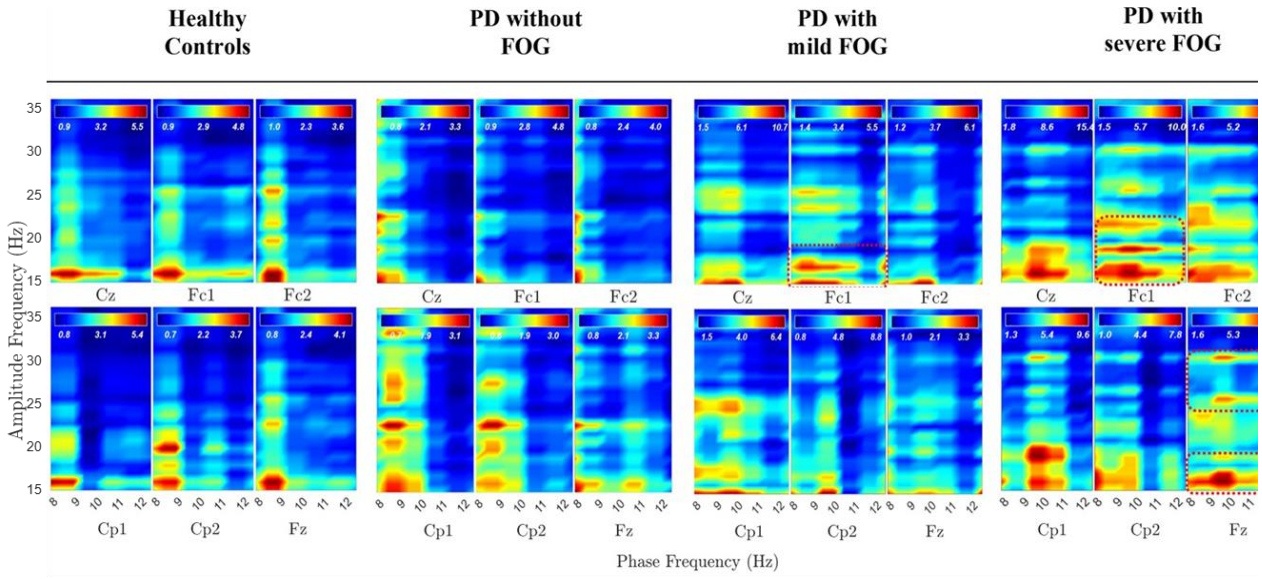

Figure 4-4. PAC between alpha and beta frequency bands without SL over [-3, 2] s in all groups. Dashed red lines represent PAC between all alpha frequency sub bands and low beta and high beta in PD with FOG.

FOG over superficial and deeper neural networks. Since the phase of the lower frequencies controls the amplitude of higher frequencies in neural oscillation and considering the fact that there are abnormal activities in the amplitude of some frequency bands, we also investigated the coupling between phase and amplitude of different frequency bands in case of observed abnormal phase synchrony associated with FOG. We found significant differences between phase features of PD with and without FOG over different cortical levels and frequency bands.

The remarkable phase-related abnormalities associated with FOG, and PD, can be summarized as: At superficial networks: 1) frontoparietal theta (left parietal areas) is

observable only in PD+FOG groups. At deeper networks: 2) frontoparietal alpha band phase synchrony was shown to be associated with FOG and its severity, especially high alpha frequency band phase synchrony. 3) Alpha phase synchrony is observable mainly on the right parietal areas in PD with FOG groups, with exaggerated phase synchrony in PD+sFOG 4) Low beta phase synchrony is missing in PD+FOG. Abnormalities reported in PLV and PAC in PD patients with FOG may represent a chain of FOG-related features in phase and amplitude that can be interpreted in a meaningful way. As the low-frequency phase controls the high-frequency amplitude, abnormal PAC between theta and beta as well as alpha and beta frequency bands in PD patients with FOG emphasizes the possible role of the phase of theta and alpha in FOG. This means that abnormal reported frontoparietal theta, and alpha phase synchrony in PD with FOG might contribute to the amplitude abnormalities in higher frequencies such as beta, which is repetitively reported in the literature.

Brain oscillations coordinate various operations within and across neural networks in a timely manner [55]. Disturbed brain oscillations and phase synchronies thus indicate uncoordinated networks. Current results suggest that significantly high frontoparietal alpha sub-bands phase synchrony, especially high alpha, replaced the beta phase synchrony in deeper networks in PD patients with FOG. This feature was the most remarkable FOG-related feature. The mechanistic role of alpha oscillations in brain function as well as their generating structures are not entirely clear [196]. Evidence suggest that alpha cortical sources are located in deeper layers (layer V) of the occipital cortex and posterior regions, with slower and faster

alpha components mainly generated in the anterior and posterior brain regions, respectively [197]. Alpha oscillations play a role in various brain functions such as attention, memory, conscious perception, and sensory information integration [198], primarily through cortical inhibition. Phase-dependent alpha inhibition of cortical neural processing is a well-supported mechanism [198][199], with the alpha phase influencing the timing and direction of inhibition changes, and consequently, attentional focus[200]. On the other hand, attentional and working memory (WM) functions are thought to operate by similar underlying principles, and they often engage overlapping frontoparietal brain regions [200][201][202]. Frontoparietal alpha-phase synchrony, in particular, reflects WM and visual attention functions [203][204], with large-scale high-alpha phase synchronization in frontoparietal network be mainly associated with visuospatial attention [205][206][207]. The results from the current study might therefore suggest unbalanced mechanisms between attention (especially visuospatial attention) and WM in PD patients with FOG. Furthermore, in the current study, alpha phase synchrony in the right hemisphere and left hemisphere showed different patterns in deeper networks (Figure 4-3). PD+FOG alpha phase synchronization between the right parietal hemisphere and the prefrontal area (Fz) is significantly higher than HC and PD-FOG. The bilateral parietal cortex has been shown to interact with WM and visual attention during dual-task demands. While the left parietal cortex strengthens the effect of WM content to guide attention toward matching visual targets, the right parietal cortex suppresses the effect of irrelevant visual distraction [201]. As a result, reported higher upper alpha phase synchrony in PD+FOG and its association with

FOG severity, especially on the right parietal areas at deeper networks, indicate that defective competition between WM with demands for subject's attention in the environment could be considered as an underlying mechanism for FOG. This view is also consistent with previous studies that reported the association of visuospatial processing deficits and attention of the patient with FOG during walking [2][175][208].

Frontoparietal theta phase synchrony at superficial networks and abnormal PAC involving theta frequency bands were other remarkable FOG-associated features. Prefrontal theta is phase-locked to hippocampal theta activity, and the frontoparietal theta is associated with visual WM [197][209]. Interestingly, a strong interplay between theta and posterior alpha phase has been reported in the literature [197][204][210]. While posterior alpha activity is related to intuitive thinking and results in autonomic access to long-term memory, frontal theta activity is correlated with analytic thinking, which is reflective of cognitive control, WM, and attention [210]. Theta frontoparietal coupling and a parallel decoupling of anterior regions in the upper alpha band have been introduced as plausible candidates for the neural correlates of the central executive function of WM [204]. Consequently, this suggests that frontoparietal theta phase synchrony in more superficial networks might be a compensatory mechanism for higher alpha phase synchrony in the deeper neural pathways in PD+FOG. Moreover, high coupling between the phase of theta and the amplitude of low and high beta suggests the possible fundamental role of theta on abnormalities associated with FOG in the beta frequency band. The interplay between upper alpha and theta in WM relies on the prioritization of

relevant information and suppression of irrelevant information. While prioritizing relevant information has been linked to theta frequency neural oscillations in the lateral prefrontal cortex, suppressing irrelevant information has been linked to alpha oscillations in the occipito-parietal cortex [211]. Therefore, it can be concluded that in the case of PD+FOG, the impairment in visual attention in the deeper networks might be compensated by visual WM in more superficial networks as coherence in the frontoparietal network has been suggested to play a role in top-down control of spatial attention [212][213]. A recent study indicated that theta rhythms temporally resolve potential functional conflicts by periodically reweighting functional connections between higher-order brain regions and sensory or motor regions [214]. Although gait is generally considered as an automatic movement, cortical control seems necessary to adapt gait patterns to environmental constraints [172]. The abnormal frontoparietal high alpha and theta phase synchrony, along with an imbalance between left and right parietal alpha and theta phase synchrony, suggest the overemphasized visuospatial attention in PD with FOG patients. In other words, unsuppressed irrelevant visual distractions might trigger FOG events, which have been described previously while walking toward doorways, and also when cued to turn in the opposite direction [130][215][216]. When the temporoparietal cortex integrates visual, proprioceptive, and vestibular sensory information timely, the PM and SMA can generate the motor program accurately. This is especially true in an unfamiliar environment [49][167]. However, perceptual malfunction of visual inputs during locomotion planning might result in decreased speed and FOG episodes [130][217][218][219].

These findings are also consistent with structural abnormalities associated with FOG such as increased FOG with either left or bilateral stimulation and decreased by right STN stimulation and the fact that reduction of the grey matter in the left parietal lobe contributes to FOG in PD [18][220][221]. Consistent with the aforementioned points, PD+FOG showed significant dopaminergic deficits in the left caudate nucleus, which exhibited altered functional connectivity with regions of the visual network and possibly visual WM in deeper networks [222]. In HC and PD-FOG, alpha phase synchronization between parietal areas and M1 might therefore indicate effective connectivity between these areas resulting in a balance between attention and target task [191].

A remarkable difference between PD groups without and with FOG was that PD-FOG represents similar distributions (frontoparietal PLV between Cp2- Fz, Cp2-Fc1, Cp1-Fc2), but over a different frequency band: low beta. PD+mFOG also represents similar frontoparietal interhemispheric patterns in the low beta frequency range at the superficial networks (with SL) between Cp2 and Fc2 as well as Cp2 and Fz, which corresponds to the low beta phase synchronizations in PD-FOG at deeper networks. Frontoparietal low beta phase synchrony in PD-FOG suggests similarity and fundamental differences between PD with and without FOG. Firstly, this pattern suggests that the frontoparietal phase synchrony in alpha versus beta can be the identifier of the fundamental difference between PD with and without FOG at deeper layers. Since large-scale phase synchronization of brain rhythms has been suggested as a main concept in neural processes underlying cognition [76][223], low beta frequency band phase

synchrony in frontoparietal networks in PD-FOG might indicate the exclusive neural activities and information transmission only about the task on hand, representing limited attention [224][225][226]. Regarding the functional role of low beta, very little was found in the literature on low beta synchrony. However, low beta oscillation of the prefrontal cortex was suggested to provide a substrate for an episodic buffer for WM, allowing a combination of executive commands (e.g., from PFC) and multimodal information into a flexible and updatable representation of recent sensory inputs [226]. The introduced alpha and beta interplay in PD with and without FOG might thus shed some light on the underlying mechanisms of the disease that lead to different symptoms in the patients.

Exaggerated low-beta power in global as well as local oscillatory synchronies in the beta frequency band within BG-thalamo-cortical network is a hallmark of PD pathophysiology [227], especially in PD with FOG. There is also evidence that there is a significant correlation between alpha and beta power spectrum and L-dopa intake, implying the role of dopaminergic mechanisms in the modulation of alpha and beta oscillations [228]. Low beta has been introduced as a locomotion-related feature in the mesencephalic locomotor region (MLR) [229]. Lack of beta phase synchrony in the PD+FOG in deeper networks is consistent with the recent findings that suggest that FOG emerges when altered cortical control of gait is combined with a limited ability of the MLR to react to that alteration [230], which might be due to environmental changes or visual attention. The increased beta amplitude may also indicate that the frontal generated motor plans failed to reach the motor cortex, resulting in the FOG events

[16]. As a consequence, coupling of the phase of theta and high alpha with low beta amplitude in PD+FOG could be considered as a compensatory mechanism for the lack of beta phase synchrony in the deeper networks.

These findings provide key new information for the basic understanding of underlying mechanisms of FOG in the field. The results of the study suggest that the breakdown during FOG in the frontal lobe-BG-thalamo-cerebellar-brainstem network, which controls gait [35], could be a result of not properly adapting to environmental stimuli. Moreover, drawn from the results and their interpretation, the large-scale frontoparietal phase synchrony of theta, alpha, and beta frequency bands along with the PAC between these frequency bands may be a useful biomarker of the severity of FOG, as well as a differential biomarker for PD with and without FOG. The phase of the brain oscillations provides a reliable yet noninvasive tool to investigate connectivity between various brain regions that can open a new window towards possibly a unified mechanism for FOG development and occurrence. However, it should be noted that, in the current study, the reference electrode was located on the soft tissue of the earlobe, contamination of which may cause distortions in PLVs. Although reference-free PLVs are also provided after applying SL, further research with other types of common reference EEG is required to confirm the PLV findings related to common reference EEG in this study.

Besides, the investigated frequency range was limited to 0.05 Hz to 35 Hz in this study. The phase of the ultra-slow oscillation (<0.05 Hz) affects the slow oscillations such as theta

and alpha and possibly higher oscillations [55]. So, it is crucial to investigate the association between the phase features of ultra slow cortical potentials and FOG. Moreover, lack of left parietal low alpha phase synchrony at superficial layers might be related to the auditory cue during the movement task in the current protocol [231][232]. Further research should be undertaken to investigate the role of the phase of the left parietal low alpha frequency band in FOG. In addition, current study involved only cue-based movement execution tasks, further studies involving self-paced movement can help with developing a full picture of brain oscillations phase synchrony associated with FOG. Studies with more focus on phase synchrony patterns in multiple FOG subgroups, including cognitive, limbic, and motor subtypes can also help clarify the role of each frequency band phase synchronization in FOG. In addition, as previously mentioned, the frontoparietal theta is considered to be associated with visual WM. On the other hand, prefrontal theta is phase-locked to hippocampal theta activity [197][209]. The amplitude of theta also varies with the temporal evolution of FOG episode. Despite the importance of this frequency band in FOG, to the best of authors knowledge phase feature of theta has not been investigated in FOG in subcortical regions [128]. Considering the coupling between the phase of theta and the amplitude of beta, it is worthwhile to investigate the phase of theta at both cortical and subcortical layers before or during FOG episodes.

Chapter 5

Altered EEG Phase-Amplitude Coupling between Theta, Alpha, and Low Beta During Freezing of Gait in Parkinson's Disease

This chapter aims to study the PAC between theta, alpha, and beta frequency bands across various cortical regions during gait-related tasks, including normal walking and freezing episodes. The method employed is based on mutual information PAC, capturing transient PAC between two frequency bands. Results from this chapter provide significant insights into the underlying mechanisms of FOG and suggest EEG signatures for use in BCI-based rehabilitation devices, noninvasive and deep brain stimulation therapeutic pathways. This chapter is ready to submit to Brain Communications.

5.1 Introduction

Freezing of Gait (FOG) is an episodic gait disturbance in PD patients that frequently leads to falls and injuries due to its sudden and unpredictable nature [4]. FOG is often categorized as a motor symptom resistant to dopaminergic therapy and observed in approximately 27% of PD patients during the early stages of the disease, while its incidence can increase to up to 86% in the advanced stages [4][39][233]. FOG is typically triggered by specific circumstances, such as initiating gait, turning, passing through narrow spaces, avoiding obstacles, or approaching a destination [2][234]. The exact mechanisms involved in

FOG are not yet fully understood, but it is widely accepted that FOG is a multifactorial problem that involves impairments across multiple domains, including motor, perceptual, and cognitive [2][235]. FOG is therefore suggested to arise from a functional disruption of a widely distributed neural network rather than structural damage to specific cortical or subcortical motor areas [236].

Emerging research into the brain network dynamics associated with FOG suggests that altered oscillatory patterns in several cortical and subcortical structures may contribute to the pathophysiology of this severe motor symptom [16][176][237]. Although the electrocortical dynamics and cortical contribution during gait in humans (upright walking) remain areas of ongoing research [238], evidence suggests that the complex and dynamic act of walking requires coordination among multiple brain regions at the cortical level, such as the supplementary motor area (SMA), premotor area, and primary motor cortex (M1), where precise motor programs are initiated and sent to the basal ganglia (BG) for refinement as well as to other subcortical areas [239]. Consequently, in recent years, there has been a growing interest in exploring brain oscillations and their mechanisms, given their role in the coordination and organization of these multiple brain areas, especially in relation to locomotion control and motor disorders. In the past decade, several studies have been conducted, primarily centred on amplitude and power spectrum analysis, to explore alterations in brain oscillations linked to FOG. However, the field has yet to establish a comprehensive and cohesive understanding of the neurophysiological mechanisms underlying FOG. Nevertheless, these

studies revealed FOG associated abnormalities within slow cortical potentials, theta, alpha, beta, and gamma frequency bands across multiple brain regions, including the frontal and parietal lobes, motor cortex, subthalamic nucleus (STN), pedunculopontine nucleus (PPN), and mesencephalic locomotor region (MLR) [16][17][127][184][240][241][242][243]. PD patients with FOG compared to those without FOG showed lower movement-related cortical potentials, reduced mid-frontal theta (4-8 Hz) power, increased midfrontal beta (13-30 Hz) power, increased high-beta (21-35 Hz) activity in the STN (during the OFF dopaminergic medication), and greater coherence in the theta band (4–8 Hz) in frontotemporal-occipital networks [17][24][127]. Abnormal coherence was also noted between the low-beta component (at C3 and C4) and high-beta frequency band (between the STN and the SMA at Cz) in PD patients who experience FOG [17]. In addition to oscillatory irregularities that were specific to PD patients with FOG compared to those without FOG and healthy individuals, certain oscillatory abnormalities were transient abnormalities that were present before or during actual FOG events both at cortical and subcortical regions. An increase in theta band power during FOG episodes within the central and frontal areas and an increase in beta activity over the parietal area during the transition from normal gait to FOG events have previously been reported [128]. Additionally, one study examining the transition from normal gait to FOG episodes, reported transient abnormalities in theta, alpha, and beta oscillations associated with FOG occurrence. These abnormalities, based on power and amplitude features of cortical oscillations, were noted in the central, parietal, and occipital areas during the transition period [244]. At the

subcortical level, the power of the low-beta and theta bands was reported to increase during FOG episodes, along with an increase in the amplitude of theta and beta bursts in STN [245]. Decoupling between the cortex and STN in the [4 13] Hz frequency range was also reported during FOG episodes. At the same time, interhemispheric STN coupling reported to be stable across theta, alpha, and beta bands during both normal walking and FOG episodes [41].

The amplitude of the higher frequencies is modulated by the phase of the lower frequency bands as an intrinsic rule of neural organization [83]. However, despite various amplitude abnormalities associated with FOG, phase-related features of the brain oscillations have been rarely investigated in relation to this phenomenon. In our recent study, phase synchronization of the brain oscillations in PD patients with FOG was investigated, and the results demonstrated significant abnormalities in the phase of different frequency bands between 0.05 Hz and 35 Hz at a large cortical scale in relation to FOG [246]. Our earlier analysis demonstrated that, during a simple lower limb movement, PD patients who experience FOG showed a significant prevalence of interhemispheric frontoparietal alpha phase synchrony, while PD patients who did not have the condition presented high beta phase synchrony [246]. In addition, our phase-amplitude coupling (PAC) analysis revealed abnormal coupling between theta and low-beta frequency bands in PD patients with severe FOG in the superficial layers over frontal areas during lower limb movement preparation and execution. In deeper brain networks, high PAC between the theta and alpha frequency bands was observed over parietal areas in PD patients with severe FOG. Additionally, alpha and low-beta frequency

bands exhibited PAC over frontal areas in PD groups with FOG [246]. Beside our study, PAC between high-beta and gamma frequency bands over the primary motor cortex was recently identified during freezing episode events [19]. Meanwhile, elevated coupling between the phase of beta band oscillations and the amplitude of gamma activity in the arm area of the primary motor cortex was previously recognized as a characteristic feature of PD [247]. These findings, combined with the knowledge that slower rhythms phase-modulate the power of faster rhythms, suggest that PAC alternations between different frequency bands could potentially contribute to FOG occurrence. Therefore, in this study, we aim to investigate PAC between theta, alpha, and beta frequency bands during normal walking and freezing episodes in PD patients with FOG and compare PAC patterns with PD patients without FOG as well as healthy controls (HC). The findings from this study provide a more profound understanding of neural coupling patterns associated with FOG, thereby lays the groundwork for developing novel non-invasive and effective therapeutic pathways for this complex phenomenon.

5.2 Materials and Methods

5.2.1 PD Patients and Healthy Participants

Twenty-four participants were included this study, nine (0 female) PD with FOG (PD+FOG), seven (1 female) PD without FOG (PD-FOG), and eight (1 female) age-matched HC. PD participants were recruited from the Movement Disorders Research and Rehabilitation Center at Wilfrid Laurier University (Waterloo, Ontario). Those with any head trauma, history

Table 5-1. Mean ± standard deviations for participant demographics and clinical characteristics.

	HC	PD without FOG	PD with FOG
N (male/female)	8 (7/1)	7 (6/1)	9 (9/0)
Age(year)	79.25 ± 6.18	76.57 ± 7.63	81.66 ± 4.55
Disease duration (year)	N/A	9.43 ± 6.67	9.55 ± 6.3
UPDRS-III	N/A	26.14 ± 7.62	35.77 ± 12.07
LED (mg/day)	N/A	370.28 ± 273.7	595.11 ± 507.08

Abbreviations: HC, Healthy Controls; UPDRS-III, Unified Parkinson's Disease Rating Scale–III; LED, Levodopa Equivalent Dose.

of other neurological disorders, severe vision or hearing problems, or severe movement control limitations were excluded. All participants with PD were on their regular antiparkinsonian medications and were assessed using the Unified Parkinson's Disease Rating Scale (UPDRS). PD with FOG was identified by the answer to question 14 in MDS-UPDRS-III (motor subsection) and the severity condition was further assessed by videotaped freezing episodes during the experimental sessions. For all PD patients, an experienced clinician initially assessed the patients who expressed FOG experience and reconfirmed the occurrence of FOG according to a standardized protocol [248]. The experienced clinician then verified the severity of FOG according to the videotaped walking tasks. To be specific, all participants were instructed to perform 20 trials of videotaped walking tasks on a 20-ft walkway, and only PD patients with FOG who experienced FOG episodes longer than 3 s during turning or normal walking were considered as PD with severe FOG and included in this study. Healthy participants were recruited from The Waterloo Research in Aging Participant (WRAP) pool at the University of Waterloo. Sample size was determined by the availability of PD with FOG

participants. The study was approved by the Research Ethics Boards at both the University of Waterloo and Wilfrid Laurier University. All participants provided written informed consent prior to the experiment in accordance with the Declaration of Helsinki. Participants were matched for age, severity of motor symptoms (UPDRS), levodopa equivalent dose (LED), and disease duration. Further details of the experimental setup can be found in our previous paper [246].

5.2.2 Experimental Protocol

During the experimental session, all participants were initially asked to perform a set of simple lower limb ankle dorsiflexion (AD) tasks while remain seated. This part of the data was used to calibrate the artifact removal algorithm in this study. More details about the experimental protocol for the initial session can found in [184]. Next, participants were instructed to complete three distinct walking tasks while walking on an electronic walkway (Zeno Walkway – ProtoKinetics) at their self-selected pace and following auditory cues.

In the first task, participants performed a walking paradigm through a narrow gate (10 feet long and 7 feet high) without any auditory cues. This narrow gate was utilized to elicit FOG episodes [249]. In the second task, following the "go" auditory cue, the participants would walk on the same walkway without any narrow gate and stop after hearing the "stop" auditory cue. Finally in the third task, participants were instructed to start walking after hearing the "ready" and "go" auditory cues with a 2-second interval between them. Following the ‘go’ cue,

they would walk through the narrow gate, perform a 360-degree turn after passing the gate, and stop. Each participant completed a minimum of four trials for each walking task, with breaks taken between them as requested. Figure 5-1 represents the experimental setup for three walking tasks.

5.2.3 Data Acquisition and Preprocessing

The electroencephalogram (EEG) data was acquired by a 32-channel wireless EEG system (g.Nautilus, Guger Technologies, Austria), sampled at a rate of 250 Hz. EEG signals were collected from 17 channels following the 10-20 international standard positions: FP1, FP2, AF3, AF4, F3, Fz, F4, FC1, FC2, C3, Cz, C4, CP1, CP2, P3, Pz, and P4. The reference electrode was placed on the right ear lobe. For all participants, electromyography (EMG) was acquired by an 8-channel TeleMyo 2400 system (NORAXON INC). Four wireless EMG sensors were placed on the tibialis anterior (TA) and the soleus muscles (SOL) of both legs, each sampled at a frequency of 1000 Hz. Gait features were collected using the 20-ft ProtoKinetics Zeno Walkway (ProtoKinetics, Haverton, Pennsylvania), wherein patients were instructed to walk between the edges of the walkway, with green tape positioned one meter away from the start and end of the mat as the start point for each trial. The ProtoKinetics PKMAS software was then used to convert the data on spatiotemporal gait parameters. Gait

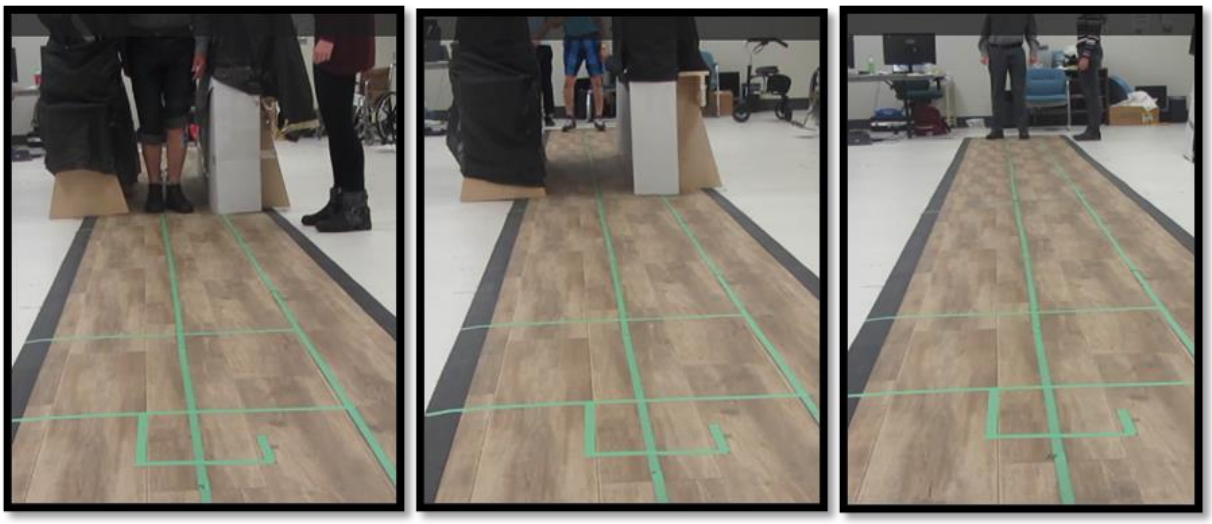

(a) (b) (c)

Figure 5-1. Experimental setup: Three groups of participants were asked to walk on an electronic walkway of 10 m length marked with green tape: (a) and (b) with narrow gate, (c) without narrow gate.

features for five recording sessions from PD+FOG were not available due to software malfunction.

Prior to EEG data pre-processing, the EEG data and synchronized EMG and walkway data (if available) from PD+FOG were labelled in accordance with the video viewing. To differentiate FOG episodes and normal walking, a set of standardized and performance-based criteria was utilized [234]. FOG episodes during walking straight ahead trials were identified across all recorded trials from PD+FOG group. FOG was defined as an unintentional and temporary failure of forward progression of the feet [91][250]. Freezing during walking was defined as an unintended pause in stepping while walking on the Zeno walkway. An FOG

episode was determined to be over when the participant managed to take a minimum of two steps close to their usual stride length [250]. For PD+FOG who had walkway gait parameters, center of pressure (COP) and gait velocity were used to reconfirm normal walking and FOG episodes. For PD+FOG group, the time series with FOG episodes and normal walking (from each task that could include multiple trials), were subsequently selected for the EEG pre-processing phase. Similarly, walking tasks that involved walking straight ahead and included at least 6 seconds of 'Normal Walk' in individual trials were selected for EEG data preprocessing in other groups.

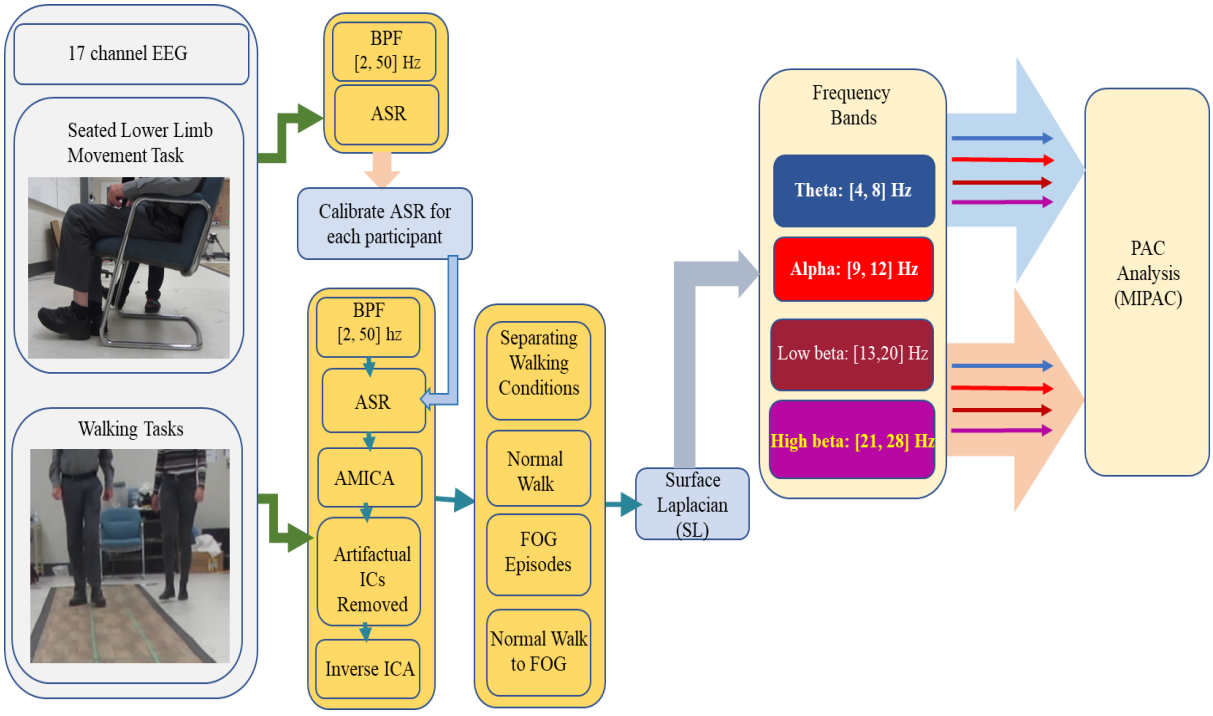

Figure 5-2. Steps in EEG processing and PAC analysis.

5.2.3.1 EEG Data Processing

Selected EEG time series of different walking tasks were initially band pass filtered between 2 and 50 Hz using a third order Butterworth filter (*filtfilt* MATLAB function). In order to remove artifacts form the walking task EEG time series, a combination of artifact subspace reconstruction (ASR) and adaptive mixture ICA (AMICA) was applied to the time series [251][252]. To calibrate ASR, we utilized data collected while the participants were seated and either performing or imagining a simple lower limb movement task. This task was selected to minimize any movement artifacts. The training data set was also ASR filtered. To remove artifacts from ASR training data set, ASR was applied to all channels. Time periods with a standard deviation exceeding 4, flatline channels lasting for 5 seconds, channel correlations below 0.8, and line noise surpassing 4 were removed from all channels, with other parameters being disabled (ASR version 2.1). AMICA was subsequently applied to EEG data to remove artefactual components from the data using EEGLAB graphical user interface. To remove artefactual ICs, ICLabel which is an automated EEG independent component classifier was initially applied and any artefactual components with 80 percent chance to be artifact were removed [253]. Surface Laplacian was then applied to Fz, Cz, Fc1, Fc2, Cp1, and Cp2 by subtracting the averaged signal of the four surrounding orthogonal electrodes from the center electrode [246]. Following the pre-processing phase, we extracted three distinct data sets for subsequent analysis:

A) Initially two sets of non-overlapping 6-s epochs were extracted from the data:

1) Normal walking (NW): identified as 6-s epochs in which the participant walks with normal strides.

2) Freeze episodes (FE): identified as 6-s epochs of severe FOG.

The 6-s length is determined based on the length of FOG episodes observed across all participants.

B) Secondly, we noted that some PD+FOG patients only experienced brief freezing episodes (< 2 s). Therefore, in addition to the NW and FE conditions, trials containing short FOG episodes were also extracted from PD+FOG walking tasks:

3) Normal walking to freeze episode (NW to FE): identified as 3-s epochs containing 2 s of normal walk followed by a short episode of FOG (less than 2 s). These epochs did not overlap with data in the NW and FE conditions.

Following the data extraction, PAC analysis was later performed for theta (4-8) Hz, alpha (9-12) Hz, low-beta (13- 20) Hz, and high-beta (21-28) Hz. The steps involved in our pre-processing pipeline and PAC analysis are illustrated in Figure 5-2.

5.2.4 Analysis of PAC

Mutual information-based phase-amplitude coupling PAC (MIPAC), which was used to quantify the PAC [84], was implemented using the PACTools plug-in for EEGLAB [254].

In detail, the PAC was estimated from the local mutual information (MI) between the phase φ_t and amplitude A_t time series. Phase and amplitude signals were initially obtained from bandpass filtering EEG segments into a low frequency band and a high frequency band using a two-way zero phase lag finite impulse response (FIR) filter. The instantaneous phase of the low frequency bandpass filtered signal and the instantaneous amplitude of the high frequency filtered signal were then extracted using the Hilbert transform. This PAC estimation method allowed a temporal dynamic description of PAC within a relatively short time window [84].

The obtained PAC values were then normalized by calculating the z-score obtained from surrogate data analysis. For each PAC estimate, 200 surrogate measures were generated using a randomized shuffling of the phase and amplitude time series, which were first divided into 20 segments. By shuffling the segments across latencies, a new PAC measure estimate was derived to obtain a distribution of MIPAC estimates that conforms to the assumption of PAC being absent beyond the chance level.

This process was repeated 200 times to ensure reliable results [255]. The mean, standard deviation, and MIPAC z-scores were calculated for each surrogate data set:

$$Z_{surr} = \frac{PAC_{measure} - \mu_{Surr}}{\delta_{surr}} \tag{5-1}$$

where μ_{Surr} and δ_{surr} are the mean and standard deviation of the surrogate PAC values, respectively.

5.2.4.1 Feature Extraction:

To quantify and compare z-scored PAC values of NW and FE conditions on a single-trial basis without losing the benefit of the temporal resolution of MIPAC, we defined a new feature by calculating the average z-scored PAC values of each trial over non-overlapping 2-second windows. Therefore, the PAC epochs of 6-s duration for each trial of NW or FE condition was initially divided into 2-s epochs. The values of z-scored PACs were then averaged across all time points in each epoch. To examine the PAC values across different frequency sub-bands, the PAC values within windows covering all included phase frequencies and amplitude frequencies of 2 Hz, 3 Hz, 4 Hz, 5 Hz, 6 Hz, and 7 Hz were averaged across all epochs for each condition. These windows were shifted in 0.5 Hz steps over the amplitude frequencies, and the resultant averaged PAC values were statistically compared.

5.2.5 Statistical Analysis of PAC

To assess the statistical significance of z-scored PAC over non-overlapping 2-s windows in each condition, we conducted one-way analysis of variance (ANOVA) on the averaged values to examine the differences among groups and conditions (in case of PD+FOG). Only windows demonstrating significant differences between PD with FOG during FOG episodes and all other three conditions were examined for further post hoc analysis. Tukey-kramer post hoc tests was then performed where significant group effects were found. In all analysis the

significance level was set to 0.01. All statistical analyses were performed using Matlab (2022b).

5.3 Results

Overall, 16 patients were included in this study and results of the participant demographics and clinical characteristics are outlined in Table 5-1. HC, PD-FOG, and PD+FOG groups were matched for age [$F_{(2,21)} = 1.37$, $p = 0.27$]. PD without FOG and PD with FOG were also matched for UPDRS, levodopa equivalent dose (LED) and disease duration ($p = 0.09$, $p = 0.3$ and $p = 0.97$, respectively). All participants were able to walk unaided during their sessions except patient SUB-8 and SUB-9 in the PD+FOG group who expressed a preference for the use of a walking aid. Patient SUB-6 and SUB-7 participated in the experiment twice, with a four-month interval. In both sessions, they were identified as PD+FOG. For all participants except five participants from PD+FOG, including SUB-2, SUB-4, SUB-5, SUB-6 (first session), and Sub-7 (first session), gait features were not available. To investigate neural activity patterns during NW and FE conditions in PD+FOG, we extracted EEG data from 21, 23, and 23 6-s long NW trials of HC, PD-FOG, and PD+FOG, respectively. Additionally, we obtained 25 trials of 6-s long FE for PD+FOG. Furthermore, we identified eight trials of normal straight walking with short FOG episodes that did not overlap with the long FOG episodes and conducted PAC analysis on 2 seconds before and 1 second after the identified short freezing

episode onset. The trials were aligned with respect to FOG onset such that every trial has 2 seconds of normal walking resulted in FOG onset.

5.3.1 Altered PAC between theta and low beta during FOG episodes

Figure 5-3 shows the comodulograms of grand average z-scored PAC maps across trials for each condition and group for each channel over theta and low-beta as well as high-beta frequency bands. We observed that, during FE, the high PAC values with statistical significance were present between theta and lower beta frequency bands, particularly between 14.5 Hz and 16.5 Hz, over Fc1, and Cp2, while no such PAC was present in other conditions (see the dashed brown lines of Figure 5-3 (a)). The boxplots for PAC values between theta and 14.5 to 16.5 Hz are presented in Figure 5-3 (c) and (d). The PAC values of FE over both Fc1 and Cp2 were significantly higher than HC, PD-FOG, and PD+FOG during NW condition (p<0.01). Additionally, the coupling between theta phase and the amplitude of low beta ([14.5, 16.5] Hz) in PD+FOG during NW over Fc1, was significantly higher than HC and PD-FOG during NW ($p < 0.01$).

5.3.1 PAC Altered PAC between alpha and low-beta during FOG episodes

Figure 5-4 shows the comodulograms of grand average z-scored PAC maps across trials for different conditions and groups for each channel over alpha and low-beta as well as high-beta

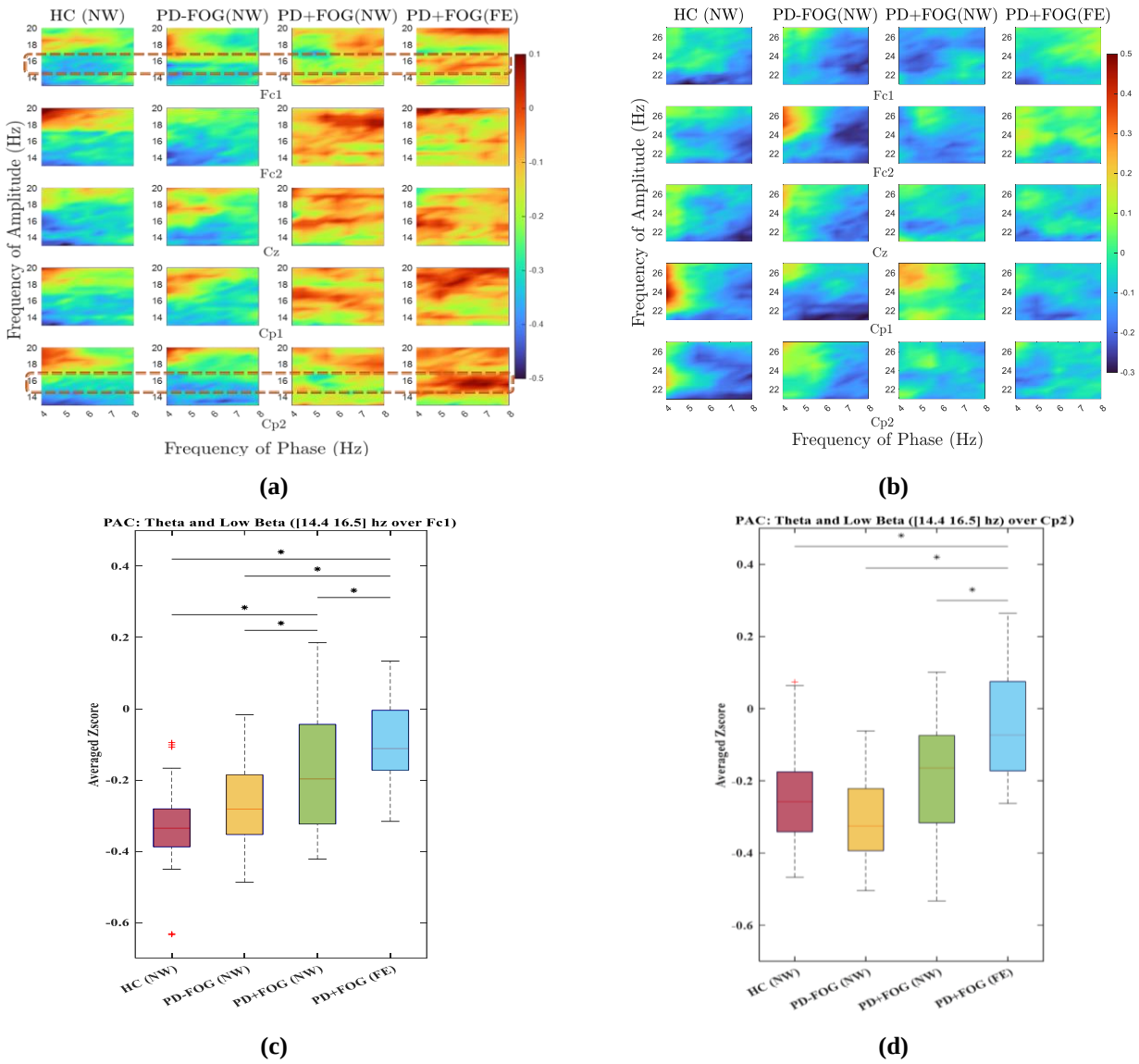

Figure 5-3. Comodulograms representing averaged z-scored PAC values for three groups during NW and FE conditions in PD+FOG. The PAC values were averaged across time points and trials for five Laplacian-filtered channels. (a) Comodulograms show PAC values within the frequency range of theta and low-beta, with dashed brown lines indicating the abnormal frequency band in which PD+FOG during FE. Inter-group comparison revealed significant differences in theta phase and low-beta amplitude, particularly in the [14.5, 16.5] Hz coupling over FC1 and Cp2 (p<0.01). (b) Comodulograms show PAC values within the frequency range of theta and high-beta, with no significant PAC values observed in this frequency band. (c) and (d) represents boxplots of averaged z-scored PAC values across trials over theta and low-beta frequencies ([14.5-16.5] Hz over Fc1 and Cp2 for HC, PD-FOG, PD+FOG during NW, and PD+FOG during FE. The asterisk (*) indicates significant differences between groups (p<0.01).

frequency bands. The results indicated that PAC between alpha and low-beta frequency bands in Cp2, particularly over [14.5, 16.5] Hz, is significantly higher during FE compared to other groups ($p<0.01$). Boxplots of averaged z-scored PAC values between theta and low-beta

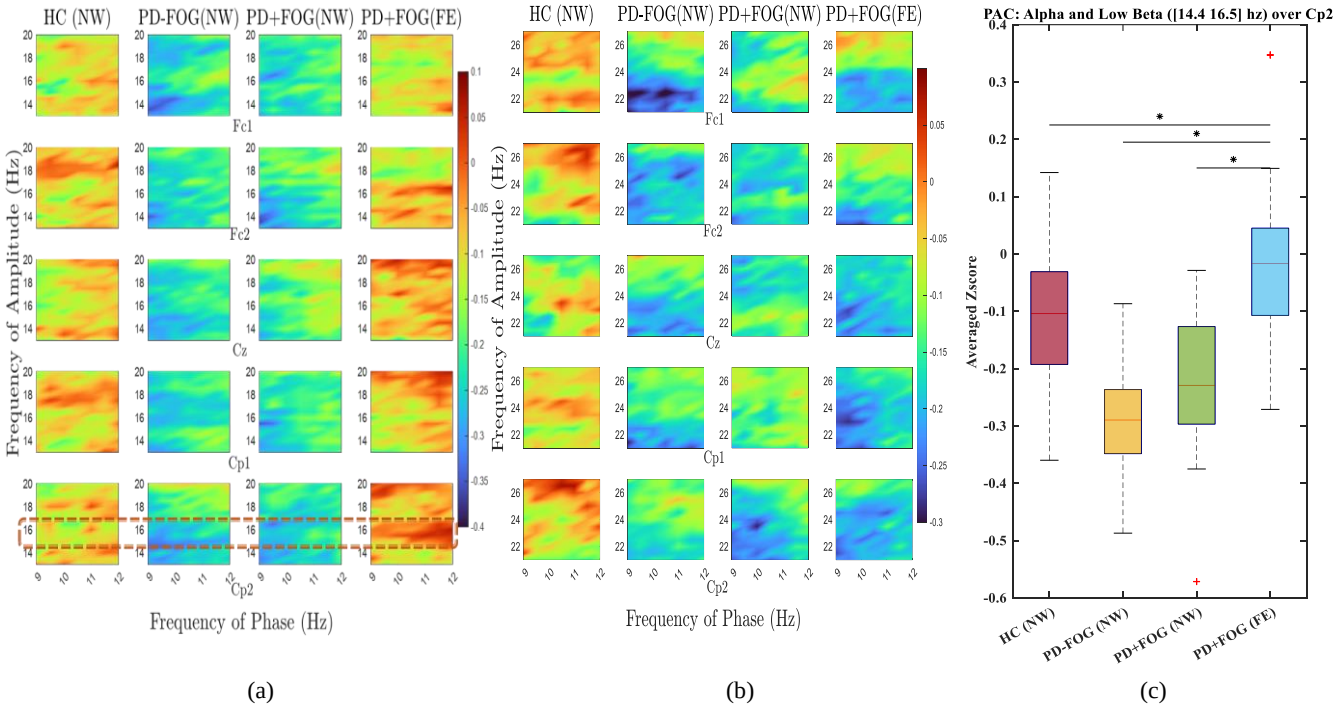

(a) (b) (c)

Figure 5-4 Comodulograms of averaged z-scored PAC values for three groups during NW and FE conditions in PD+FOG group. The PAC values were averaged across time points and trials for five Laplacian-filtered channels. (a) Comodulograms show PAC values within the frequency range of alpha and low-beta, with dashed brown lines indicating the abnormal frequency band in which PD+FOG experience freezing episodes. Inter-group comparison revealed significant differences in alpha phase and low-beta amplitude, particularly in the [14.5, 16.5] Hz coupling over Cp2 ($p<0.01$). (b) Comodulograms show PAC values within the frequency range of alpha and high beta, with no significant PAC values observed in these frequency bands. (c) Boxplot of averaged z-scored PAC values across trials over alpha and low-beta frequencies ([14.5-16.5] Hz over Cp2) for HC, PD-FOG, PD+FOG during NW, and PD+FOG during FE. The asterisk (*) indicates significant differences between groups ($p<0.01$).

([14.5, 16.5] Hz) over Cp2 are presented in Figure 5-4 (c). In addition to the significant FOG related PAC between alpha and [14.5 16.5] Hz over Cp2, PAC between alpha and low-beta frequency bands of PD+FOG during FE was higher in all channels compared to the NW condition of both PD+FOG and PD-FOG ($p<0.01$). However, it was not significantly different from HC, other than in Cp2 channel. Figure 5-4 (b) represents PAC values between alpha and high-beta frequency bands over all five channels. The results suggested that coupling between alpha and high-beta is lower in participants with PD compared to HC regardless of condition.

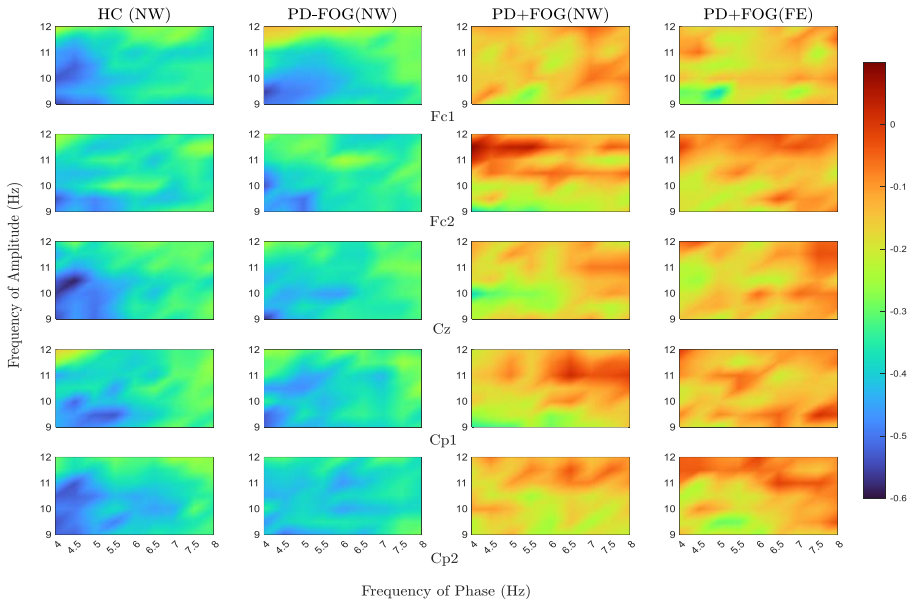

Figure 5-5. Comodulograms of z-scored PAC between theta and alpha frequencies for three groups during NW and FE conditions in PD+FOG. PAC values were averaged across time points and trials for five Laplacian-filtered channels. Inter-group comparisons revealed significant differences in PAC values between the PD+FOG group during both NW and FOG conditions and both HC and PD-FOG groups across all channels ($p<0.01$).

5.3.2 Elevated PAC between theta and alpha in PD+FOG group

Figure 5-5 represents the comodulograms of grand average z-scored PAC maps across trials for each condition and group over theta and alpha frequency bands. The results indicated that PAC between theta and alpha frequency bands is significantly higher in PD+FOG during both NW and FE conditions compared to PD-FOG and HC during NW (p<0.01). However, no significant difference was observed between PD+FOG during NW and FE, which is distinctively different from the PAC between theta and low-beta.

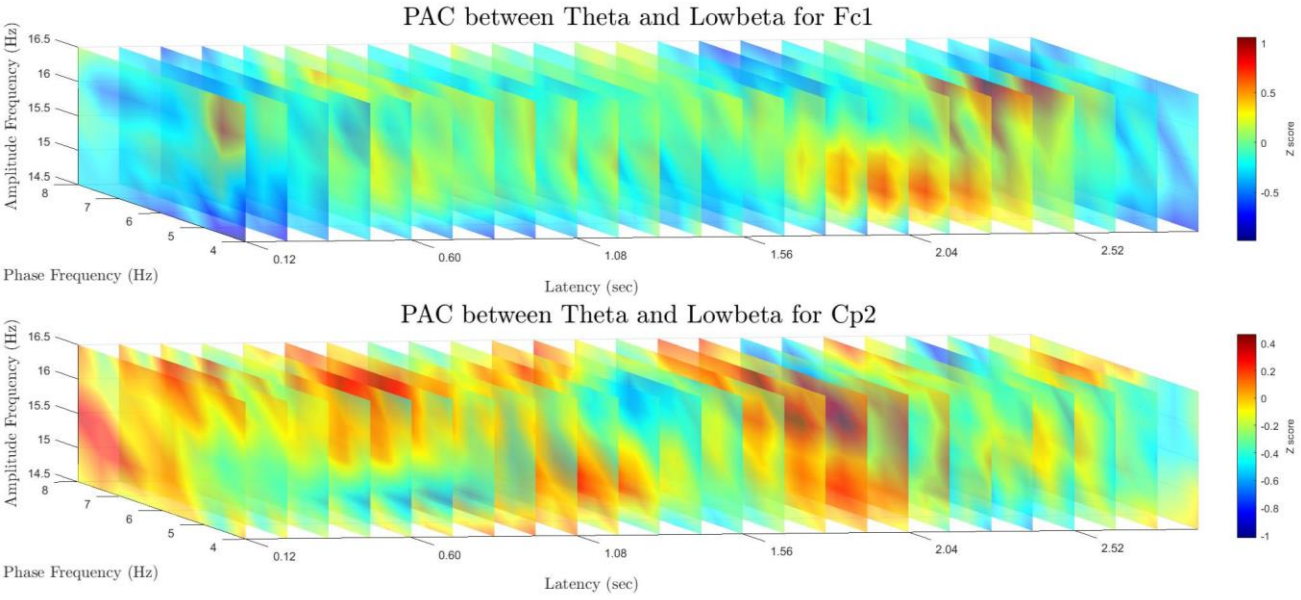

Figure 5-6. Temporal evolution of PAC between theta and low beta frequency bands ([14.5, 16.5] Hz) for Fc1 and Cp2 electrodes across eight aligned trials (with respect to FOG onset). Each trial includes two seconds of Normal Walk, followed by a brief episode of FOG. Time point 2 sec represents FOG onset.

5.3.1 Higher PAC between theta and low beta at FOG onset for NW to FE

Grand mean z-scored PAC across latencies was also computed for eight aligned trials over theta and low beta ([14.5, 16.5] Hz) frequency bands for normal walk followed by a short episode of FOG (less than 2 s) as presented in Figure 5-6. Temporal evolution of PAC between theta and low beta observable during FOG (~2-s represents FOG onset) confirmed the existence of PAC at the investigated frequencies. In Figure 5-6 only [-2, 1] s of the averaged z-scored PAC over the time course of effective walking to short FOG episodes are presented for Fc1 and Cp2.

5.4 Discussion

In this study, the alternations in PAC associated with FOG in lower frequency bands, including theta, alpha, and beta in PD patients without and with FOG as well as HC during effective walking and FOG episodes were examined. Results revealed that PAC patterns between theta and low-beta in PD+FOG patients during FOG episodes exhibit atypical pattern in comparison to HC, PD-FOG, and even within themselves during normal gait (i.e., when FOG is not occurring). The abnormal PAC occurred over the (pre-) SMA (Fc1) and parietal areas (Cp2). Notably, these PAC patterns demonstrated transient deviations in connection with FOG (Figure 5-6). Findings also demonstrated that the PD+FOG group generally manifests higher levels of PAC between alpha and theta frequency bands than both HC and PD-FOG, regardless of walking condition. Additionally, we found significantly higher PAC levels in the

alpha and low-beta frequency bands over Cp2 in PD+FOG during freezing episodes (Figure 5-4).

These findings underscore the significance of the theta frequency band in relation to FOG episodes. Theta oscillation, primarily generated in the hippocampus, plays a crucial role in spatial navigation, contextual interpretation, and memory. The bidirectional transmission of environmental signals between the neocortex and the hippocampus highlights the role of hippocampus in providing the neocortex with context for interpretation. This interaction is facilitated by the theta rhythm, which may act as a timing mechanism, ensuring the relevance and coherence of brain output in a dynamically changing environment to provide coordinated movement sequences and plan spatial navigation trajectories [256][257]. It is intriguing to consider that memory mechanisms might have developed from those governing physical navigation, suggesting a fundamental similarity between the neuronal algorithms driving real and conceptual space navigation [258]. Despite ongoing debates regarding the specific functional role of theta frequency oscillations [259], the significance of hippocampal theta in temporally structuring movement sequences, memory consolidation, and the planning of spatial paths is increasingly recognized [257]. Similar to other neural oscillation, theta is not unique to the hippocampus and theta coordinates neural networks across wide range spatial and temporal scales [260]. Theta band rhythms, primarily in the prefrontal cortex and mid-frontal areas, are associated with executive function, and conflict/error processing [261][262]. Mid-frontal theta, in addition to previously known alpha, has been recently introduced as a

moderator for visuomotor coordination when there is increased need of cognitive control. In this case, theta further moderates the well-established link between beta oscillations and visuomotor precision control [263]. Theta band abnormalities has been previously reported in association with FOG and has been highlighted as a key neural mechanism associated with executive processes in individuals with PD who experience FOG [127][128][245][264]. These processes are vital for effectively managing complex motor tasks such as gait and adapting to changes in the environment [264]. Theta abnormalities have been repetitively reported in relation to FOG. FOG-related decoupled theta synchronization between the cortex and STN [41] in addition to FOG-related low-beta and theta band activities within the STN area [245] represent the crucial role of this particular frequency band in adaptive locomotion control that involves widespread networks. Considering the observed abnormalities between the phase of theta with the amplitude of alpha and low-beta in association with FOG and previously reported amplified theta activities in frontal cortex and STN in response to conflict scenarios [265], altered PAC manifestations during FOG episodes over SMA and parietal areas might therefore suggest impairment in resolving conflicting information, possibly proprioceptive input in a real-world environment, that leads to FOG occurrence.

The findings of this study suggest that the amplitude of alpha was strongly linked with the phase of theta in PD patients with FOG during normal walking and FOG episodes, and this differed from the patterns observed in HC and PD-FOG. While alpha was traditionally studied in sensorimotor cortex and associated with an idling state of the sensorimotor system, recent

research indicates that alpha is involved in more complex and dynamic processes such as visuomotor processing in sensorimotor cortex, working memory (WM) encoding and maintenance, attention, and proactive inhibition [263][266]. In contrast, theta is involved in response to high levels of conflict and when task settings requires updating [266]. Recent research suggests that alpha oscillatory activity is responsible for maintaining representations in WM for intervals of several seconds, via stabilizing mechanisms that involve cortico-thalamic loops. However, when unpredictable information is encountered, these stability intervals are disrupted by sporadic bursts of inhibitory activity in the theta and delta frequency ranges, which leads to the suppression of excitatory patterns within the cortico-thalamic loops [266]. The prominent high coupling between theta and alpha oscillations in large-scale networks in PD+FOG may be attributed to the significant involvement of theta oscillations in visuomotor processes and the destabilization of WM via theta-triggered interruptions, particularly in PD with FOG experiencing unpredictable information or conflicts. Specifically, frontal cortex theta oscillations and occipito-parietal alpha oscillations have been identified as two distinct modes of thinking, and their functions have been also associated with prioritizing relevant information and inhibiting irrelevant information, respectively, in WM processes [210][267]. The significant high coupling between theta and alpha oscillations in large-scale networks may therefore indicate the inappropriate inhibition of prepotent responses in visuomotor processing in PD+FOG. Therefore, FOG may be linked to changes in the inhibition and release of motor programs rather than a general executive deficit.

High PAC between alpha and low-beta over parietal areas (Cp2) during freezing episodes is another finding of the current study. High PAC between alpha and low-beta over parietal areas (Cp2) as well as high coupling between theta phase and the amplitude of low beta over (pre-)SMA (Fc1) and parietal areas (Cp2) during freezing episodes represent the central role of low-beta in FOG events. As mentioned before, beta and its sub-bands have been repetitively reported to represent abnormalities associated with PD and FOG both at cortical and subcortical networks. Beta frequency range oscillations are extensively present across the motor system, and their modulation is influenced by dopaminergic medications. These oscillations are locally produced within STN and ventral intermediate nucleus of the thalamus [268] and are found in other subcortical regions such as PPN area of the MLR. Low beta, more localized in STN, and high beta, related to long-distance coupling, are two beta frequency sub bands that represent distinct properties related to motor functions [269]. Prolonged beta oscillations in the STN during FOG occurrence has been reported as a biomarker of FOG [237]. The control framework for human locomotion originates from the SMA, progresses to the BG for refinement, and ultimately converges with cerebellar inputs in the MLR, which descends to the spinal cord [179][270]. Crucial to supraspinal network is the STN, which receives direct afferents from the SMA and projects to both the MLR and the output nuclei of the BG which also project to the MLR [271]. The STN modulates the integration of cortical and cerebellar information by either activating or inhibiting the MLR. Theta oscillations in the midfrontal region are hypothesized to be produced by the dorsal anterior cingulate cortex and (Pre-) SMA.

These oscillations are considered to be a physiological mechanism that indicates the need for enhanced cognitive control, as evidenced by several previous studies that primarily employed conflict control tasks [263]. The abnormal coupling between the amplitude of low beta and the phase of theta as well as alpha might reflect a compensatory mechanism of locomotion control during FOG that emphasizes in the medial frontal cortex and particularly (pre-) SMA.

In this study, PAC was estimated using a recently introduced method (MIPAC), which is based on mutual information measures. Entropy based features have been previously introduced as neural correlates of FOG at both cortical and subcortical levels [243][272]. Among different PAC computing methods [273], which mostly utilize the instantaneous phase and amplitude of band-pass filtered signals to determine a metric reflecting the strength of coupling, this approach is based on a measure of the entropy of the phase-amplitude distribution and has been shown to yield reliable results in previous studies [274]. Importantly, MIPAC is one of the few PAC estimation methods that can be used to estimate time-resolved PAC with high temporal resolution. Hence, this method exhibits potential for investigating transient PAC that arises from FOG and can potentially be utilized for real-time detection or prediction of FOG episodes.

A major challenge in the research field of FOG is the identification of dependable biomarkers that can be obtained from real-life walking scenarios to guide more effective treatments and validate medical and therapeutic interventions. The findings of the current study

suggest that PAC between various frequency bands of brain oscillation can provide crucial insight into the neurobiological basis of FOG, and the potential to identify reliable biomarkers for FOG that can lead into novel therapies for FOG based on deep brain stimulation (DBS) and transcranial magnetic stimulation (TMS). In addition, the transient estimation of PAC used in this paper paves the way for identifying reliable EEG features to develop brain-computer interface (BCI)-based rehabilitative systems.

Chapter 6

Conclusion and Future Work

This chapter outlines the findings of the thesis and suggests potential future directions.

6.1 Summary and Concluding Remarks

FOG is a debilitating and poorly understood symptom of PD, with limited effective management options available. This thesis aimed to investigate novel EEG features associated with FOG and its severity, as well as EEG alterations related to FOG occurrence, using an integrative approach. The main objective was to uncover new insights that could potentially lead to the development of innovative therapeutic strategies, rehabilitative devices and neuromodulation paradigms, such as BCI, adaptive DBS, and TMS in addition to introducing EEG-based biomarkers for FOG diagnosis and monitoring.

The thesis primarily aimed to explore the amplitude and phase characteristics of low-frequency brain oscillations, particularly the low frequency movement-related EEG component known as MRCP, and higher frequency bands (theta, alpha, and beta) during a basic lower limb movement task. This analysis was conducted by comparing PD patients with and without FOG, as well as age-matched health controls. Notably, the analysis took into account sub-bands within each frequency band, considering their reported functional differences and the impact of dopaminergic treatments.

Chapter three demonstrated altered MRCP morphology in PD patients with FOG, which correlated with the severity of FOG during the lower limb task. Abnormalities in theta and beta frequency bands associated with FOG were also identified. These findings suggest that MRCP could potentially serve as a novel biomarker for FOG and its severity.

Chapter four explored the phase synchronization of investigated frequency bands in PD patients with FOG, revealing significant associations and differences between healthy individuals, PD patients without FOG, and PD patients with FOG. The results suggested that phase alterations in various frequency bands, along with abnormal large-scale phase synchronization in specific frequency bands, could underlie the reported abnormalities in beta frequency band power noted in the literature. Furthermore, the findings suggest that the phase synchronization linked to FOG and its severity has potential as biomarkers for the condition.

In the final chapter, the thesis investigated the relationships between the phase of lower frequency bands and the amplitude of higher frequency bands during normal walking and freezing episodes. We found significantly high PAC between theta/low-beta and alpha/low-beta frequency bands during FOG episodes, shedding light on this complex phenomenon and offering promising paths for FOG rehabilitation and treatment as well as potential biomarkers.

Overall, the findings of this thesis contribute to the interpretation of oscillatory activity associated with FOG, emphasizing the need to shift research focus towards meaningful relationships between brain oscillations and the importance of cortical involvement in FOG

development. These insights have the potential to advance our understanding of FOG and inspire the development of targeted therapeutic interventions.

6.2 Future Work

The current thesis represented significant EEG abnormalities associated with FOG, but there remains a lot to learn. There are several important questions that remain to be addressed in future studies.

The findings from Chapter three indicate that early components of MRCP, which have been utilized to predict movement up to 2 seconds before its initiation, are significantly reduced in PD patients with FOG. This discovery suggests that MRCP is not suitable for closed-loop BCI-base FOG rehabilitation applications as previously was suggested for stroke patients [275]. However, it is important to note that in our study, the measure used to align the MRCPs was the onset of movement (passing a threshold), and MRCP morphology was not investigated using aligned EMG based on the maximum contraction (EMG peak). Therefore, further investigation into MRCP in PD patients with FOG is required, specifically by considering EMG activities and patterns. Notably, clear patterns of EMG activities are evident during FOG episodes, particularly in the TA and Gastrocnemius muscles [25][276]. This highlights the importance of conducting necessary studies on leg muscle activation patterns and the interactions between brain activity and leg muscle activation. Specifically, there is a need to emphasize the examination of leg muscle activation patterns during FOG episodes. These

studies will contribute to a more comprehensive understanding of the mechanisms underlying FOG and may provide valuable insights into the potential use of leg muscle activation patterns in evaluating MRCP in PD patients with FOG.

While the sample size utilized in this thesis can be considered average, future research should aim to incorporate data from larger groups of individuals experiencing FOG. It is particularly important to note that the results concerning PD patients with severe FOG were based on data from only five participants. This limited sample size calls for a cautious approach in interpreting or generalizing the findings. Expanding the sample size to include a broader spectrum of individuals, both mild and severe freezers, will enhance our understanding of the condition and significantly contribute to the robustness of the biomarkers being evaluated. Moreover, the limited sample size makes it impossible to characterize within-group consistency for the introduced potential biomarkers. Although efforts were made to control potential confounders and ensure a homogeneous sample, variability within groups might still influence the results. Future research would benefit from incorporating methodologies specifically aimed at quantifying and addressing within-group variability. In addition, given the highly variable nature of FOG across patients and the multitude of factors contributing to FOG episodes, including more participants will aid in result generalization and facilitate analysis of FOG subtypes. Specifically, investigating FOG subtypes and other contributing factors such as left and right brain dominance, as well as the most affected side of the brain in PD, may have an impact on the outcomes.

The observation of these findings has prompted the suggestion that PAC and phase-related features have the potential to serve as control or trigger signals for controlling BCI-based exoskeletons, assistive devices, and adaptive DBSs. Although the algorithms employed have demonstrated effective removal of movement artifacts and noise, the real-time detection of FOG still requires robust and fast algorithms that can reliably identify FOG episodes based on the suggested EEG features.

References

[1] A. Fasano *et al.*, "Unfreezing of gait in patients with Parkinson's disease," *Lancet Neurol.*, vol. 14, no. 7, pp. 675–677, Jul. 2015, doi: 10.1016/S1474-4422(15)00053-8.

[2] J. G. Nutt, B. R. Bloem, N. Giladi, M. Hallett, F. B. Horak, and A. Nieuwboer, "Freezing of gait: Moving forward on a mysterious clinical phenomenon," *Lancet Neurol.*, vol. 10, no. 8, pp. 734–744, Aug. 2011, doi: 10.1016/S1474-4422(11)70143-0.

[3] B. R. Bloem, J. M. Hausdorff, J. E. Visser, and N. Giladi, "Falls and freezing of gait in Parkinson's disease: a review of two interconnected, episodic phenomena.," *Mov. Disord.*, vol. 19, no. 8, pp. 871–84, Aug. 2004, doi: 10.1002/mds.20115.

[4] B. R. Bloem, J. M. Hausdorff, J. E. Visser, and N. Giladi, "Falls and freezing of Gait in Parkinson's disease: A review of two interconnected, episodic phenomena," *Mov. Disord.*, vol. 19, no. 8, pp. 871–884, Aug. 2004, doi: 10.1002/MDS.20115.

[5] J. G. Nutt, B. R. Bloem, N. Giladi, M. Hallett, F. B. Horak, and A. Nieuwboer, "Freezing of gait: moving forward on a mysterious clinical phenomenon," *Lancet Neurol.*, vol. 10, no. 8, pp. 734–744, Aug. 2011, doi: 10.1016/S1474-4422(11)70143-0.

[6] N. Giladi and A. Nieuwboer, "Understanding and treating freezing of gait in Parkinsonism, proposed working definition, and setting the stage," *Mov. Disord.*, vol. 23, no. SUPPL. 2, 2008, doi: 10.1002/MDS.21927.

[7] S. K. Bansal, B. Basumatary, R. Bansal, and A. K. Sahani, “Techniques for the detection and management of freezing of gait in Parkinson’s disease - A systematic review and future perspectives,” *MethodsX*, vol. 10, Jan. 2023, doi: 10.1016/J.MEX.2023.102106.

[8] C. M. Gray, “Synchronous Oscillations in Neuronal Systems: Mechanisms and Functions,” *J. Comput. Neurosci.*, vol. 1, no. 9, pp. 11–38, 1994.

[9] J. M. Shine, S. L. Naismith, and S. J. G. Lewis, “The pathophysiological mechanisms underlying freezing of gait in Parkinson’s Disease.,” *J. Clin. Neurosci.*, vol. 18, no. 9, pp. 1154–7, Sep. 2011, doi: 10.1016/j.jocn.2011.02.007.

[10] L. Niu *et al.*, “Effect of bilateral deep brain stimulation of the subthalamic nucleus on freezing of gait in Parkinson’s disease.,” *J. Int. Med. Res.*, vol. 40, no. 3, pp. 1108–13, 2012.

[11] A. Delval, C. Tard, and L. Defebvre, “Why we should study gait initiation in Parkinson’s disease.,” *Neurophysiol. Clin.*, vol. 44, no. 1, pp. 69–76, Jan. 2014, doi: 10.1016/j.neucli.2013.10.127.

[12] A. Nieuwboer, “Cueing for freezing of gait in patients with Parkinson’s disease: a rehabilitation perspective.,” *Mov. Disord.*, vol. 23 Suppl 2, pp. S475-81, 2008, doi: 10.1002/mds.21978.

[13] A. M. Cebolla and G. Cheron, “Understanding neural oscillations in the human brain: From movement to consciousness and vice versa,” *Front. Psychol.*, vol. 10, no. AUG,

2019, doi: 10.3389/FPSYG.2019.01930.

[14] C. Gao, J. Liu, Y. Tan, and S. Chen, “Freezing of gait in Parkinson’s disease: pathophysiology, risk factors and treatments,” doi: 10.1186/s40035-020-00191-5.

[15] A. M. A. Handojoseno, J. M. Shine, T. N. Nguyen, Y. Tran, S. J. G. Lewis, and H. T. Nguyen, “Analysis and Prediction of the Freezing of Gait Using EEG Brain Dynamics.,” *IEEE Trans. Neural Syst. Rehabil. Eng.*, vol. 23, no. 5, pp. 887–96, Sep. 2015, doi: 10.1109/TNSRE.2014.2381254.

[16] J. S. Marquez *et al.*, “Neural Correlates of Freezing of Gait in Parkinson’s Disease: An Electrophysiology Mini-Review,” *Front. Neurol.*, vol. 0, p. 1303, Nov. 2020, doi: 10.3389/FNEUR.2020.571086.

[17] J. Toledo *et al.*, “High Beta Activity In The Subthalamic Nucleus And Freezing Of Gait In Parkinson’s Disease.,” *Neurobiol. Dis.*, vol. 64, 2013, doi: 10.1016/j.nbd.2013.12.005.

[18] N. G. Pozzi *et al.*, “Freezing of gait in Parkinson’s disease reflects a sudden derangement of locomotor network dynamics,” *Brain*, vol. 142, pp. 2037–2050, 2019.

[19] Z. Yin *et al.*, “Cortical phase-amplitude coupling is key to the occurrence and treatment of freezing of gait,” *Brain*, Apr. 2022, doi: 10.1093/BRAIN/AWAC121.

[20] A. R. John *et al.*, “Predicting the Onset of Freezing of Gait Using EEG Dynamics,”

Appl. Sci., vol. 13, no. 1, 2023, doi: 10.3390/app13010302.

[21] Z. Cao *et al.*, "Identification of EEG Dynamics during Freezing of Gait and Voluntary Stopping in Patients with Parkinson's Disease.", IEEE Trans. Neural Syst. Rehabilitation Eng. 29, 1774–1783. 2021, doi: 10.1109/TNSRE.2021.3107106

[22] E. E. Asher *et al.*, "Connectivity of EEG synchronization networks increases for Parkinson's disease patients with freezing of gait," *Commun. Biol.*, vol. 4, no. 1, Dec. 2021, doi: 10.1038/S42003-021-02544-W.

[23] D.-F. Liu *et al.*, "Synchronized Intracranial Electrical Activity and Gait Recording in Parkinson's Disease Patients With Freezing of Gait.," *Front. Neurosci.*, vol. 16, p. 795417, 2022, doi: 10.3389/fnins.2022.795417.

[24] M. Gérard *et al.*, "EEG-based functional connectivity and executive control in patients with Parkinson's disease and freezing of gait," *Clin. Neurophysiol.*, vol. 137, pp. 207–215, May 2022, doi: 10.1016/J.CLINPH.2022.01.128.

[25] M. Günther *et al.*, "Coupling Between Leg Muscle Activation and EEG During Normal Walking, Intentional Stops, and Freezing of Gait in Parkinson's Disease," *Front. Physiol.*, vol. 10, p. 870, 2019, doi: 10.3389/fphys.2019.00870.

[26] W. Zhang *et al.*, "Multimodal Data for the Detection of Freezing of Gait in Parkinson's Disease," *Sci. Data*, vol. 9, no. 1, Dec. 2022, doi: 10.1038/S41597-022-01713-8.

[27] M. Bayot *et al.*, “Functional networks underlying freezing of gait: a resting-state electroencephalographic study,” *Neurophysiol. Clin.*, vol. 52, no. 3, pp. 212–222, Jun. 2022, doi: 10.1016/J.NEUCLI.2022.03.003.

[28] T. J. Bosch, A. I. Espinoza, M. Mancini, F. B. Horak, and A. Singh, “Functional Connectivity in Patients With Parkinson’s Disease and Freezing of Gait Using Resting-State EEG and Graph Theory,” *Neurorehabil. Neural Repair*, vol. 36, no. 10–11, pp. 715–725, 2022, doi: 10.1177/15459683221129282.

[29] O. B. Tysnes and A. Storstein, “Epidemiology of Parkinson’s disease,” *J. Neural Transm.*, vol. 124, no. 8, pp. 901–905, Aug. 2017, doi: 10.1007/S00702-017-1686-Y.

[30] W. H. Organization, “Atlas : country resources for neurological disorders 2004 : results of a collaborative study of the World Health Organization and the World Federation of Neurology.” World Health Organization, p. 59 p., 2004.

[31] H. B. Estifanos, G. Udo, R. Hansjürgen, B. Kelly, and D. Tredici, “Stages in the development of Parkinson’s disease-related pathology,” *Cell Tissue Res*, vol. 318, pp. 121–134, 2004, doi: 10.1007/s00441-004-0956-9.

[32] H. Bergman, “The Hidden Life of the Basal Ganglia,” *Hidden Life Basal Ganglia*, Oct. 2021, doi: 10.7551/MITPRESS/14075.001.0001.

[33] D. Weiss *et al.*, “Freezing of gait: Understanding the complexity of an enigmatic phenomenon,” *Brain*. 2020, doi: 10.1093/brain/awz314.

[34] N. Giladi and A. Nieuwboer, “Understanding and treating freezing of gait in Parkinsonism, proposed working definition, and setting the stage,” *Mov. Disord.*, vol. 23 Suppl 2, pp. S423-5, 2008, doi: 10.1002/mds.21927.

[35] N. Browner and N. Giladi, “What can we learn from freezing of gait in Parkinson’s disease?,” *Curr. Neurol. Neurosci. Rep.*, vol. 10, no. 5, pp. 345–351, Sep. 2010, doi: 10.1007/S11910-010-0127-1.

[36] M. M. Mcgregor and A. B. Nelson, “Circuit Mechanisms of Parkinson’s Disease,” 2019, doi: 10.1016/j.neuron.2019.03.004.

[37] P. J. Garcia-Ruiz, “Gait disturbances in Parkinson disease. Did freezing of gait exist before levodopa? Historical review,” *J. Neurol. Sci.*, vol. 307, no. 1–2, pp. 15–17, Aug. 2011, doi: 10.1016/J.JNS.2011.05.019.

[38] S. A. Factor *et al.*, “Freezing of gait subtypes have different cognitive correlates in Parkinson’s disease,” *Park. Relat. Disord.*, vol. 20, no. 12, pp. 1359–1364, Dec. 2014, doi: 10.1016/J.PARKRELDIS.2014.09.023.

[39] A. Nieuwboer and N. Giladi, “Characterizing freezing of gait in Parkinson’s disease: models of an episodic phenomenon,” *Mov. Disord.*, vol. 28, no. 11, pp. 1509–1519, Sep. 2013, doi: 10.1002/MDS.25683.

[40] S. J. G. Lewis and J. M. Shine, “The Next Step: A Common Neural Mechanism for Freezing of Gait,” *Neuroscientist*, vol. 22, no. 1, pp. 72–82, Feb. 2016, doi:

10.1177/1073858414559101.

[41] N. G. Pozzi *et al.*, “Freezing of gait in Parkinson’s disease reflects a sudden derangement of locomotor network dynamics,” *Brain*, vol. 142, no. 7, pp. 2037–2050, Jul. 2019, doi: 10.1093/BRAIN/AWZ141.

[42] S. J. G. Lewis and R. A. Barker, “A pathophysiological model of freezing of gait in Parkinson’s disease,” *Park. Relat. Disord.*, vol. 15, no. 5, pp. 333–338, Jun. 2009, doi: 10.1016/J.PARKRELDIS.2008.08.006.

[43] J. V. Jacobs, J. G. Nutt, P. Carlson-Kuhta, M. Stephens, and F. B. Horak, “Knee trembling during freezing of gait represents multiple anticipatory postural adjustments,” *Exp. Neurol.*, vol. 215, no. 2, pp. 334–341, Feb. 2009, doi: 10.1016/j.expneurol.2008.10.019.

[44] S. Muralidhar, Y. Wang, and H. Markram, “Synaptic and cellular organization of layer 1 of the developing rat somatosensory cortex,” *Front. Neuroanat.*, vol. 7, no. JAN, p. 52, Jan. 2014, doi: 10.3389/FNANA.2013.00052.

[45] E. T. Rolls, “Cerebral Cortex,” *Cereb. Cortex*, Nov. 2016, doi: 10.1093/ACPROF:OSO/9780198784852.001.0001.

[46] R. Iansek, J. L. Bradshaw, J. G. Phillips, R. Cunnington, and M. E. Morris, “Chapter 3 Interaction of the basal ganglia and supplementary motor area in the elaboration of movement,” *Adv. Psychol.*, vol. 111, no. C, pp. 37–59, Jan. 1995, doi: 10.1016/S0166-

4115(06)80006-3.

[47] D. W. Pfaff, “Neuroscience in the 21st century: From basic to clinical,” *Neurosci. 21st Century From Basic to Clin.*, pp. 1–3111, Nov. 2013, doi: 10.1007/978-1-4614-1997-6.

[48] S. Rahimpour *et al.*, “Freezing of Gait in Parkinson’s Disease: Invasive and Noninvasive Neuromodulation,” *Neuromodulation Technol. Neural Interface*, vol. 24, no. 5, pp. 829–842, Jul. 2021, doi: 10.1111/NER.13347.

[49] K. Takakusaki, “Neurophysiology of gait: From the spinal cord to the frontal lobe,” *Mov. Disord.*, vol. 28, no. 11, pp. 1483–1491, Sep. 2013, doi: 10.1002/MDS.25669.

[50] G. E. Alexander, M. R. DeLong, and P. L. Strick, “Parallel organization of functionally segregated circuits linking basal ganglia and cortex,” *Annu. Rev. Neurosci.*, vol. 9, p. 357—381, 1986, doi: 10.1146/annurev.ne.09.030186.002041.

[51] W. Thevathasan *et al.*, “Alpha oscillations in the pedunculopontine nucleus correlate with gait performance in parkinsonism,” *Brain*, vol. 135, no. 1, pp. 148–160, 2012, doi: 10.1093/BRAIN/AWR315.

[52] M. X. Cohen, *Analyzing Neural Time Series Data*. MIT Press, 2019.

[53] P. J. Uhlhaas and W. Singer, “Neural Synchrony in Brain Disorders: Relevance for Cognitive Dysfunctions and Pathophysiology,” *Neuron*, vol. 52, no. 1, pp. 155–168, Oct. 2006, doi: 10.1016/J.NEURON.2006.09.020.

[54] A. L. Valencia and T. Froese, “What binds us? Inter-brain neural synchronization and its implications for theories of human consciousness,” *Neurosci. Conscious.*, vol. 2020, no. 1, Jan. 2020, doi: 10.1093/NC/NIAA010.

[55] G. Buzsáki, *Rhythms of the Brain*. Oxford University Press, 2009.

[56] G. Buzsáki, N. Logothetis, and W. Singer, “Scaling Brain Size, Keeping Timing: Evolutionary Preservation of Brain Rhythms,” *Neuron*, vol. 80, no. 3, pp. 751–764, Oct. 2013, doi: 10.1016/J.NEURON.2013.10.002.

[57] P. J. Uhlhaas *et al.*, “Neural synchrony in cortical networks: history, concept and current status.,” *Front. Integr. Neurosci.*, vol. 3, p. 17, 2009, doi: 10.3389/neuro.07.017.2009.

[58] B. van Wijk, P. Beek, and A. Daffertshofer, “Neural synchrony within the motor system: what have we learned so far?,” *Front. Hum. Neurosci.*, vol. 6, p. 252, 2012, doi: 10.3389/fnhum.2012.00252.

[59] M. A. Whittington, R. D. Traub, and N. E. Adams, “A future for neuronal oscillation research.,” *Brain Neurosci. Adv.*, vol. 2, p. 2398212818794827, 2018, doi: 10.1177/2398212818794827.

[60] R. Caton , "The electric currents of the brain.”, American Journal of EEG Technology. 1970;10(1):12-14.

[61] H. Berger, “Über das Elektrenkephalogramm des Menschen,” *Arch. Psychiatr.*

Nervenkr., vol. 87, no. 1, pp. 527–570, Dec. 1929, doi: 10.1007/BF01797193.

[62] P. L. Nunez and R. Srinivasan, "Electric Fields of the Brain The Neurophysics of EEG Second Edition,". Oxford Univ. Press, 2006.

[63] C. J. Stam, "Nonlinear dynamical analysis of EEG and MEG: review of an emerging field," *Clin. Neurophysiol.*, vol. 116, no. 10, pp. 2266–2301, Oct. 2005, doi: 10.1016/J.CLINPH.2005.06.011.

[64] J. M. Palva and S. Palva, "Functional integration across oscillation frequencies by cross-frequency phase synchronization.," *Eur. J. Neurosci.*, vol. 48, no. 7, pp. 2399–2406, Dec. 2017, doi: 10.1111/EJN.13767.

[65] S. Sanei and J. Chambers, "EEG signal processing," , 2007, Jan. , 2023.

[66] G. Pfurtscheller and F. H. Lopes Da Silva, "Event-related EEG/MEG synchronization and desynchronization: basic principles.," *Clin. Neurophysiol.*, vol. 110, pp. 1842–1857, 1999.

[67] C. Kufta, "Event-related desynchronization and movement-related cortical potentials on the ECoG and EEG," *Electroencephalogr. Clin. Neurophysiol. Potentials Sect.*, vol. 93, no. 5, pp. 380 – 389, 1994.

[68] M. Jahanshahi and M. Hallett, "The Bereitschaftspotential: what does it measure and where does it come from?," in *The Bereitschaftspotential*, Springer, 2003.

[69] A. Shakeel, M. S. Navid, M. N. Anwar, S. Mazhar, M. Jochumsen, and I. K. Niazi, "A Review of Techniques for Detection of Movement Intention Using Movement-Related Cortical Potentials," *Comput. Math. Methods Med.*, vol. 2015, no. 6, pp. 1–13, Oct. 2015, doi: 10.1155/2015/346217.

[70] K. Dremstrup, Y. Gu, O. F. do Nascimento, and D. Farina, "Movement-Related Cortical Potentials and Their Application in Brain-Computer Interfacing," in *Introduction to Neural Engineering for Motor Rehabilitation*, Hoboken, NJ, USA: John Wiley & Sons, Inc., 2013, pp. 253–266.

[71] H. Shibasaki and M. Hallett, "What is the Bereitschaftspotential?," *Clin. Neurophysiol.*, vol. 117, no. 11, pp. 2341–56, Nov. 2006, doi: 10.1016/j.clinph.2006.04.025.

[72] D. J. Wright, P. S. Holmes, and D. Smith, "Using the Movement-Related Cortical Potential to Study Motor Skill Learning," *J. Mot. Behav.*, vol. 43, no. 3, pp. 193–201, May 2011, doi: 10.1080/00222895.2011.557751.

[73] B. Fisch, "Fisch and Spehlmann's Digital and Analog EEG Primer," 1999.

[74] A. Kübler and D. Mattia, "Brain-Computer Interface Based Solutions for End-Users with Severe Communication Disorders," *Neurol. Conscious. Cogn. Neurosci. Neuropathol.*, pp. 217–240, Jan. 2015, doi: 10.1016/B978-0-12-800948-2.00014-5.

[75] C. L. Groth, A. Singh, Q. Zhang, B. D. Berman, and N. S. Narayanan, "GABAergic Modulation in Movement Related Oscillatory Activity: A Review of the Effect

Pharmacologically and with Aging," *Tremor Other Hyperkinet. Mov. (N. Y).*, vol. 11, no. 1, 2021, doi: 10.5334/TOHM.655.

[76] F. Varela, J. P. Lachaux, E. Rodriguez, and J. Martinerie, "The brainweb: Phase synchronization and large-scale integration," *Nat. Rev. Neurosci.*, vol. 2, no. 4, pp. 229–239, 2001, doi: 10.1038/35067550.

[77] R. T. Canolty and R. T. Knight, "The functional role of cross-frequency coupling," *Trends Cogn. Sci.*, vol. 14, no. 11, pp. 506–515, Nov. 2010, doi: 10.1016/J.TICS.2010.09.001.

[78] W. Klimesch, "The frequency architecture of brain and brain body oscillations: an analysis," *Eur. J. Neurosci.*, vol. 48, pp. 2431–2453, 2018.

[79] A. M. Bastos and J. M. Schoffelen, "A tutorial review of functional connectivity analysis methods and their interpretational pitfalls," *Front. Syst. Neurosci.*, vol. 9, no. JAN2016, Jan. 2016, doi: 10.3389/FNSYS.2015.00175.

[80] C. Demanuele, C. J. James, and E. J. S. Sonuga-Barke, "Distinguishing low frequency oscillations within the 1/f spectral behaviour of electromagnetic brain signals," *Behav. Brain Funct.*, vol. 3, Dec. 2007, doi: 10.1186/1744-9081-3-62.

[81] M. S. Keshner, "1/f noise," *Proc. IEEE*, vol. 70, no. 3, pp. 212–218, 1982, doi: 10.1109/PROC.1982.12282.

[82] G. Buzsáki and A. Draguhn, “Neuronal olscillations in cortical networks,” *Science (80-.).*, vol. 304, no. 5679, pp. 1926–1929, Jun. 2004, doi: 10.1126/SCIENCE.1099745.

[83] G. Buzsáki and B. O. Watson, “Brain rhythms and neural syntax: Implications for efficient coding of cognitive content and neuropsychiatric disease,” *Dialogues Clin. Neurosci.*, vol. 14, no. 4, pp. 345–367, Dec. 2012, doi: 10.31887/DCNS.2012.14.4/GBUZSAKI.

[84] R. Martínez-Cancino, J. Heng, A. Delorme, K. Kreutz-Delgado, R. C. Sotero, and S. Makeig, “Measuring transient phase-amplitude coupling using local mutual information,” *Neuroimage*, vol. 185, pp. 361–378, Jan. 2019, doi: 10.1016/J.NEUROIMAGE.2018.10.034.

[85] R. T. Canolty *et al.*, “High gamma power is phase-locked to theta oscillations in human neocortex,” *Science (80-.).*, vol. 313, no. 5793, pp. 1626–1628, Sep. 2006, doi: 10.1126/SCIENCE.1128115.

[86] C. MX, *Analyzing Neural Time Series Data The MIT Press*, 2014.

[87] Y. Salimpour and W. S. Anderson, “Cross-frequency coupling based neuromodulation for treating neurological disorders,” *Front. Neurosci.*, vol. 13, no. FEB, 2019, doi: 10.3389/FNINS.2019.00125.

[88] T. Li and W. Le, “Biomarkers for Parkinson’s Disease: How Good Are They?,” *Neurosci. Bull.*, vol. 36, no. 2, pp. 183–194, Feb. 2020, doi: 10.1007/s12264-019-

00433-1.

[89] E. Sarasso *et al.*, “MRI biomarkers of freezing of gait development in Parkinson’s disease,” *npj Park. Dis.*, vol. 8, no. 1, p. 158, 2022, doi: 10.1038/s41531-022-00426-4.

[90] A. Surguchov, “Biomarkers in Parkinson’s Disease,” *Neuromethods*, vol. 173, pp. 155–180, 2022, doi: 10.1007/978-1-0716-1712-0_7.

[91] G. Baldazzi, E. Sulas, M. Urru, R. Tumbarello, L. Raffo, and D. Pani, “Wavelet denoising as a post-processing enhancement method for non-invasive foetal electrocardiography,” *Comput. Methods Programs Biomed.*, vol. 195, p. 105558, Oct. 2020, doi: 10.1016/j.cmpb.2020.105558.

[92] F. B. Horak and M. Mancini, “Objective biomarkers of balance and gait for Parkinson’s disease using body-worn sensors.,” *Mov. Disord.*, vol. 28, no. 11, pp. 1544–1551, Sep. 2013, doi: 10.1002/mds.25684.

[93] S. T. Moore, H. G. MacDougall, and W. G. Ondo, “Ambulatory monitoring of freezing of gait in Parkinson’s disease.,” *J. Neurosci. Methods*, vol. 167, no. 2, pp. 340–8, Jan. 2008, doi: 10.1016/j.jneumeth.2007.08.023.

[94] M. Bächlin *et al.*, “Wearable Assistant for Parkinson’s Disease Patients With the Freezing of Gait Symptom,” *Inf. Technol. Biomed. IEEE Trans.*, vol. 14, pp. 436–446, 2010.

[95] A. Delval *et al.*, “Objective detection of subtle freezing of gait episodes in Parkinson’s disease.,” *Mov. Disord.*, vol. 25, no. 11, pp. 1684–93, Aug. 2010, doi: 10.1002/mds.23159.

[96] S. Lewis, S. Factor, N. Giladi, A. Nieuwboer, J. Nutt, and M. Hallett, “Stepping up to meet the challenge of freezing of gait in Parkinson’s disease,” *Transl. Neurodegener.*, vol. 11, no. 1, pp. 1–12, Dec. 2022, doi: 10.1186/S40035-022-00298-X.

[97] Y. Zhang, W. Yan, Y. Yao, J. B. Ahmed, Y. Tan, and D. Gu, “Prediction of Freezing of Gait in Patients With Parkinson’s Disease by Identifying Impaired Gait Patterns.,” *IEEE Trans. neural Syst. Rehabil. Eng. a Publ. IEEE Eng. Med. Biol. Soc.*, vol. 28, no. 3, pp. 591–600, Mar. 2020, doi: 10.1109/TNSRE.2020.2969649.

[98] A. Mirelman *et al.*, “Gait impairments in Parkinson’s disease,” *The Lancet Neurology*. 2019, doi: 10.1016/S1474-4422(19)30044-4.

[99] E. Heremans, A. Nieuwboer, and S. Vercruysse, “Freezing of gait in Parkinson’s disease: where are we now?,” *Curr. Neurol. Neurosci Rep* 13, 350 (2013). https://doi.org/10.1007/s11910-013-0350-7.

[100] F. T. Phibbs, P. G. Arbogast, and T. L. Davis, “60-Hz Frequency Effect on Gait in P arkinson’s Disease With Subthalamic Nucleus Deep Brain Stimulation,” *Neuromodulation Technol. Neural Interface*, vol. 17, no. 8, pp. 717–720, 2014.

[101] R. J. Vorovenci, R. Biundo, and • Angelo Antonini, “Therapy-resistant symptoms in

Parkinson's disease," *J. Neural Transm.*, vol. 123, doi: 10.1007/s00702-015-1463-8.

[102] J. Vaamonde Gamo, J. P. Cabello, M. J. Gallardo Alcañiz, J. M. Flores Barragan, S. Carrasco García de León, and R. E. Ibañez Alonso, "Freezing of gait unresponsive to dopaminergic stimulation in patients with severe Parkinsonism," *Neurol. (English Ed.*, vol. 25, no. 1, pp. 27–31, Jan. 2010, doi: 10.1016/S2173-5808(10)70005-5.

[103] M. Gilat, A. Lígia Silva de Lima, B. R. Bloem, J. M. Shine, J. Nonnekes, and S. J. G. Lewis, "Freezing of gait: Promising avenues for future treatment," *Parkinsonism and Related Disorders*. 2018, doi: 10.1016/j.parkreldis.2018.03.009.

[104] D. Caligiore *et al.*, "Parkinson's disease as a system-level disorder," *npj Parkinson's Disease*. 2016, doi: 10.1038/npjparkd.2016.25.

[105] R. S. Turner and M. Desmurget, "Basal ganglia contributions to motor control: a vigorous tutor," *Curr. Opin. Neurobiol.*, vol. 20, no. 6, pp. 704–716, 2010.

[106] M. Jochumsen *et al.*, "Detection of movement intentions through a single channel of electroencephalography," in *Replace, Repair, Restore, Relieve--Bridging Clinical and Engineering Solutions in Neurorehabilitation*, Springer, 2014, pp. 465–472.

[107] M. Jahanshahi, I. H. Jenkins, R. G. Brown, C. D. Marsden, R. E. Passingham, and D. J. Brooks, "Self-initiated versus externally triggered movements: I. An investigation using measurement of regional cerebral blood flow with PET and movement-related potentials in normal and Parkinson's disease subjects," *Brain*, vol. 118, no. 4, pp. 913–933, 1995.

[108] R. Cunnington, R. Iansek, J. L. Bradshaw, and J. G. Phillips, “Movement-related potentials in Parkinson’s disease: presence and predictability of temporal and spatial cues,” *Brain*, vol. 118, no. 4, pp. 935–950, 1995.

[109] D. Georgiev, F. Lange, C. Seer, B. Kopp, and M. Jahanshahi, “Movement-related potentials in Parkinson’s disease,” *Clin. Neurophysiol.*, vol. 127, no. 6, pp. 2509–2519, 2016.

[110] M. Vidailhet. F. tocchi , J.C. Rothwell, P.D. Thompson, B.L. Day BL, D.J. Brooks, C.D. Marsden, “The Bereitschaftspotential preceding simple foot movement and initiation of gait in Parkinson’s disease.,” *Neurology*, vol. 43, no. 9, pp. 1784–8, Sep. 1993, doi: 10.1212/wnl.43.9.1784.

[111] A. Patil, S. Sood, V. Goyal, and K. Kochhar, “Cortical Potentials Prior to Movement in Parkinson’s Disease,” *J. Clin. Diagnostic Res.*, vol. 11, pp. CC13–CC16, 2017, doi: 10.7860/JCDR/2017/25520.9598.

[112] S. Yazawa, H. Shibasaki, A. Ikeda, K. Terada, T. Nagamine, and M. Honda, “Cortical mechanism underlying externally cued gait initiation studied by contingent negative variation,” *Electroencephalogr. Clin. Neurophysiol. Mot. Control*, vol. 105, no. 5, pp. 390–399, 1997, doi: 10.1016/s0924-980x(97)00034-9.

[113] M. Oishi, Y. Mochizuki, C. Du, and T. Takasu, “Contingent negative variation and movement-related cortical potentials in parkinsonism.,” *Electroencephalogr. Clin.*

Neurophysiol., vol. 95, no. 5, pp. 346–9, Nov. 1995, doi: 10.1016/0013-4694(95)00084-c.

[114] J. B. Renfroe, M. M. Bradley, M. S. Okun, and D. Bowers, "Motivational engagement in Parkinson's disease: preparation for motivated action," *Int. J. Psychophysiol.*, vol. 99, pp. 24–32, 2016, doi: 10.1016/j.ijpsycho.2015.11.014.

[115] E. Wascher, R. Verleger, P. Vieregge, P. Jaskowski, S. Koch, and D. Kömpf, "Responses to cued signals in Parkinson's disease. Distinguishing between disorders of cognition and of activation.," *Brain a J. Neurol.*, vol. 120, no. 8, pp. 1355–1375, 1997, doi: 10.1093/brain/120.8.1355.

[116] J. P. R. Dick *et al.*, "The Bereitschaftspotential, L-DOPA and Parkinson's disease," *Electroencephalogr. Clin. Neurophysiol.*, vol. 66, no. 3, pp. 263–274, 1987, doi: 10.1016/0013-4694(87)90075-7.

[117] A. P. Feve, N. Bathien, and P. Rondot, "Chronic administration of L-dopa affects the movement-related cortical potentials of patients with Parkinson's disease.," *Clin. Neuropharmacol.*, vol. 15, no. 2, pp. 100–108, 1992, doi: 10.1097/00002826-199204000-00003.

[118] T. Fumuro *et al.*, "Bereitschaftspotential augmentation by neuro-feedback training in Parkinson's disease," *Clin. Neurophysiol.*, vol. 124, no. 7, pp. 1398–1405, 2013, doi: 10.1016/j.clinph.2013.01.026.

[119] A. Gironell, A. Rodriguez-Fornells, J. Kulisevsky, B. Pascual, M. Barbanoj, and P. Otermin, “Motor circuitry re-organization after pallidotomy in Parkinson disease: a neurophysiological study of the bereitschaftspotential, contingent negative variation, and N30,” *J. Clin. Neurophysiol.*, vol. 19, no. 6, pp. 553–561, 2002, doi: 10.1097/00004691-200212000-00009.

[120] R. G. Brown *et al.*, “Impact of deep brain stimulation on upper limb akinesia in Parkinson’s disease,” *Ann. Neurol. Off. J. Am. Neurol. Assoc. Child Neurol. Soc.*, vol. 45, no. 4, pp. 473–488, 1999, doi: 10.1002/1531-8249(199904)45:4<473::aid-ana9>3.0.co;2-v.

[121] W. Gerschlager *et al.*, “Bilateral subthalamic nucleus stimulation improves frontal cortex function in Parkinson’s disease: An electrophysiological study of the contingent negative variation,” *Brain*, vol. 122, no. 12, pp. 2365–2373, 1999, doi: 10.1093/brain/122.12.2365.

[122] V. M, A. PR, S. F, T. PD, R. JC, and M. CD, “The bereitschaftspotential preceding stepping in patients with isolated gait ignition failure,” *Mov. Disord.*, vol. 10, no. 1, pp. 18–21, 1995, doi: 10.1002/MDS.870100105.

[123] D. Williams *et al.*, “Dopamine-dependent changes in the functional connectivity between basal ganglia and cerebral cortex in humans,” *Brain*, vol. 125, pp. 1558–1569, 2002, doi: 10.1093/brain/awf156.

[124] A. Sharott *et al.*, “Spatio-temporal dynamics of cortical drive to human subthalamic nucleus neurons in Parkinson’s disease,” *Neurobiol. Dis.*, vol. 112, 2018, doi: 10.1016/j.nbd.2018.01.001.

[125] A. Holt *et al.*, “Phase-Dependent Suppression of Beta Oscillations in Parkinson’s Disease Patients,” *J. Neurosci.*, vol. 39, pp. 1913–1918, 2018, doi: 10.1523/JNEUROSCI.1913-18.2018.

[126] V. K. Lim, J. P. Hamm, W. D. Byblow, and I. J. Kirk, “Decreased desychronisation during self-paced movements in frequency bands involving sensorimotor integration and motor functioning in Parkinson’s disease,” *Brain Res. Bull.*, vol. 71, no. 1–3, pp. 245–251, 2006, doi: 10.1016/j.brainresbull.2006.09.009.

[127] A. Singh, R. Cole, A. Espinoza, D. Brown, J. Cavanagh, and N. Narayanan, “Frontal theta and beta oscillations during lower-limb movement in Parkinson’s disease,” 2019, doi: 10.1101/634808.

[128] J. Shine *et al.*, “Abnormal patterns of theta frequency oscillations during the temporal evolution of freezing of gait in Parkinson’s disease,” *Clin. Neurophysiol.*, vol. 125, 2013, doi: 10.1016/j.clinph.2013.09.006.

[129] M. J. Georgiades *et al.*, “Hitting the brakes: Pathological subthalamic nucleus activity in Parkinson’s disease gait freezing,” *Brain*, vol. 142, no. 12, pp. 3906–3916, Dec. 2019, doi: 10.1093/brain/awz325.

[130] Q. J. Almeida and C. A. Lebold, “Freezing of gait in Parkinson’s disease: a perceptual cause for a motor impairment?,” *J. Neurol. Neurosurg. Psychiatry*, vol. 81, no. 5, pp. 513–8, May 2010, doi: 10.1136/jnnp.2008.160580.

[131] S. Solnik, P. Rider, K. Steinweg, P. DeVita, and T. Hortobágyi, “Teager--Kaiser energy operator signal conditioning improves EMG onset detection,” *Eur. J. Appl. Physiol.*, vol. 110, no. 3, pp. 489–498, 2010, doi: 10.1007/s00421-010-1521-8.

[132] A. Delorme and S. Makeig, “EEGLAB: an open source toolbox for analysis of single-trial EEG dynamics including independent component analysis,” *J. Neurosci. Methods*, vol. 134, no. 1, pp. 9–21, 2004, doi: 10.1016/j.jneumeth.2003.10.009.

[133] E. López-Larraz, L. Montesano, Á. Gil-Agudo, and J. Minguez, “Continuous decoding of movement intention of upper limb self-initiated analytic movements from pre-movement EEG correlates,” *J. Neuroeng. Rehabil.*, vol. 11, no. 1, p. 153, 2014, doi: 10.1186/1743-0003-11-153.

[134] D. Liu, W. Chen, R. Chavarriaga, Z. Pei, and J. del R. Millán, “Decoding of self-paced lower-limb movement intention: A case study on the influence factors,” *Front. Hum. Neurosci.*, vol. 11, p. 560, 2017, doi: 10.3389/fnhum.2017.00560.

[135] Y. Gu, K. Dremstrup, and D. Farina, “Single-trial discrimination of type and speed of wrist movements from EEG recordings,” *Clin. Neurophysiol.*, vol. 120, no. 8, pp. 1596–1600, 2009, doi: 10.1016/j.clinph.2009.05.006.

[136] B. Graimann and G. Pfurtscheller, “Quantification and visualization of event-related changes in oscillatory brain activity in the time--frequency domain,” *Prog. Brain Res.*, vol. 159, pp. 79–97, 2006, doi: 10.1016/S0079-6123(06)59006-5.

[137] E. Maris and R. Oostenveld, “Nonparametric statistical testing of EEG-and MEG-data,” *J. Neurosci. Methods*, vol. 164, no. 1, pp. 177–190, 2007, doi: 10.1016/j.jneumeth.2007.03.024.

[138] Karimi F. FOG severity EEG/EMG. IEEE Dataport. 2021, doi: /10.21227/5ch0-8b29.

[139] D. Lindenbach and C. Bishop, “Critical Involvement of the Motor Cortex in the Pathophysiology and Treatment of Parkinson’s Disease,” *Neurosci. Biobehav. Rev.*, vol. 37, 2013, doi: 10.1016/j.neubiorev.2013.09.008.

[140] J. B. Green, P. A. St. Arnold, L. Rozhkov, D. M. Strother, and N. Garrott, “Bereitschaft (readiness potential) and supplemental motor area interaction in movement generation: Spinal cord injury and normal subjects,” *J. Rehabil. Res. Dev.*, 2003.

[141] L. H. Goldstein, “The frontal lobes and voluntary action,” *Behav. Res. Ther.*, 1996, doi: 10.1016/0005-7967(96)87642-x.

[142] P. Nachev, C. Kennard, and M. Husain, “Functional role of the supplementary and pre-supplementary motor areas,” *Nat. Rev. Neurosci.*, vol. 9, no. 11, pp. 856–869, 2008, doi: 10.1038/nrn2478.

[143] G. Cona and C. Semenza, “Supplementary motor area as key structure for domain-general sequence processing: A unified account,” *Neuroscience and Biobehavioral Reviews*. 2017, doi: 10.1016/j.neubiorev.2016.10.033.

[144] E. C. Leek, K. S. L. Yuen, and S. J. Johnston, “Domain general sequence operations contribute to pre-SMA involvement in visuo-spatial processing,” *Front. Hum. Neurosci.*, 2016, doi: 10.3389/fnhum.2016.00009.

[145] E. Travers, M. Friedemann, and P. Haggard, “The Readiness Potential reflects planning-based expectation, not uncertainty, in the timing of action,” *Cogn. Neurosci.*, 2020, doi: 10.1080/17588928.2020.1824176.

[146] P. Alm, “Stuttering and the basal ganglia circuits: A critical review of possible relations,” *J. Commun. Disord.*, vol. 37, pp. 325–369, 2004, doi: 10.1016/j.jcomdis.2004.03.001.

[147] A. H. Snijders *et al.*, “Physiology of freezing of gait,” *Annals of Neurology*. 2016, doi: 10.1002/ana.24778.

[148] R. M. Camicioli, C. C. Hanstock, T. P. Bouchard, M. Gee, N. J. Fisher, and W. R. W. Martin, “Magnetic resonance spectroscopic evidence for presupplementary motor area neuronal dysfunction in Parkinson’s disease,” *Mov. Disord.*, 2007, doi: 10.1002/mds.21288.

[149] V. MacDonald and G. Halliday, “Selective loss of pyramidal neurons in the pre-

supplementary motor cortex in Parkinson's disease," *Mov. Disord.*, vol. 17, pp. 1166–1173, 2002, doi: 10.1002/mds.10258.

[150] J. A. Obeso *et al.*, "Missing pieces in the Parkinson's disease puzzle," *Nature Medicine*. 2010, doi: 10.1038/nm.2165.

[151] J. P. Dick *et al.*, "The Bereitschaftspotential is abnormal in Parkinson's disease.," *Brain*, pp. 233–44, Feb. 1989, doi: 10.1093/brain/112.1.233.

[152] J. S. Butler, C. Fearon, I. Killane, S. M. Waechter, R. B. Reilly, and T. Lynch, "Motor preparation rather than decision-making differentiates Parkinson's disease patients with and without freezing of gait," *Clin. Neurophysiol.*, vol. 128, no. 3, pp. 463–471, 2017, doi: 10.1016/j.clinph.2016.12.019.

[153] V. Siemionow, G. Yue, V. Ranganathan, J. Liu, and V. Sahgal, "Relationship between motor activity-related cortical potential and voluntary muscle activation," *Exp. Brain Res.*, vol. 133, pp. 303–311, 2000, doi: 10.1007/s002210000382.

[154] A. C. Etchell, B. W. Johnson, and P. F. Sowman, "Beta oscillations, timing, and stuttering," *Front. Hum. Neurosci.*, vol. 8, p. 1036, 2015, doi: 10.3389/fnhum.2014.01036.

[155] R. Bartolo, L. Prado, and H. Merchant, "Information Processing in the Primate Basal Ganglia during Sensory-Guided and Internally Driven Rhythmic Tapping," *J. Neurosci.*, vol. 34, pp. 3910–3923, 2014, doi: 10.1523/JNEUROSCI.2679-13.2014.

[156] S. Lehéricy *et al.*, "3-D Diffusion Tensor Axonal Tracking shows Distinct SMA and Pre-SMA Projections to the Human Striatum," *Cereb. Cortex*, vol. 14, pp. 1302–1309, 2005, doi: 10.1093/cercor/bhh091.

[157] C. Tzagarakis, S. West, and G. Pellizzer, "Brain oscillatory activity during motor preparation: Effect of directional uncertainty on beta, but not alpha, frequency band," *Front. Neurosci.*, 2015, doi: 10.3389/fnins.2015.00246.

[158] J. P. Solomon, S. N. Kraeutner, T. Bardouille, and S. G. Boe, "Probing the temporal dynamics of movement inhibition in motor imagery," *Brain Res.*, 2019, doi: 10.1016/j.brainres.2019.146310.

[159] A. Singh and K. Bötzel, "Globus pallidus internus oscillatory activity is related to movement speed," *Eur. J. Neurosci.*, 2013, doi: 10.1111/ejn.12369.

[160] C. Neuper and G. Pfurtscheller, "Evidence for distinct beta resonance frequencies in human EEG related to specific cortical areas," *Clin. Neurophysiol.*, vol. 112, pp. 2084–2097, 2001, doi: 10.1016/S1388-2457(01)00661-7.

[161] O. Talakoub *et al.*, "Time-course of coherence in the human basal ganglia during voluntary movements," *Sci. Rep.*, 2016, doi: 10.1038/srep34930.

[162] G. Foffani, A. M. Bianchi, G. Baselli, and A. Priori, "Movement-related frequency modulation of beta oscillatory activity in the human subthalamic nucleus," *J. Physiol.*, 2005, doi: 10.1113/jphysiol.2005.089722.

[163] A. Canessa, C. Palmisano, I. U. Isaias, and A. Mazzoni, “Gait-related frequency modulation of beta oscillatory activity in the subthalamic nucleus of parkinsonian patients,” *Brain Stimul.*, vol. 13, no. 6, pp. 1743–1752, 2020, doi: 10.1016/j.brs.2020.09.006.

[164] S. N. Meissner, V. Krause, M. Südmeyer, C. J. Hartmann, and B. Pollok, “The significance of brain oscillations in motor sequence learning: Insights from Parkinson’s disease,” *NeuroImage Clin.*, 2018, doi: 10.1016/j.nicl.2018.08.009.

[165] M. Jochumsen *et al.*, “Quantification of movement-related EEG correlates associated with motor training: A study on movement-related cortical potentials and sensorimotor rhythms,” *Front. Hum. Neurosci.*, 2017, doi: 10.3389/fnhum.2017.00604.

[166] T. M. Mi *et al.*, “High-frequency rTMS over the supplementary motor area improves freezing of gait in Parkinson’s disease: a randomized controlled trial,” *Park. Relat. Disord.*, 2019, doi: 10.1016/j.parkreldis.2019.10.009.

[167] C. Gao, J. Liu, Y. Tan, and S. Chen, “Freezing of gait in Parkinson’s disease: pathophysiology, risk factors and treatments,” *Transl. Neurodegener. 2020 91*, vol. 9, no. 1, pp. 1–22, Apr. 2020, doi: 10.1186/S40035-020-00191-5.

[168] C. Jin *et al.*, “Altered Degree Centrality of Brain Networks in Parkinson’s Disease With Freezing of Gait: A Resting-State Functional MRI Study,” *Front. Neurol.*, vol. 12, p. 1759, Oct. 2021, doi: 10.3389/FNEUR.2021.743135.

[169] Y. Li *et al.*, “Aberrant Advanced Cognitive and Attention-Related Brain Networks in Parkinson’s Disease with Freezing of Gait,” *Neural Plast.*, vol. 2020, 2020, doi: 10.1155/2020/8891458.

[170] R. Iansek and M. Danoudis, “Freezing of Gait in Parkinson’s Disease: Its Pathophysiology and Pragmatic Approaches to Management,” *Mov. Disord. Clin. Pract.*, vol. 4, no. 3, pp. 290–297, May 2017, doi: 10.1002/MDC3.12463.

[171] R. Iansek, F. Huxham, and J. McGinley, “The sequence effect and gait festination in Parkinson disease: contributors to freezing of gait?,” *Mov. Disord.*, vol. 21, no. 9, pp. 1419–1424, Sep. 2006, doi: 10.1002/MDS.20998.

[172] A. Delval, M. Bayot, L. Defebvre, and K. Dujardin, “Cortical oscillations during gait: Wouldn’t walking be so automatic?,” *Brain Sci.*, vol. 10, no. 2, Feb. 2020, doi: 10.3390/BRAINSCI10020090.

[173] J. A. Beeler and J. K. Dreyer, “Synchronicity: The Role of Midbrain Dopamine in Whole-Brain Coordination,” *eNeuro*, vol. 6, no. 2, Mar. 2019, doi: 10.1523/ENEURO.0345-18.2019.

[174] V. Marinho *et al.*, “The dopaminergic system dynamic in the time perception: a review of the evidence,” *Int. J. Neurosci.*, vol. 128, no. 3, pp. 262–282, Mar. 2018, doi: 10.1080/00207454.2017.1385614.

[175] J. Nantel, J. C. McDonald, S. Tan, and H. Bronte-Stewart, “Deficits in visuospatial

processing contribute to quantitative measures of freezing of gait in Parkinson's disease," *Neuroscience*, vol. 221, pp. 151–156, Sep. 2012, doi: 10.1016/J.NEUROSCIENCE.2012.07.007.

[176] D. D. Wang and J. T. Choi, "Brain Network Oscillations During Gait in Parkinson's Disease," *Front. Hum. Neurosci.*, vol. 14, p. 455, Oct. 2020, doi: 10.3389/FNHUM.2020.568703.

[177] T. Flash, E. Henis, R. Inzelberg ', and A. D. Korczyn "," 'i, "Timing and sequencing of human arm trajectories: Normal and abnormal motor behaviour *," *Hum. Mov. Sci.*, vol. 11, pp. 83–100, 1992.

[178] M. X. Cohen, "It's about time," *Front. Hum. Neurosci.*, vol. 0, no. JANUARY, pp. 1–16, 2011, doi: 10.3389/FNHUM.2011.00002.

[179] G. Arnulfo *et al.*, "Phase matters: A role for the subthalamic network during gait," *PLoS One*, vol. 13, no. 6, Jun. 2018, doi: 10.1371/JOURNAL.PONE.0198691.

[180] T. T. K. Munia and S. Aviyente, "Time-Frequency Based Phase-Amplitude Coupling Measure For Neuronal Oscillations," *Sci. Reports 2019 91*, vol. 9, no. 1, pp. 1–15, Aug. 2019, doi: 10.1038/s41598-019-48870-2.

[181] J. Kayser and C. E. Tenke, "Issues and considerations for using the scalp surface Laplacian in EEG/ERP research: A tutorial review," *Int. J. Psychophysiol.*, vol. 97, no. 3, pp. 189–209, Sep. 2015, doi: 10.1016/J.IJPSYCHO.2015.04.012.

[182] S. Vercruysse *et al.*, “Freezing in Parkinson’s disease: a spatiotemporal motor disorder beyond gait,” *Mov. Disord.*, vol. 27, no. 2, pp. 254–263, Feb. 2012, doi: 10.1002/MDS.24015.

[183] J. M. Shine, S. L. Naismith, and S. J. G. Lewis, “The pathophysiological mechanisms underlying freezing of gait in Parkinson’s Disease,” *J. Clin. Neurosci.*, vol. 18, no. 9, pp. 1154–1157, Sep. 2011, doi: 10.1016/J.JOCN.2011.02.007.

[184] F. Karimi, J. Niu, K. Gouweleeuw, Q. Almeida, and N. Jiang, “Movement-related EEG signatures associated with freezing of gait in Parkinson’s disease: an integrative analysis,” *Brain Commun.*, vol. 3, no. 4, Oct. 2021, doi: 10.1093/BRAINCOMMS/FCAB277.

[185] Ren Xu, Ning Jiang, Chuang Lin, N. Mrachacz-Kersting, K. Dremstrup, and D. Farina, “Enhanced Low-Latency Detection of Motor Intention From EEG for Closed-Loop Brain-Computer Interface Applications,” *IEEE Trans. Biomed. Eng.*, vol. 61, no. 2, pp. 288–296, Feb. 2014, doi: 10.1109/TBME.2013.2294203.

[186] J. Lu, D. J. McFarland, and J. R. Wolpaw, “Adaptive Laplacian filtering for sensorimotor rhythm-based brain-computer interfaces,” *J. Neural Eng.*, vol. 10, no. 1, 2013, doi: 10.1088/1741-2560/10/1/016002.

[187] C. E. Tenke and J. Kayser, “Surface Laplacians (SL) and phase properties of EEG rhythms: simulated generators in a volume-conduction model,” *Int. J. Psychophysiol.*,

vol. 97, no. 3, p. 285, Sep. 2015, doi: 10.1016/J.IJPSYCHO.2015.05.008.

[188] W. Jian, M. Chen, and D. J. McFarland, “EEG based zero-phase phase-locking value (PLV) and effects of spatial filtering during actual movement,” *Brain Res. Bull.*, vol. 130, pp. 156–164, Apr. 2017, doi: 10.1016/J.BRAINRESBULL.2017.01.023.

[189] W. Jian, M. Chen, and D. J. McFarland, “Use of Phase-locking Value in Sensorimotor Rhythm-based Brain-Computer Interface: Zero-phase Coupling and Effects of Spatial Filters,” *Med. Biol. Eng. Comput.*, vol. 55, no. 11, p. 1915, Nov. 2017, doi: 10.1007/S11517-017-1641-Y.

[190] B. Hjorth, “An on-line transformation of EEG scalp potentials into orthogonal source derivations,” *Electroencephalogr. Clin. Neurophysiol.*, vol. 39, no. 5, pp. 526–530, Nov. 1975, doi: 10.1016/0013-4694(75)90056-5.

[191] A. Zazio, C. Miniussi, and M. Bortoletto, “Alpha-band cortico-cortical phase synchronization is associated with effective connectivity in the motor network,” *Clin. Neurophysiol.*, vol. 132, no. 10, pp. 2473–2480, Oct. 2021, doi: 10.1016/J.CLINPH.2021.06.025.

[192] S. Aydore, D. Pantazis, and R. M. Leahy, “A note on the phase locking value and its properties,” *Neuroimage*, 2013, doi: 10.1016/j.neuroimage.2013.02.008.

[193] N. Fisher, *Statistical Analysis of Circular Data*. Cambridge University Press, Cambridge, 1993.

[194] A. Shakeel, T. Tanaka, and K. Kitajo, “Time-series prediction of the oscillatory phase of eeg signals using the least mean square algorithm-based ar model,” *Appl. Sci.*, vol. 10, no. 10, May 2020, doi: 10.3390/APP10103616.

[195] P. Berens, “CircStat : A MATLAB Toolbox for Circular Statistics ,” *J. Stat. Softw.*, vol. 31, no. 10, 2009, doi: 10.18637/JSS.V031.I10.

[196] S. Sadaghiani and A. Kleinschmidt, “Brain Networks and α-Oscillations: Structural and Functional Foundations of Cognitive Control,” *Trends Cogn. Sci.*, vol. 20, no. 11, pp. 805–817, Nov. 2016, doi: 10.1016/J.TICS.2016.09.004.

[197] G. G. Knyazev, “Motivation, emotion, and their inhibitory control mirrored in brain oscillations,” *Neurosci. Biobehav. Rev.*, vol. 31, no. 3, pp. 377–395, Jan. 2007, doi: 10.1016/J.NEUBIOREV.2006.10.004.

[198] J. I. Chapeton, R. Haque, J. H. Wittig, S. K. Inati, and K. A. Z. Correspondence, “Large-Scale Communication in the Human Brain Is Rhythmically Modulated through Alpha Coherence,” *Curr. Biol.*, vol. 29, pp. 2801-2811.e5, 2019, doi: 10.1016/j.cub.2019.07.014.

[199] K. E. Mathewson, A. Lleras, D. M. Beck, M. Fabiani, T. Ro, and G. Gratton, “Pulsed out of awareness: EEG alpha oscillations represent a pulsed-inhibition of ongoing cortical processing,” *Front. Psychol.*, vol. 2, no. MAY, 2011, doi: 10.3389/FPSYG.2011.00099.

[200] W. Klimesch, “Alpha-band oscillations, attention, and controlled access to stored information,” *Trends Cogn. Sci.*, vol. 16, no. 12, pp. 606–617, Dec. 2012, doi: 10.1016/J.TICS.2012.10.007.

[201] A. Kiyonaga, J. P. Powers, Y. C. Chiu, and T. Egner, “Hemisphere-specific Parietal Contributions to the Interplay between Working Memory and Attention,” *J. Cogn. Neurosci.*, vol. 33, no. 8, pp. 1428–1441, Jul. 2021, doi: 10.1162/JOCN_A_01740.

[202] D. Van Moorselaar, J. J. Foster, D. W. Sutterer, J. Theeuwes, C. N. L. Olivers, and E. Awh, “Spatially Selective Alpha Oscillations Reveal Moment-by-Moment Trade-offs between Working Memory and Attention,” *J. Cogn. Neurosci.*, vol. 30, no. 2, pp. 256–266, 2022, doi: 10.1162/jocn_a_01198.

[203] G. Kwon *et al.*, “Frontoparietal EEG alpha-phase synchrony reflects differential attentional demands during word recall and oculomotor dual-tasks,” *Neuroreport*, vol. 26, no. 18, pp. 1161–1167, 2015, doi: 10.1097/WNR.0000000000000494.

[204] P. Sauseng, W. Klimesch, M. Schabus, and M. Doppelmayr, “Fronto-parietal EEG coherence in theta and upper alpha reflect central executive functions of working memory,” in *International Journal of Psychophysiology*, 2005, vol. 57, no. 2, pp. 97–103, doi: 10.1016/j.ijpsycho.2005.03.018.

[205] M. Lobier, J. M. Palva, and S. Palva, “High-alpha band synchronization across frontal, parietal and visual cortex mediates behavioral and neuronal effects of visuospatial

attention," *Neuroimage*, vol. 165, pp. 222–237, 2018, doi: 10.1016/j.neuroimage.2017.10.044.

[206] S. Sadaghiani *et al.*, "Lesions to the Fronto-Parietal Network Impact Alpha-Band Phase Synchrony and Cognitive Control," *Cereb. Cortex*, vol. 29, no. 10, pp. 4143–4153, Sep. 2019, doi: 10.1093/CERCOR/BHY296.

[207] S. Sadaghiani *et al.*, "Alpha-Band Phase Synchrony Is Related to Activity in the Fronto-Parietal Adaptive Control Network," *J. Neurosci.*, vol. 32, no. 41, p. 14305, Oct. 2012, doi: 10.1523/JNEUROSCI.1358-12.2012.

[208] C. R. A. Silveira, K. A. Ehgoetz Martens, F. Pieruccini-Faria, D. Bell-Boucher, E. A. Roy, and Q. J. Almeida, "Disentangling perceptual judgment and online feedback deficits in Parkinson's freezing of gait," *J. Neurol.*, vol. 262, no. 7, pp. 1629–1636, Jul. 2015, doi: 10.1007/S00415-015-7759-7.

[209] M. Kawasaki, K. Kitajo, and Y. Yamaguchi, "Fronto-parietal and fronto-temporal theta phase synchronization for visual and auditory-verbal working memory," *Front. Psychol.*, vol. 5, no. MAR, p. 200, 2014, doi: 10.3389/FPSYG.2014.00200.

[210] C. C. Williams, M. Kappen, C. D. Hassall, B. Wright, and O. E. Krigolson, "Thinking theta and alpha: Mechanisms of intuitive and analytical reasoning," *Neuroimage*, vol. 189, pp. 574–580, Apr. 2019, doi: 10.1016/J.NEUROIMAGE.2019.01.048.

[211] J. Riddle, J. M. Scimeca, D. Cellier, S. Dhanani, and M. D'Esposito, "Causal Evidence

for a Role of Theta and Alpha Oscillations in the Control of Working Memory," *Curr. Biol.*, vol. 30, no. 9, pp. 1748-1754.e4, May 2020, doi: 10.1016/J.CUB.2020.02.065.

[212] M. R. van Schouwenburg, T. P. Zanto, and A. Gazzaley, "Spatial attention and the effects of frontoparietal alpha band stimulation," *Front. Hum. Neurosci.*, vol. 10, p. 658, Jan. 2017, doi: 10.3389/FNHUM.2016.00658.

[213] K. E. Mathewson *et al.*, "Dynamics of alpha control: preparatory suppression of posterior alpha oscillations by frontal modulators revealed with combined EEG and event-related optical signal," *J. Cogn. Neurosci.*, vol. 26, no. 10, pp. 2400–2415, Oct. 2014, doi: 10.1162/JOCN_A_00637.

[214] I. C. Fiebelkorn and S. Kastner, "A Rhythmic Theory of Attention," *Trends Cogn. Sci.*, vol. 23, no. 2, pp. 87–101, Feb. 2019, doi: 10.1016/J.TICS.2018.11.009.

[215] P. Knobl, L. Kielstra, and Q. Almeida, "The relationship between motor planning and freezing of gait in Parkinson's disease," *J. Neurol. Neurosurg. Psychiatry*, vol. 83, no. 1, pp. 98–101, 2012, doi: 10.1136/jnnp-2011-300869.

[216] C. A. Lebold and Q. J. Almeida, "An evaluation of mechanisms underlying the influence of step cues on gait in Parkinson's disease," *J. Clin. Neurosci.*, vol. 18, no. 6, pp. 798–802, Jun. 2011, doi: 10.1016/J.JOCN.2010.07.151.

[217] D. Cowie, P. Limousin, A. Peters, and B. L. Day, "Insights into the neural control of locomotion from walking through doorways in Parkinson's disease,"

Neuropsychologia, vol. 48, no. 9, pp. 2750–2757, Jul. 2010, doi: 10.1016/j.neuropsychologia.2010.05.022.

[218] D. Cowie, P. Limousin, A. Peters, M. Hariz, and B. L. Day, "Doorway-provoked freezing of gait in Parkinson's disease," *Mov. Disord.*, vol. 27, no. 4, pp. 492–499, 2012, doi: 10.1002/mds.23990.

[219] R. G. Cohen, A. Chao, J. G. Nutt, and F. B. Horak, "Freezing of gait is associated with a mismatch between motor imagery and motor execution in narrow doorways, not with failure to judge doorway passability," *Neuropsychologia*, vol. 49, no. 14, pp. 3981–3988, 2011, doi: 10.1016/j.neuropsychologia.2011.10.014.

[220] S. Mei *et al.*, "New onset on-medication freezing of gait after STN-DBS in Parkinson's disease," *Front. Neurol.*, vol. 10, no. JUN, p. 659, 2019, doi: 10.3389/FNEUR.2019.00659.

[221] A. Rubino *et al.*, "Does a volume reduction of the parietal lobe contribute to freezing of gait in Parkinson's disease?," *Parkinsonism Relat. Disord.*, vol. 20, no. 10, pp. 1101–1103, Oct. 2014, doi: 10.1016/J.PARKRELDIS.2014.07.002.

[222] K. Steidel *et al.*, "Dopaminergic pathways and resting-state functional connectivity in Parkinson's disease with freezing of gait," *NeuroImage Clin.*, vol. 32, p. 102899, Jan. 2021, doi: 10.1016/J.NICL.2021.102899.

[223] X. J. Wang, "Neurophysiological and computational principles of cortical rhythms in

cognition," *Physiol. Rev.*, vol. 90, no. 3, pp. 1195–1268, Jul. 2010, doi: 10.1152/PHYSREV.00035.2008.

[224] E. G. Antzoulatos and E. K. Miller, "Synchronous beta rhythms of frontoparietal networks support only behaviorally relevant representations," *Elife*, vol. 5, Nov. 2016, doi: 10.7554/eLife.17822.

[225] A. D'Andrea *et al.*, "Alpha and alpha-beta phase synchronization mediate the recruitment of the visuospatial attention network through the Superior Longitudinal Fasciculus," *Neuroimage*, vol. 188, pp. 722–732, Mar. 2019, doi: 10.1016/j.neuroimage.2018.12.056.

[226] A. Gelastopoulos, M. A. Whittington, and N. J. Kopell, "Parietal low beta rhythm provides a dynamical substrate for a working memory buffer," *Proc. Natl. Acad. Sci. U. S. A.*, vol. 116, no. 33, pp. 16613–16620, 2019, doi: 10.1073/pnas.1902305116.

[227] J. W. Choi *et al.*, "Altered Pallidocortical Low-Beta Oscillations During Self-Initiated Movements in Parkinson Disease," *Front. Syst. Neurosci.*, vol. 14, Jul. 2020, doi: 10.3389/FNSYS.2020.00054.

[228] J. M. Melgari *et al.*, "Alpha and beta EEG power reflects L-dopa acute administration in parkinsonian patients," *Front. Aging Neurosci.*, vol. 6, no. OCT, p. 302, 2014, doi: 10.3389/FNAGI.2014.00302.

[229] B. R. Noga *et al.*, "LFP oscillations in the mesencephalic locomotor region during

voluntary locomotion," *Front. Neural Circuits*, vol. 11, p. 34, May 2017, doi: 10.3389/FNCIR.2017.00034.

[230] A. H. Snijders *et al.*, "Gait-related cerebral alterations in patients with Parkinson's disease with freezing of gait," *Brain*, 2011, doi: 10.1093/brain/awq324.

[231] L. Meyer, J. Obleser, and A. D. Friederici, "Left parietal alpha enhancement during working memory-intensive sentence processing," *Cortex*, vol. 49, no. 3, pp. 711–721, Mar. 2013, doi: 10.1016/J.CORTEX.2012.03.006.

[232] Y. Deng, R. M. G. Reinhart, I. Choi, and B. Shinn-Cunningham, "Causal links between parietal alpha activity and spatial auditory attention," *Elife*, vol. 8, Nov. 2019, doi: 10.7554/ELIFE.51184.

[233] D. M. Tan, J. L. McGinley, M. E. Danoudis, R. Iansek, and M. E. Morris, "Freezing of gait and activity limitations in people with parkinson's disease," *Arch. Phys. Med. Rehabil.*, vol. 92, no. 7, pp. 1159–1165, Jul. 2011, doi: 10.1016/J.APMR.2011.02.003.

[234] J. D. Schaafsma, Y. Balash, T. Gurevich, A. L. Bartels, J. M. Hausdorff, and N. Giladi, "Characterization of freezing of gait subtypes and the response of each to levodopa in Parkinson's disease," *Eur. J. Neurol.*, vol. 10, no. 4, pp. 391–398, Jul. 2003, doi: 10.1046/J.1468-1331.2003.00611.X.

[235] J. G. Nutt, F. B. Horak, and B. R. Bloem, "Milestones in gait, balance, and falling," *Mov. Disord.*, vol. 26, no. 6, pp. 1166–1174, May 2011, doi: 10.1002/MDS.23588.

[236] K. Bharti *et al.*, “Neuroimaging advances in Parkinson’s disease with freezing of gait: A systematic review,” *Neuroimage (Amst).*, vol. 24, p. 102059, Jan. 2019, doi: 10.1016/J.NICL.2019.102059.

[237] C. Anidi *et al.*, “Neuromodulation targets pathological not physiological beta bursts during gait in Parkinson’s disease,” *Neurobiol. Dis.*, vol. 120, pp. 107–117, Dec. 2018, doi: 10.1016/J.NBD.2018.09.004.

[238] M. Seeber, R. Scherer, J. Wagner, T. Solis-Escalante, and G. R. Müller-Putz, “EEG beta suppression and low gamma modulation are different elements of human upright walking,” *Front. Hum. Neurosci.*, vol. 8, no. JULY, p. 485, Jul. 2014, doi: 10.3389/FNHUM.2014.00485.

[239] K. Takakusaki, “Functional Neuroanatomy for Posture and Gait Control,” *J. Mov. Disord.*, vol. 10, no. 1, pp. 1–17, Jan. 2017, doi: 10.14802/JMD.16062.

[240] R. O. Nwogo, S. Kammermeier, and A. Singh, “Abnormal neural oscillations during gait and dual-task in Parkinson’s disease,” *Front. Syst. Neurosci.*, vol. 16, p. 107, Sep. 2022, doi: 10.3389/FNSYS.2022.995375.

[241] A. Singh, A. Plate, S. Kammermeier, J. H. Mehrkens, J. Ilmberger, and K. Bötzel, “Freezing of gait-related oscillatory activity in the human subthalamic nucleus,” *Basal Ganglia*, vol. 3, no. 1, pp. 25–32, Mar. 2013, doi: 10.1016/J.BAGA.2012.10.002.

[242] A. M. A. Handojoseno, J. M. Shine, T. N. Nguyen, Y. Tran, S. J. G. Lewis, and H. T.

Nguyen, “Using EEG spatial correlation, cross frequency energy, and wavelet coefficients for the prediction of Freezing of Gait in Parkinson’s Disease patients,” in *2013 35th Annual International Conference of the IEEE Engineering in Medicine and Biology Society (EMBC)*, 2013, pp. 4263–4266.

[243] A. M. A. Handojoseno, J. M. Shine, T. N. Nguyen, Y. Tran, S. J. G. Lewis, and H. T. Nguyen, “The detection of Freezing of Gait in Parkinson’s disease patients using EEG signals based on Wavelet decomposition,” in *2012 Annual International Conference of the IEEE Engineering in Medicine and Biology Society*, 2012, pp. 69–72.

[244] A. M. A. Handojoseno, J. M. Shine, T. N. Nguyen, Y. Tran, S. J. G. Lewis, and H. T. Nguyen, “Analysis and prediction of the freezing of gait using EEG brain dynamics,” *IEEE Trans. neural Syst. Rehabil. Eng.*, vol. 23, no. 5, pp. 887–896, 2014.

[245] C. C. Chen *et al.*, “Subthalamic nucleus oscillations correlate with vulnerability to freezing of gait in patients with Parkinson’s disease,” *Neurobiol. Dis.*, vol. 132, p. 104605, Sep. 2019, doi: 10.1016/J.NBD.2019.104605.

[246] F. Karimi, Q. Almeida, and N. Jiang, “Large-scale frontoparietal theta, alpha, and beta phase synchronization: A set of EEG differential characteristics for freezing of gait in Parkinson’s disease?,” *Front. Aging Neurosci.*, vol. 14, p. 1245, Oct. 2022, doi: 10.3389/FNAGI.2022.988037.

[247] C. De Hemptinne *et al.*, “Exaggerated phase-amplitude coupling in the primary motor

cortex in Parkinson disease," *Proc. Natl. Acad. Sci. U. S. A.*, vol. 110, no. 12, pp. 4780–4785, Mar. 2013, doi: 10.1073/PNAS.1214546110.

[248] Q. J. Almeida and C. A. Lebold, "Freezing of gait in Parkinson's disease: a perceptual cause for a motor impairment?," *J. Neurol. Neurosurg. Psychiatry*, vol. 81, no. 5, pp. 513–518, 2010, doi: 10.1136/JNNP.2008.160580.

[249] S. Rahman, H. J. Griffin, N. P. Quinn, and M. Jahanshahi, "The factors that induce or overcome freezing of gait in Parkinson's disease," *Behav. Neurol.*, vol. 19, no. 3, pp. 127–136, 2008, doi: 10.1155/2008/456298.

[250] R. Chee, A. Murphy, M. Danoudis, N. Georgiou-Karistianis, and R. Iansek, "Gait freezing in Parkinson's disease and the stride length sequence effect interaction," *Brain*, vol. 132, no. 8, pp. 2151–2160, 2009, doi: 10.1093/BRAIN/AWP053.

[251] D. Gorjan, K. Gramann, K. De Pauw, and U. Marusic, "Removal of movement-induced EEG artifacts: current state of the art and guidelines," *J. Neural Eng.*, vol. 19, no. 1, p. 011004, Feb. 2022, doi: 10.1088/1741-2552/AC542C.

[252] E. Arad, R. Bartsch, J. Kantelhardt, and M. Plotnik, "Performance-based approach for movement artifact removal from electroencephalographic data recorded during locomotion," *PLoS One*, vol. 13, p. e0197153, 2018, doi: 10.1371/journal.pone.0197153.

[253] L. Pion-Tonachini, K. Kreutz-Delgado, and S. Makeig, "ICLabel: An automated

electroencephalographic independent component classifier, dataset, and website," 2019, doi: 10.1016/j.neuroimage.2019.05.026.

[254] R. Martinez-Cancino, A. Delorme, K. Kreutz-Delgado, and S. Makeig, "Computing Phase Amplitude Coupling in EEGLAB: PACTools," *Proc. - IEEE 20th Int. Conf. Bioinforma. Bioeng. BIBE 2020*, pp. 387–394, Oct. 2020, doi: 10.1109/BIBE50027.2020.00070.

[255] A. B. L. Tort, R. Komorowski, H. Eichenbaum, and N. Kopell, "Measuring phase-amplitude coupling between neuronal oscillations of different frequencies," *J. Neurophysiol.*, vol. 104, no. 2, pp. 1195–1210, 2010, doi: 10.1152/JN.00106.2010.

[256] V. Itskov, E. Pastalkova, K. Mizuseki, G. Buzsaki, and K. D. Harris, "Theta-mediated dynamics of spatial information in hippocampus.," *J. Neurosci. Off. J. Soc. Neurosci.*, vol. 28, no. 23, pp. 5959–5964, Jun. 2008, doi: 10.1523/JNEUROSCI.5262-07.2008.

[257] A. Nuñez and W. Buño, "The Theta Rhythm of the Hippocampus: From Neuronal and Circuit Mechanisms to Behavior," *Front. Cell. Neurosci.*, vol. 15, p. 31, Mar. 2021, doi: 10.3389/FNCEL.2021.649262.

[258] G. Buzsáki and E. I. Moser, "Memory, navigation and theta rhythm in the hippocampal-entorhinal system," *Nat. Neurosci.*, vol. 16, no. 2, pp. 130–138, 2013, doi: 10.1038/nn.3304.

[259] M. E. Hasselmo and C. E. Stern, "Theta rhythm and the encoding and retrieval of space

and time.," *Neuroimage*, vol. 85 Pt 2, no. 0 2, pp. 656–666, Jan. 2014, doi: 10.1016/j.neuroimage.2013.06.022.

[260] H. Zhang, A. J. Watrous, A. Patel, and J. Jacobs, "Theta and Alpha Oscillations Are Traveling Waves in the Human Neocortex," *Neuron*, vol. 98, no. 6, pp. 1269-1281.e4, Jun. 2018, doi: 10.1016/J.NEURON.2018.05.019.

[261] H. Mizuhara and Y. Yamaguchi, "Human cortical circuits for central executive function emerge by theta phase synchronization," *Neuroimage*, vol. 36, no. 1, pp. 232–244, May 2007, doi: 10.1016/J.NEUROIMAGE.2007.02.026.

[262] E. Beldzik, M. Ullsperger, A. Domagalik, and T. Marek, "Conflict- and error-related theta activities are coupled to BOLD signals in different brain regions," *Neuroimage*, vol. 256, p. 119264, Aug. 2022, doi: 10.1016/J.NEUROIMAGE.2022.119264.

[263] T. Watanabe, T. Mima, S. Shibata, and H. Kirimoto, "Midfrontal theta as moderator between beta oscillations and precision control," *Neuroimage*, vol. 235, p. 118022, Jul. 2021, doi: 10.1016/J.NEUROIMAGE.2021.118022.

[264] A. Zampogna, V. D'Onofrio, and A. Suppa, "Theta rhythms may support executive functions in Parkinson's disease with freezing of gait," *Clin. Neurophysiol.*, vol. 137, pp. 181–182, May 2022, doi: 10.1016/J.CLINPH.2022.02.007.

[265] P. Moolchand, S. R. Jones, and M. J. Frank, "Biophysical and Architectural Mechanisms of Subthalamic Theta under Response Conflict," *J. Neurosci.*, vol. 42, no.

22, pp. 4470–4487, Jun. 2022, doi: 10.1523/JNEUROSCI.2433-19.2022.

[266] G. M. Clements, D. C. Bowie, M. Gyurkovics, K. A. Low, M. Fabiani, and G. Gratton, "Spontaneous Alpha and Theta Oscillations Are Related to Complementary Aspects of Cognitive Control in Younger and Older Adults," *Front. Hum. Neurosci.*, vol. 15, p. 106, Mar. 2021, doi: 10.3389/FNHUM.2021.621620.

[267] A. Justin Riddle, "Causal Evidence for a Role of Theta and Alpha Oscillations in the Control of Working Memory," *Curr. Biol.*, vol. 30, pp. 1748-1754.e4, 2020, doi: 10.1016/j.cub.2020.02.065.

[268] R. N. Holdefer, B. A. Cohen, and K. A. Greene, "Intraoperative local field recording for deep brain stimulation in Parkinson's disease and essential tremor," *Mov. Disord.*, vol. 25, no. 13, pp. 2067–2075, Oct. 2010, doi: 10.1002/MDS.23232.

[269] Z. Yin *et al.*, "Local field potentials in Parkinson's disease: A frequency-based review," *Neurobiol. Dis.*, vol. 155, p. 105372, Jul. 2021, doi: 10.1016/J.NBD.2021.105372.

[270] K. Takakusaki, "Forebrain control of locomotor behaviors," *Brain Res. Rev.*, vol. 57, no. 1, pp. 192–198, Jan. 2008, doi: 10.1016/J.BRAINRESREV.2007.06.024.

[271] A. Parent and L. N. Hazrati, "Functional anatomy of the basal ganglia. II. The place of subthalamic nucleus and external pallidium in basal ganglia circuitry," *Brain Res. Rev.*, vol. 20, no. 1, pp. 128–154, 1995, doi: 10.1016/0165-0173(94)00008-D.

[272] J. Syrkin-Nikolau *et al.*, “Subthalamic neural entropy is a feature of freezing of gait in freely moving people with Parkinson’s disease,” *Neurobiol. Dis.*, vol. 108, pp. 288–297, Dec. 2017, doi: 10.1016/J.NBD.2017.09.002.

[273] M. J. Hülsemann, E. Naumann, and B. Rasch, “Quantification of phase-amplitude coupling in neuronal oscillations:comparison of phase-locking value, mean vector length, modulation index, and generalized-linear-modeling-cross-frequency-coupling,” *Front. Neurosci.*, vol. 13, no. JUN, p. 573, 2019, doi: 10.3389/FNINS.2019.00573.

[274] A. Farokhniaee, C. Palmisano, J. Del Vecchio, D. Vecchio, and J. Volkmann, “Gait-related cross-frequency coupling in the subthalamic nucleus of parkinsonian patients,” 2022, doi: 10.21203/rs.3.rs-2105705/v1.

[275] Ren Xu *et al.*, “A Closed-Loop Brain-Computer Interface Triggering an Active Ankle-Foot Orthosis for Inducing Cortical Neural Plasticity,” *IEEE Trans. Biomed. Eng.*, vol. 61, no. 7, pp. 2092–2101, Jul. 2014, doi: 10.1109/TBME.2014.2313867.

[276] A. Nieuwboer, R. Dom, W. De Weerdt, K. Desloovere, L. Janssens, and V. Stijn, “Electromyographic profiles of gait prior to onset of freezing episodes in patients with Parkinson’s disease,” *Brain*, vol. 127, no. 7, pp. 1650–1660, Jul. 2004, doi: 10.1093/BRAIN/AWH189.

[277] J. A. Obeso, M. C. Rodriguez-Oroz, M. Stamelou, K. P. Bhatia, and D. J. Burn, “The expanding universe of disorders of the basal ganglia,” *Lancet (London, England)*, vol.

384, no. 9942, pp. 523–531, 2014, doi: 10.1016/S0140-6736(13)62418-6.